# COUPLED MOLECULE - RADIATION FIELD EFFECTS IN AN AMMONIA BEAM MASER.

Thesis submitted to the University of Keele

for the Degree of Doctor of Philosophy

by

Paul R. Lefrère.

Department of Physics,

University of Keele,

May 1974.

ACKNOWLEDGEMENTS

The Author would like to thank

Professor D. J. E. Ingram for the provision of experimental facilities.

Dr. D. C. Lainé for his active concern and encouragement.

His colleagues in the Maser Group.

The Technical Staff of the Department for their willing assistance.

The University for personal finance.

Mrs. M. Taylor, for her care in typing this thesis.

## ABSTRACT

Details are given of a number of phenomena which have been observed in an advanced ammonia beam maser. These include cooperative effects arising during the build-up of oscillations , regenerative nutation, pulling and quenching of oscillations, induced spiking, biharmonic operation in a magnetic field, hysteresis effects and polarization transients.

The relevance of each of these to other areas of quantum electronics is discussed.

CONTENTS

# CHAPTER ONE

## Aspects of maser theory and design.

### Section 1.1. Introduction.

Any physicist entering the field of Quantum Electronics will find that current textbooks place a greater emphasis on lasers than on masers (e.g. Yariv 1967). This is justified from an engineering standpoint, since more applications exist for a laser, as a source of coherent electromagnetic radiation producing perhaps kilowatts of power in, or near, the visible region of the spectrum, than for its much weaker (nW) equivalent in the microwave region.

However, the number of experimental parameters for typical lasers may be very large. For example, the resonators used in lasers have both a multimode character and a high quality factor (i.e. narrow bandwidth) for each mode. Furthermore, laser media may be optically inhomogeneous. Thus, the observation that the output radiation from certain lasers consists of a continuous train of sharp spikes of irregular spacing and amplitude (Collins et al 1960) has not, as yet, been satisfactorily explained, although it has been the subject of considerable discussion (see, e.g. Birnbaum 1964). Clearly, a beam maser which exhibited such behaviour would enable this situation to be resolved, firstly since the number of parameters involved in maser operation is far smaller, and secondly because potential factors such as resonator mode structure can be varied independently of others such as beam flux. Unfortunately, an early theoretical analysis of the 'spiking' phenomenon indicated that it would be most unlikely to occur in ammonia beam masers (Singer and Wang 1961). However, a later experiment (Bardo and Lainé 1969) revealed that amplitude fluctuations

of similar appearance ('induced spiking') could arise in a strongly oscillating ammonia beam maser, provided that it was perturbed by an external microwave source.

It was suggested to the author at this stage that this particular aspect of molecule - radiation field interactions might prove of interest. Accordingly, since the maser used in the 'induced spiking' study was available, a series of modifications, chosen to increase the radiation field strength in the resonator of this maser, were undertaken.

It seemed feasible that as each improvement was introduced, it would be possible to reduce by a slight amount the intensity of the external perturbation referred to earlier, so that eventually self-induced pulsations, akin to those in lasers, would ensue.

The present chapter is only concerned with outlining (i) the details of the modifications undertaken, and (ii) the 'semiclassical' approach to maser theory, but chapters two and three show that this supposition about spiking effects was not, in fact, physically realistic.

## Section 1.2. Maximizing the oscillation power in an ammonia maser.

Ammonia maser oscillators have four essential components: (i) a beam source, (ii) a state separator, which should focus only those molecules which are in a net emissive state, (iii) a tuned resonant cavity with a large quality factor, and (iv) a pumping system which can maintain a long mean free path in the system.

In simple versions of molecular beam masers the source, focuser and cavity are housed in a single vacuum compartment. This means that whenever molecules are scattered, the vacuum will be degraded. There is, therefore, considerable advantage to be gained by having the source in a separately pumped compartment, and coupling this to

the main cavity by a variable iris, set in the dividing wall. The maser used by the author had in fact been designed with this scheme in mind (Bardo and Lainé 1971), and could oscillate without the cryogenic pumping needed in a single ~~cavity~~ chamber ammonia maser. The high degree of operational efficiency implied by this is a result of the fact that only those molecules that can be captured by the state focuser and focused into the microwave cavity need enter the main chamber with this arrangement.

Since operation with a higher beam flux was eventually envisaged by the author, the diffusion pumps fitted to each chamber were removed and replaced with larger pumps. The resulting 50% increase in pump speed produced an immediate four kilovolt reduction (to 17 kV) in focuser voltage at the threshold of oscillation. In other respects, however, the vacuum chambers were as described in the doctoral thesis of the previous researcher, which is henceforth termed 'WSB' (Bardo 1969).

Having achieved this increase in pumping speed, attention was then paid to the possibility that the focuser design could be improved. The state focuser used by the previous researcher was of the ring type (Krupnov 1959), consisting of a series of ring-like structures (safety pins) alternately charged positive and negative. Safety pins were chosen because their spiral ends, which consist of a $1\frac{1}{2}$-turn helix, have a smooth profile that decreases the tendency towards electrical breakdown. The two ends of each ring were mounted in a smooth metal base that was set in a PTFE support; the two sets of rings were separated by Sintox ceramic tubes, capable of withstanding voltages in excess of 50 kV between each base. The field between rings was then of the order

200 kV $cm^{-1}$, since there was a separation of approximately 3 mm between adjacent (oppositely charged) rings. This spacing represented a compromise between the need for a high field strength (since the separation of molecules in the upper and lower inversion levels is effected by a quadratic Stark interaction) and transparency (to permit unimpeded deflection of lower state molecules), (Bardo and Lainé 1971). It seemed unlikely to the author that the field strength could be increased without breakdown occurring, so an attempt was made to design a focuser with a greater degree of transparency than that of the WSB system. The scheme with most promise used safety pins of varying diameters, tapering towards the cavity, in a manner similar to that employed in a tapered quadrupole focuser (Helmer et al 1960).

Consideration of the design principle for ring focusers that the ratio of ring radius to ring separation should be close to unity (Krupnov 1959) indicates that the transparency of a tapered ring focuser of this type should indeed be greater than that of a conventional 'straight' ring focuser, assuming that the final ring diameter is the same in both cases. However, although the tapered focuser was found on construction to have a lower oscillation threshold voltage (15 kV), it was, in fact, much more prone to breakdown at high voltages than the WSB focuser. Eventually, therefore, this new focuser was discarded, being replaced by the original (WSB) device.

Additional experiments were then undertaken to find out whether any significant improvement in the efficiency of this focuser could be achieved. The first of these involved finding the most appropriate region for a cryogenically-cooled plate, designed to trap defocused molecules. It was known that molecules which leave the focuser may

rotate in space, following the fringe field between the focuser and earthed objects. Furthermore, the orientation of focused molecules relative to the resonator radiation field determines the strength of this microwave field. Attempts were therefore made by the author to reduce the oscillation threshold without cryogenic cooling, by bringing a small earthed probe near the focuser, thus perturbing its stray fields slightly. This met with some success, so a larger copper plate, milled lengthways to increase its eventual trapping area, was placed at a similar distance (about 15 mm) from the side of the focuser. Two such plates, when cooled with liquid nitrogen, allowed the flux of ammonia molecules through the focuser to be increased substantially, without a corresponding increase in background pressure occurring.

It was established in a further experiment that an increase in the number of active molecules entering the resonator could be achieved by reducing the distance between the focuser and the iris to perhaps 4 mm, and reducing the iris diameter to 1 mm.

One further possibility that presented itself was that the efficiency of the state selection process could be increased by using a small earthed beam stop, placed on the axis before the focuser. Since only those molecules with a non-zero quantum number $M_J$ (where $M_J$ is the projection of the J quantum number on the direction of the focuser field) contribute to the emission in the resonator, and states with $M_J = 0$ are not affected by the focuser field, this procedure could allow the density of active molecules in the resonator to be increased.

This can be seen from the equation for the energy of the inversion states, W, remembering that in an inhomogeneous field these molecules

experience a force F = - grad W:

$$W = W_o \pm \left[ \left( \frac{h \nu_o}{2} \right)^2 + \left( \frac{\mu E M_J K}{J(J+1)} \right)^2 \right]^{\frac{1}{2}} \qquad 1.1.$$

where $W_o$ is the average energy of the upper and lower inversion levels, neglecting hyperfine effects, $\mu$ is the permanent dipole moment that the molecule would exhibit in the absence of inversion, and E is the electric field strength (see, e.g. Gordon et al 1955). However, on due consideration it was realized that the use of a beam stop would inevitably reduce the maximum possible beam flux, so this experiment was not taken further.

Instead, attention was turned to the beam source used by the previous researcher. This was basically a single nozzle, 1 cm long and 1 mm in diameter. A multiple-channel nozzle, taken from another maser, was tried in its place, but gave inferior results. This was, perhaps, to be expected, since any nozzle used in a maser must be matched to the state focuser. For example, both the spatial divergence of the emerging beam and the distribution of molecules over energy states may vary from one focuser to another.

The author therefore decided to use the original source-focuser combination, but modified the mechanical mounting arrangements somewhat. In particular, the nozzle was soldered to a cryogenically-cooled tube which could be displaced both laterally and transversely while the maser was operating. The distance between the nozzle and the iris could therefore be optimized for any given beam flux, whilst cooling of the beam was taking place.

One effect associated with cooling the gas is that the population in the J = K = 3 inversion state increases, since it varies with absolute

temperature as $T^{-3/2}$ (Townes and Schawlow 1955). However, the average molecular velocity is reduced, thus increasing the time of interaction in the cavity. While this latter factor serves to lower the threshold of oscillation, it should be borne in mind that the number of molecules entering the cavity every second may also decrease as the source temperature is reduced, unless this temperature reduction is the result of dynamic cooling under conditions of quasi-supersonic flow, as may occur with high nozzle pressures.

The advantage gained by cooling the beam in this fashion may be gauged by the fall in threshold focuser voltage to 7 kV when cryogenic cooling was used in both chambers. In passing, it should be noted that while the nozzle could be operated down to temperatures near 170 K and ammonia gas pressures of a few torr, oscillations sometimes ceased at lower temperatures. Presumably this observation is related to the fact that the triple point of ammonia is at 195 K and 45 torr.

The final component considered was the microwave resonator. The need here was to find a method of increasing the interaction between the maser molecules and the cavity radiation field, without broadening the spectral line appreciably.

Clearly, this interaction can be maximized by choosing a cavity mode with both a high quality factor and a microwave electric field that is axially uniform and has a maximum on the beam axis. The closest approach to this ideal situation is obtained if a weakly-coupled cavity operating in the $E_{010}$ mode is used (Shimoda et al 1956). In this mode the radiofrequency field E is parallel to the resonator axis, but decreases in the transverse direction away from the beam axis.

Furthermore, the $E_{010}$ mode is independent of length, so the interaction time can be maximized for a given beam flux by using a long cavity. These considerations had in fact already been put into practice within the Keele maser group, and an $E_{010}$ mode cavity made of electroformed OFHC copper (to minimize ohmic losses) had been fitted to this particular maser during the initial stages of its construction by WSB . This cavity, which was fitted with end-caps of diameter beyond cutoff for the mode, had an effective length of 124 mm; additionally, it was much undercoupled, thereby yielding a high value of loaded Q (estimated at 9000) .

Since the surface conductivity of metals is known to increase when their temperature is reduced, an attempt was made to improve the cavity Q factor by cooling to just above the point at which appreciable quantities of ammonia condense inside the cavity. To this end, a cavity was electroformed that was slightly oversize at room temperature (9.63 mm in diameter, rather than 9.61 mm), but was of comparable length. When this cavity was cooled to about 150 K, a near doubling in the Q factor was observed, although the maser operation time was reduced because of temperature instabilities. However, further cooling was found to simultaneously detune the cavity and broaden the spectral line, presumably because ammonia molecules then condensed, and collected charge.

In conclusion, it is noted that little further improvement in quality factor can be expected at this high frequency (23,870 MHz), regardless of the nature of the refrigerating arrangements (Biquard and Septier 1966) .

Section 1.3. Theory of molecular beam masers.

In this section, a short summary of the rationale of three different approaches to the theory of quantum oscillators is given; further details of each can be found in standard texts (e.g. Pantell and Puthoff 1969). Examples are then given of the way in which the results of the second of these, the semiclassical approach, may be interpreted geometrically.

The simplest method of interpreting the behaviour of quantum oscillators involves the neglect of all phase relationships between radiation field and molecules. Two equations are thereby obtained which relate to the time evolution of population differences and to field fluctuations respectively. Such a set of rate equations provides a phenomenological description of situations which involve gross effects, such as the oscillation threshold condition, but may be inappropriate for certain other situations, as explained in section 3.2.

A more sophisticated analysis of the molecule - radiation field interaction can be obtained by including the back reaction of any radiation emitted by each molecule in the ensemble on itself. This reaction is included by requiring that the field be self-consistent, that is, that the field which acts upon the molecules is consistent with the field radiated by these molecules.

That this automatically ensures the inclusion of all possible emission processes is perhaps not always appreciated, as some authors sometimes add extra terms, relating to effects such as coherent spontaneous emission, after making this self-consistent field (SCF) approximation (e.g. Ponte Goncalves et al 1969).

The SCF approach is generally taken to be semiclassical; that is, the radiating molecules are treated quantum-mechanically, while the radiation field is described classically. It is possible, though, to start with a quantized radiation field and then make the approximation that molecule-field correlations can be neglected (Jaynes and Cummings 1963). However, this approximation in fact brings one back to a self-consistent semiclassical theory.

The derivation of SCF equations used in standard texts (e.g. Pantell and Puthoff 1969) proceeds via Maxwell's equations and the dynamical equations for the statistical density operator, written in the Schrodinger picture, for an ideal two-level system, usually with an electric dipole interaction. A closed system of equations is then obtained, which can be used to calculate both static and dynamic properties of those molecular oscillators for which the two-level approximation is appropriate.

From the standpoint of beam maser theory, these equations may be written in the form:

$$\left.\begin{aligned} &\ddot{P} + \frac{2\dot{P}}{T} + (\omega_o^2 + T^{-2})P = -2N\frac{\omega_o}{\hbar}\left|\mu_{12}\right|^2 E \\ &\ddot{E} + 4\pi\ddot{P} + \frac{\omega_c}{Q_c}\dot{E} + \omega_c^2 E = 0 \\ &\dot{N} + \frac{1}{T}(N - N_o) = \frac{2}{\hbar\omega_o}E\left(\dot{P} + \frac{1}{T}P\right) \end{aligned}\right\} \quad 1.2.$$

where $N_o$ and N are the number of active molecules per unit volume in the absence and presence of the resonator field respectively, $\omega_o$ is the molecular resonance frequency, $\omega_c$ and $Q_c$ are the natural

frequency and quality factor of the resonator, $T$ is the average transit time of the molecules through the resonator and $\mu_{12}$ is the dipole matrix element for the transition ( Fain 1958).

Although it is not immediately apparent from individual papers in the literature, several important assumptions must be made before a set of equations which are in the form given previously can be obtained:

(a) it is implied that macroscopic variables such as the population difference $(N - N_o)$ decay exponentially; this is equivalent to neglecting quantum-mechanical damping,

(b) the molecular distribution function for times of flight through the cavity is taken to be of the form $(1/T)\exp(-t/T)$, although experiments have shown that molecular beams may be deficient in very slow molecules (Barnes 1959),

(c) the molecular polarization P must not be averaged simultaneously over the two independent variables, resonator length and molecular velocity distribution, since no information on possible instabilities can then be obtained (Mukhamedgalieva and Khoklov 1961).

Nevertheless, self-consistent field equations of this general type can account for phenomena as diverse as two-frequency operation, superradiance and radiative echoes.

If a more detailed description of a system is required, it is possible to proceed via the equations of motion for the dynamical operators of the system, written in the Heisenberg picture. This enables damping processes to be pictured, since equations of motion for the operators have the same form as those for a classical damped

system subject to fluctuating forces (the Langevin equations).

One example of the use which can be made of this resemblance relates to an evaluation, in terms of a univelocity model, of the noise properties of a beam maser amplifier (Gordon et al 1955). The requisite large number of degrees of freedom can be conferred upon the maser by considering each of the active molecules entering the cavity as equivalent to an excited oscillatory circuit, so that the ensemble can be regarded as a medium with negative loss. This simple approach makes the system amenable to treatment as a dispersive medium. However, the equations which result are only valid for single-frequency processes, since the concept of a dielectric constant is only applicable in this case.

It will therefore be appreciated that the semiclassical approach, which can easily be modified to cope with multi-frequency processes such as may occur in a Zeeman beam maser, is employed more frequently than any other by workers in the general field of quantum electronics.

A discussion of the semiclassical theory of beam masers would be incomplete without giving an outline of a geometrical representation of the equations of motion for the density matrix, based upon the fact that linear combinations of density matrix elements can give a set of equations analogous to the Bloch equations of magnetic resonance (Feynman et al 1957).

These equations can be derived by associating the components of a three-dimensional vector $\underline{r}^*$ with various elements of the density

matrix $\rho$ :

$$\left.\begin{aligned} r_1^* &= \rho_{ab} + \rho_{ba} \\ r_2^* &= i(\rho_{ab} - \rho_{ba}) \\ r_3^* &= \rho_{aa} - \rho_{bb} \end{aligned}\right\} \quad 1.3.$$

Representing the coupling to an external radiation field E by the interaction

$$H = -\mu E \cos \omega t \qquad 1.4.$$

where $\mu$ is the projection of the induced dipole moment along the polarization direction of the field, then allows $\underline{r}^*$ to be transformed into a new vector $\underline{r}$ by using a rotating frame. If this frame revolves at the angular frequency $\omega$ around the $r_3^*$ axis, and terms oscillating at $2\omega$ are ignored, then a Bloch - type vector relating to the molecules in the resonator is obtained:

$$\dot{\underline{r}} = \omega_{eff} \times \underline{r} \qquad 1.5.$$

where $\omega_{eff}$ is also a three-vector,

$$\omega_{eff} = (\omega_1 , 0 , \omega_o - \omega) \qquad 1.6.$$

$\omega_o$ is the frequency of the maser resonance, and $\omega_1 = \mu E / h$ .

However, while the Bloch vector for a spin - $\frac{1}{2}$ particle in a magnetic field B may be resolved into components in the x, y and z directions, where $\omega_1$ , $\omega_2$ and $\omega_3$ are proportional to the field components $B_x$ , $B_y$ and $B_z$ , the analogous Bloch vector for the electric dipole

case can only be considered as rotating in a mathematical three-dimensional 'space' , unrelated to real physical space. If the axes of this space correspond to the axes of $\omega_{eff}$, then the 1 - 2 plane can be thought of as a complex plane representing relative phase, with the 2 - axis being the imaginary axis. Accordingly, the projection of the Bloch vector on this plane will be proportional to the polarization (or to the experimental value of induced dipole moment).

The 3 - axis will then be the 'energy' axis, and the projection of the vector in this direction will be proportional to the difference in level populations for an ensemble of molecules.

As an example of the uses to which this representation may be put, consider the case of an ensemble subjected to a steady radiation field. When the radiation field is tuned to resonance, the $\underline{r}$ vector will precess in the 1 - 3 plane, about the 2 - axis , as shown in figure 1.a.

If the field is reduced to zero at the instant of maximum inversion, (i.e. when $\underline{r}$ has its maximum extension in the positive direction of the 3 - axis), the vector will maintain a vertical orientation, but will gradually change in magnitude, as a result of relaxation processes, until it is eventually fully extended in the negative direction. (Note: this behaviour may be modified when the system is superradiant, as discussed in subsequent chapters).

However, if an off-resonant field is now applied, $\underline{r}$ will nutate about $\omega_{eff}$ . This nutation may be looked upon as a precession by $\underline{r}$ about a vector formed from $\omega_1$ and $\omega_2$ which is itself rotating in the 1 - 2 plane, as shown in figure 1.b.

Use of the geometrical representation can also allow any informa-

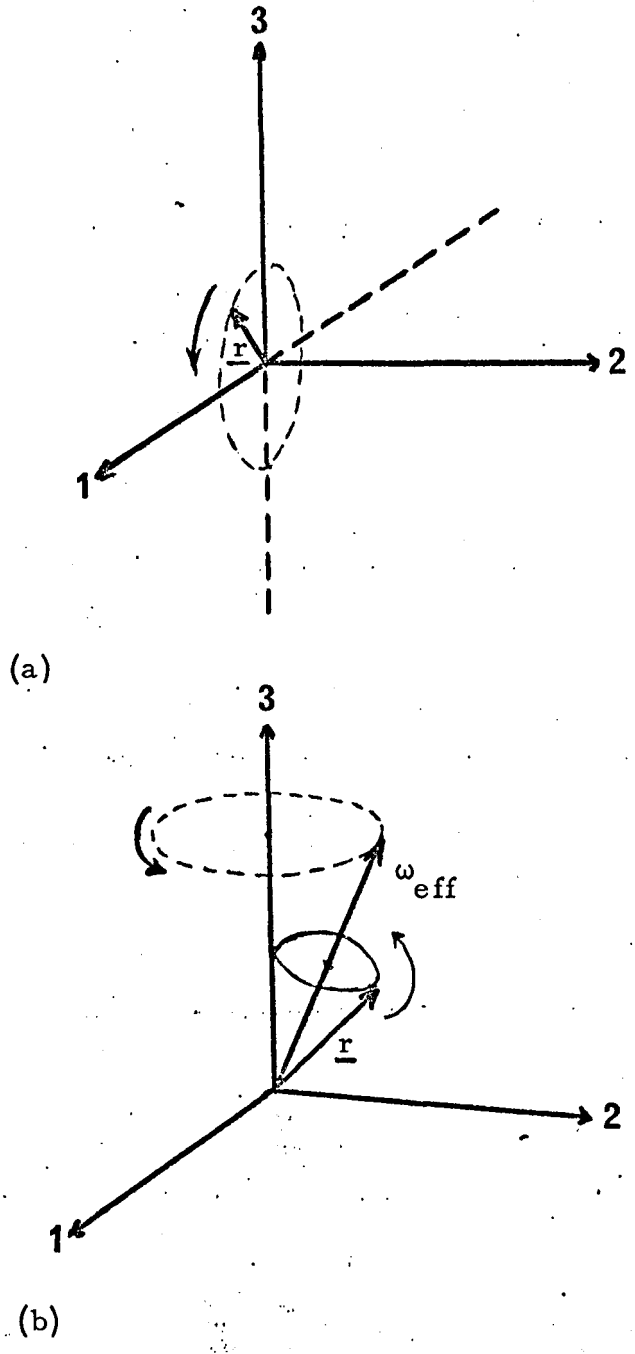


Figure 1.1. (a) Precession of $\underline{r}$ when a resonant radiation field is applied; (b) nutation in an off-resonant field.

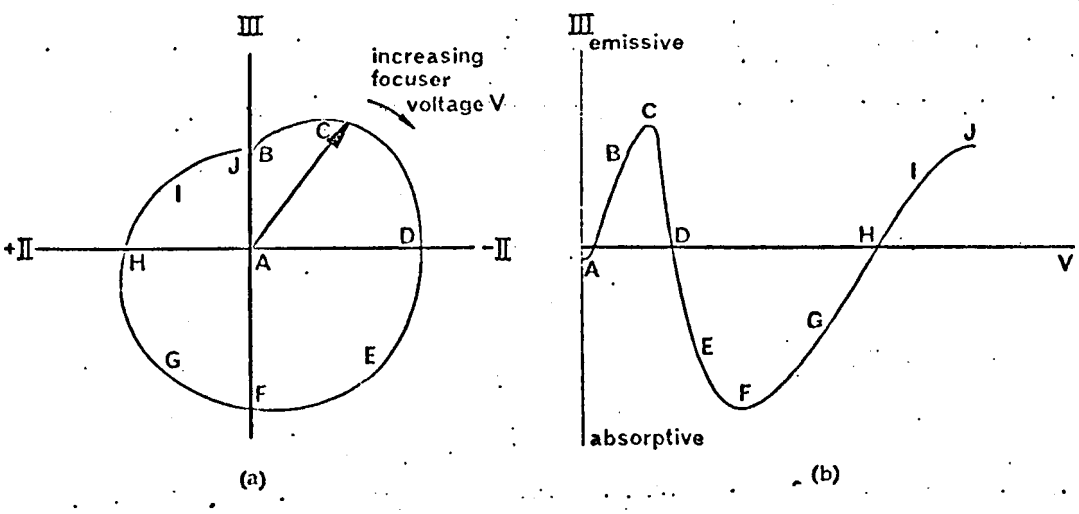


Figure 1.2. (a) The locus of $\underline{r}$ as a parametric function of focuser voltage V, at zero resonator detuning, for a narrow distribution of molecular velocities; (b) form of variation of amplitude of spectral line in cavity 2 at zero detuning for both cavities (After Bardo and Lainé 1971*).

tion concerning polarizations and populations which is gleaned in beam maser experiments to be displayed particularly concisely, as shown in figure 2.a. This figure depicts the variation with excitation of both the polarization carried by the beam from the maser cavity and the state in which the molecules emerge from this cavity. It may be compared with an alternative presentation of these results, shown in figure 2.b. (Bardo and Lainé 1971*).

In conclusion, it may be stated that the picture of maser design and theory given by the author must reflect to a considerable degree the programme of investigations being undertaken by the Keele maser group into the analogies existing between different quantum electronic systems.

REFERENCES

Bardo W.S., (1969), Thesis, University of Keele, unpublished.

Bardo W.S.,and Lainé D.C., (1969), Electron.Lett.5 , 688-9.

Bardo W.S. and Lainé D.C., (1971), J.Phys.E (Sci.Instrum.)4, 595-7.

Bardo W.S. and Lainé D.C., (1971*), J.Phys.B(Atom.Mol.Phys.)4, 1523-35.

Barnes F.S., (1959), Proc.IRE 47 , 2085-98.

Biquard F. and Septier A., (1966), Nucl.Instrum.and Methods 44,18-28.

Birnbaum G., (1964), Adv.in Electronics and Electron Phys., Suppl.2.

Collins R.J. et al, (1960), Phys.Rev.Lett.5 , 303.

Fain V.M., (1958), Sov.Phys.-JETP, 6 , 726-8.

Feynman R.P. et al, (1957), J.Appl.Phys. 28 , 49-52.

Gordon J.P. et al, (1955), Phys.Rev. 99, 1264-74.

Helmer J.C. et al, (1960), J.Appl.Phys. 31 , 458-63.

Jaynes E.T. and Cummings F.W., (1963), Proc.IEEE 51 , 89-109.

Krupnov A.F., (1959), Sov.Radiophys. 2 , 658-9.

Mukhamedgalieva A.F. and Khoklov R.V., (1961), Sov.Radiophys. 4 , 259-62.

Pantell R.H. and Puthoff H.E., (1969), "Fundamentals of Quantum Electronics", John Wiley (publ.), New York.

Ponte-Goncalves A.M. et al, (1969), Phys.Rev. 188 , 576.

Shimoda K. et al, (1956), Phys.Rev. 102, 1308-21.

Singer J.R. and Wang S., (1961), Phys.Rev.Lett. 6 , 351-4.

Townes C.H. and Schawlow A.C., (1955), "Microwave Spectroscopy", McGraw-Hill (publ.), New York.

Yariv A., (1967), "Quantum Electronics", John Wiley (publ.), New York.

## CHAPTER TWO

### Properties of a Zeeman maser and other coupled systems.

### Section 2.1. Introduction.

It has long been known that coupling two or more classical oscillators together will result in frequency pulling effects. Early work on beam maser frequency standards showed that quantum oscillators exhibit similar behaviour. However, since the response of the quantum systems in a quantum oscillator has a sharply resonant character it is not necessary to couple two separate quantum oscillators together for frequency pulling to occur. This is because a quantum oscillator such as a molecular beam maser, although normally thought of as a single frequency system, is in fact essentially a coupled system of two oscillators, one a "polarization" oscillator, of frequency $\nu_o$, and the other a "cavity-field" oscillator, of frequency $\nu_c$.

Thus, although the oscillation frequency of an ammonia beam maser depends to some extent on parameters such as beam flux and separator voltage, it is mainly determined by the tuning of the cavity resonator relative to the peak of the spectral line. The actual oscillation frequency $\nu$ will depend on the frequency $\nu_o$ of the molecular resonance, the quality factor $Q_m$ of the spectral line, the quality factor $Q_c$ and the frequency $\nu_c$ of the resonator, and the output power- (saturation-) factor, $f(\theta)$ of the oscillation (Gordon et al 1955):

$$\nu = \nu_o \left[ 1 - \frac{\nu_c - \nu_o}{\nu_o} \frac{Q_c}{Q_m} f(\theta) \right] \qquad 2.1.$$

Such a system is particularly easy to study, since ammonia beam masers can be operated well above the threshold of oscillation when the $J = 3$, $K = 3$ inversion of $N^{14}H_3$ is used. Indeed, under

strong oscillation conditions such a maser will continue to oscillate when the spectral line is broadened (or even split) by a magnetic field. If the field is large enough, (~0.2mT), c.w. oscillation may take place simultaneously on the two weak-field Zeeman components of the spectral line.

A detailed study of this situation is made in the first half of this chapter, but it should be noted that such a double oscillation is only possible over a small range of magnetic field values, since at low fields the two oscillations, which are subject to mutual frequency pulling, lock together to produce a single oscillation. The Zeeman maser therefore provides a good example of a system of two coupled quantum oscillators. There does exist a related problem: the frequency locking of a single mode laser operating in a magnetic field (a Zeeman laser). This has been studied by a number of authors (e.g. Sargent et al 1967), although no direct comparison with the maser may be made because the roles of cavity and molecular linewidths are reversed in the laser case.

The remainder of this chapter is concerned with other effects which may be observed in both classical and quantum oscillators, such as frequency entrainment. The first theoretical work directly applicable to quantum oscillators dealt with coupled electronic circuits (van der Pol 1934), although Huygens also seems to have observed frequency locking phenomena (in clocks, quoted in Minorsky 1947). Since both electronic and quantum oscillators exhibit oscillation entrainment phenomena (e.g. injection phase-locking and oscillation quenching) one section is devoted to the classical van der Pol oscillator model. Although only qualitative experiments on locking are reported in this thesis, the question of whether the van der Pol approach to such effects may be validly applied to the forced locking of quantum oscillators would still appear to be worthy

of consideration. In particular, a number of analyses (e.g. Tang and Statz 1967) of the locking of one laser oscillator to another (Stover and Steier 1966) rely on results obtained from an approximate treatment, derived for electronic oscillators with special feedback characteristics (Adler 1946), rather than for the more general van der Pol oscillators.

The conclusions drawn in this chapter may therefore be relevant to quantum oscillators in general.

## Section 2.2 The Zeeman effect in $N^{14}H_3$.

The change in linewidth produced by the magnetic field makes observation of Zeeman beats in a maser possible only if the unperturbed maser is operated considerably above the threshold of oscillation. This criterion for Zeeman maser operation has only been satisfied so far by masers operated on the J = 3, K = 3 inversion transition of $N^{14}H_3$.

Unfortunately, no detailed data on magnetic effects in the (3,3) line appear to be available for the range of field values used for Zeeman maser operation (approximately 0.3 to 1 mT), and it is therefore necessary to consider how the linewidth is observed to change in lower fields.

In such a case the line broadening produced by Zeeman splitting is given approximately by:

$$\Delta\nu_L = \left[ (\Delta\nu_o)^2 + (\Delta\nu_B)^2 \right]^{\frac{1}{2}} \qquad 2.2.$$

where $\Delta\nu_o$ is the unperturbed linewidth for the transition and $\Delta\nu_B$ is the splitting in a magnetic field.

Since the molecular quality factor, $Q_M$, depends on the linewidth, magnetic fields may be used to tune the maser oscillation frequency fairly near to the peak of the spectral line. In practice

the magnetic field is modulated at some angular frequency $\omega_m$. The linewidth modulation produces a modulation term proportional to the frequency difference $\nu_o - \nu_c$ between the cavity and the spectral line in the resulting pulling equation (Barnes et al 1961):

$$\nu = \nu_o - \frac{\Delta\nu_o}{\Delta\nu_c}\left(1 + \tfrac{1}{2}x^2\right)^{\frac{1}{2}}\left(\nu_o - \nu_c\right) + \frac{\Delta\nu_o}{\Delta\nu_c}\,\frac{\tfrac{1}{2}x^2\left(\nu_o - \nu_c\right)}{\left(4 + 2x^2\right)^{\frac{1}{2}}}\cos 2\omega_m t \qquad 2.3.$$

where x is defined as the ratio of the peak line width (with magnetic perturbation) to the natural (unperturbed) width.

Both small, (flux density $\sim$ 0.1 mT), fairly homogeneous magnetic fields (Shimoda et al 1956) and stronger ($\sim$ 1 mT) local fields (Hellwig 1966) have been found suitable for modulation. The actual peak line width is thus not critical, although it is generally assumed in calculations of the sensitivity of this method of tuning that the relevant g-factor is approximately that measured in bulk gas at high ($\gtrsim$ 0.1 T) fields (Jen 1948). This assumption certainly does not hold in the case of the (3,3) line of $N^{14}H_3$, because the central hyperfine components of this line (figure 2.1.) exhibit level-crossing and level-anticrossing effects in the region 0.1 to 1 mT. This results in an apparent non-linearity in the effective g-factor (figure 2.2) in this region, although at higher fields the g-factor tends to the value of 0.47 measured by Jen.

The total g-factor for the (3,2) line of $N^{14}H_3$ appears to be much more linear, however, because this transition consists of a strong main line with only two pairs of magnetic hyperfine satellites, and level crossing of main line components does not occur. The uncertainty in the determination of the line centre is therefore small, and a maser operated on such a transition can be tuned very precisely, to give a reproducibility of a few parts in $10^{11}$

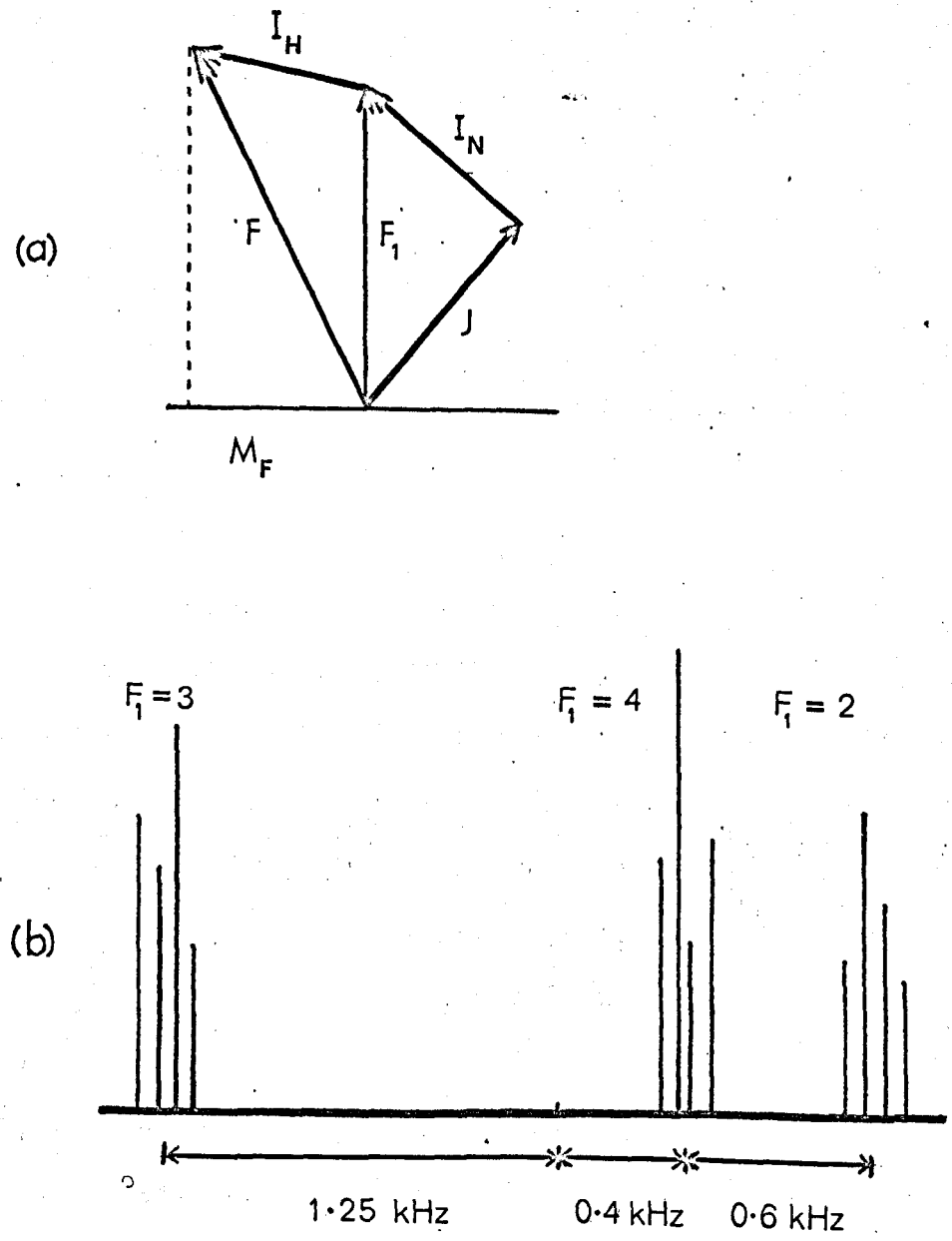


FIGURE 2.1. Inversion line of $^{14}NH_3$, $J = 3$, $K = 3$, $\Delta F = 0$, $\Delta F_1 = 0$. (a) Coupling scheme, (b) structure. (After Oraevskii 1963).

(Hellwig 1966).

The complicated structure of the (3,3) line arises because of the quadrupole interaction of the $N^{14}$ nucleus with the molecular field and the dependence exhibited by the total hydrogen spin $I_H$ on the value of K ($I_H = \frac{3}{2}$ when K is a multiple of 3, while for all other values of K, $I_H = \frac{1}{2}$).

In the case of the 3,3 line the quadrupole interaction, which is proportional to $eqQ\ (1 - \frac{3K^2}{J(J+1)})$, produces an uncertainty of over 100 Hz in the determination of the line centre, whereas the uncertainty is much less in the 3,2 line since only magnetic hyperfine structure is present.

The appropriate selection rules for the ammonia inversion spectrum are $\Delta J = 0$, $\Delta K = 0$, where J is the total angular momentum excluding nuclear spin and K is the projection of J on the symmetry axis of the molecule. Additional selection rules apply to the coupling scheme of figure 2.1. for the 3,3 line:

$\Delta F_1 = 0, \pm 1$, where $F_1 = J + I_N$ and $I_N$ is the spin of the nitrogen nucleus;

$\Delta F = 0, \pm 1$, where $F = F_1 + I_H$ and $I_H$ is the total spin of the hydrogen nuclei.

These give rise to a central group of lines with twelve hyperfine components, for which $\Delta F = \Delta F_1 = 0$, closely flanked on either side by the magnetic satellites, with $\Delta F_1 = 0, \Delta F = \pm 1$. The quadrupole satellites, $\Delta F_1 = \pm 1$, and their associated magnetic structure ($\Delta F = 0, +1$, or $0, -1$) lie somewhat further away. The slight difference in quadrupole coupling constants between the upper and the lower inversion levels splits the twelve components of the main line into three close groups of lines corresponding to $F_1 = 3$, 4 and 2, with relative strengths in emission in the ratio of 1 to 0.92 to 0.05 respectively, (Shimoda 1957). It should be noted that

the g-factor measured by Jen was for bulk gas, where the molecules are in thermal equilibrium. The relative intensities of the three $F_1$ components are then proportional to $2F_1+1$, and the weighted average Zeeman splitting measured by Jen will therefore appear to be slightly less than the weighted splitting in the state selected case.

The frequency shift of the central line Zeeman components ($\Delta F = 0, \Delta M = \pm 1$) is given by Jen as:

$$\Delta\nu_o = \pm \frac{\mu_o B}{h} \left\{ \frac{g_M+g_N}{2} + \frac{J(J+1)-I(I+1)}{F(F+1)} \frac{(g_M-g_N)}{2} \right\} \qquad 2.4.$$

where $g_M$ is the g-factor of the molecule along J, $g_N$ is the g-factor of the nucleus coupled with the molecule, and $\mu_o$ is the nuclear magneton.

For the (3,3) line this becomes:

$$\Delta\nu_o = \pm \frac{\mu_o B}{h} \left\{ 0{\cdot}441 + \frac{0{\cdot}4}{F(F+1)} \right\} \qquad 2.5.$$

However, this shift is modified in fields of 0.1 to 1 mTesla, because all M components of the central groups of lines ($F_1$ = 3, 4 and 2) tend to cross. In time-independent perturbation theory "levels of the same M never cross" on an energy level diagram. If we are considering the breakdown of I-J coupling, for example, the hyperfine interaction $a\underline{I}.\underline{J}$, which has non-vanishing matrix elements between states of the same value of $M = (M_I + M_J)$, causes repulsion of such levels. It can thus be seen that the effective g-factor of the (3,3) line may vary somewhat in the region 0.1 to 1 mTesla. This was confirmed by direct measurement of the spacing of Zeeman components in the emission line of a maser operated below oscillation threshold. (The same maser was used for all the experiments

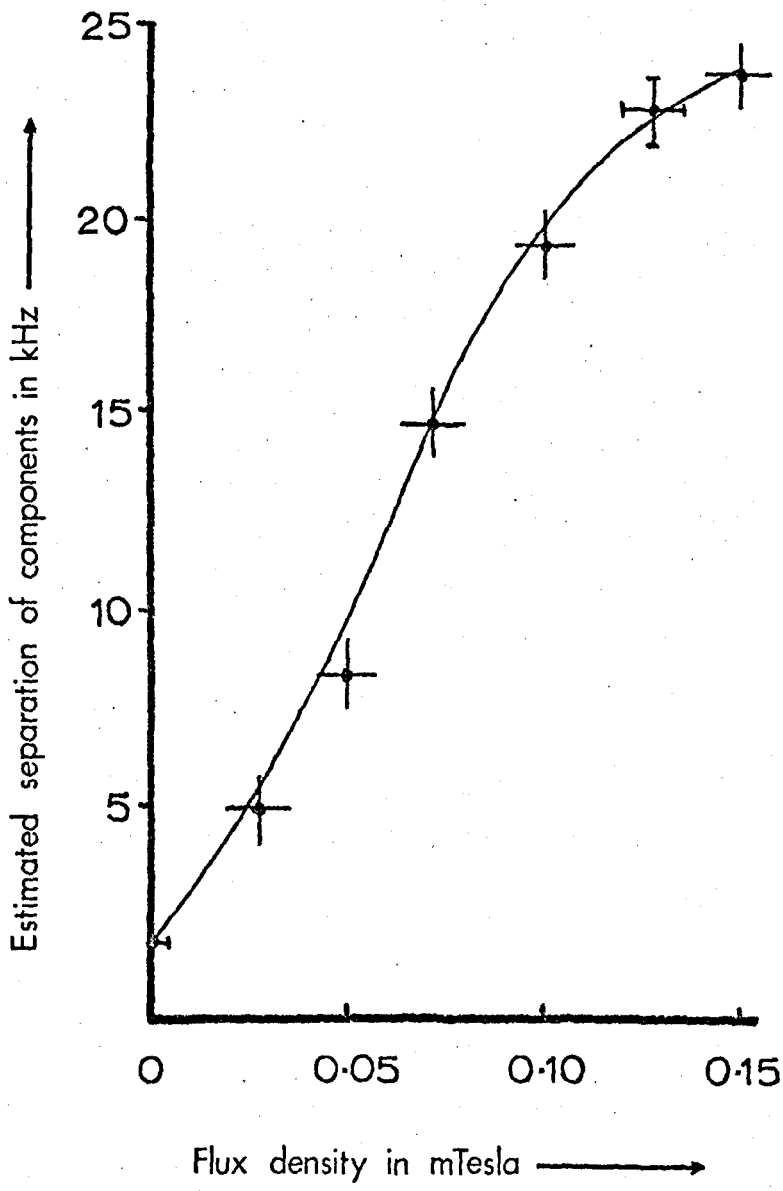


FIGURE **2.2.** Low field Zeeman splitting: 3,3 line of ammonia in emission.

described in this thesis.) The results are summarized in figure 2.2. These results are only approximate, however, for three reasons:

(i) an acceptable signal-to-noise ratio was only obtained when the maser was operated under conditions such that the spectral line was slightly power broadened.

(ii) the magnetic field coils (calibrated using a Newport Instruments Hall Probe) were found to produce a field which varied by up to 10% in value over the length of the cavity.

(iii) the $E_{010}$ mode cavity used was 124 mm long. This was not long enough to resolve the central Zeeman components until their frequency separation was greater than 7-10 kHz. The Zeeman spacing was therefore estimated from photographs of the resulting asymmetrical line shape. The equivalent method of fast passage through the line to produce an electric dipole "beating of beats" pattern (Lainé and Smart, unpublished) was found to give similar results.

Section 2.3. The Zeeman maser I - locking, hysteresis, and the maximum emission principle.

If locking phenomena did not occur in quantum oscillators then a magnetic field of any value applied to a maser oscillating at a single frequency $\nu$ would produce two oscillations at frequencies $\nu_+$, $\nu_-$, separated by the Zeeman splitting.

Experimentally, however, it is found that at low fields the Zeeman components lock together to produce a single oscillation. In intermediate fields what is effectively a "Zeeman dip" appears on the line profile, inhibiting the previous oscillation, but Zeeman beats are only found to occur when the magnetic field exceeds a certain critical value, $B_{cr}$.

It is therefore necessary to have an intuitive picture of the mechanisms responsible for locking in quantum oscillators if the

conditions for the Zeeman beat mode are to be determined.

Frequency locking in multi-mode lasers was first observed by Javan (quoted in Lamb 1964). The necessary modifications to single-frequency laser theory are given in Lamb's paper, which shows that locking in low power multi-mode gas lasers results from partial saturation of the output and subsequent generation of "combination tones". Later work (Stenholm and Lamb 1969) showed that this pertubation approach is reasonable for low power gas lasers, although the Lamb theory requires the knowledge of a number of parameters of the atomic system if the relative phases of individual lasing modes are to be calculated.

A less complicated approach relies on the radiation field in the cavity adjusting itself until the maximum possible cavity field amplitude (equivalent to a $\pi$-pulse for molecules which leave the cavity in an absorptive state) is obtained. However, even though ammonia masers oscillate at levels sufficient to produce at least a $\pi$-pulse excitation of the beam as a whole (Lainé and Bardo 1970), this "maximum emission" principle (Tang and Statz 1967) cannot predict the precise point at which the system will make a transition from one polarization state to another, although it will assist in the physical interpretation of this transition. The critical field value, $B_{cr}$, can be found in principle, at least, if simultaneous solutions are obtained to sets of the molecular oscillator equations for the Zeeman transitions.

The ammonia beam maser used in these experiments is shown in figure 2.3. It uses a combination of differential pumping and cryogenic cooling to produce a large radiation field in the first resonator (length 124 mm, Q~9000). After leaving the high Q resonator the molecular beam enters a second cavity with a lower Q, which is used for experiments on state populations and for

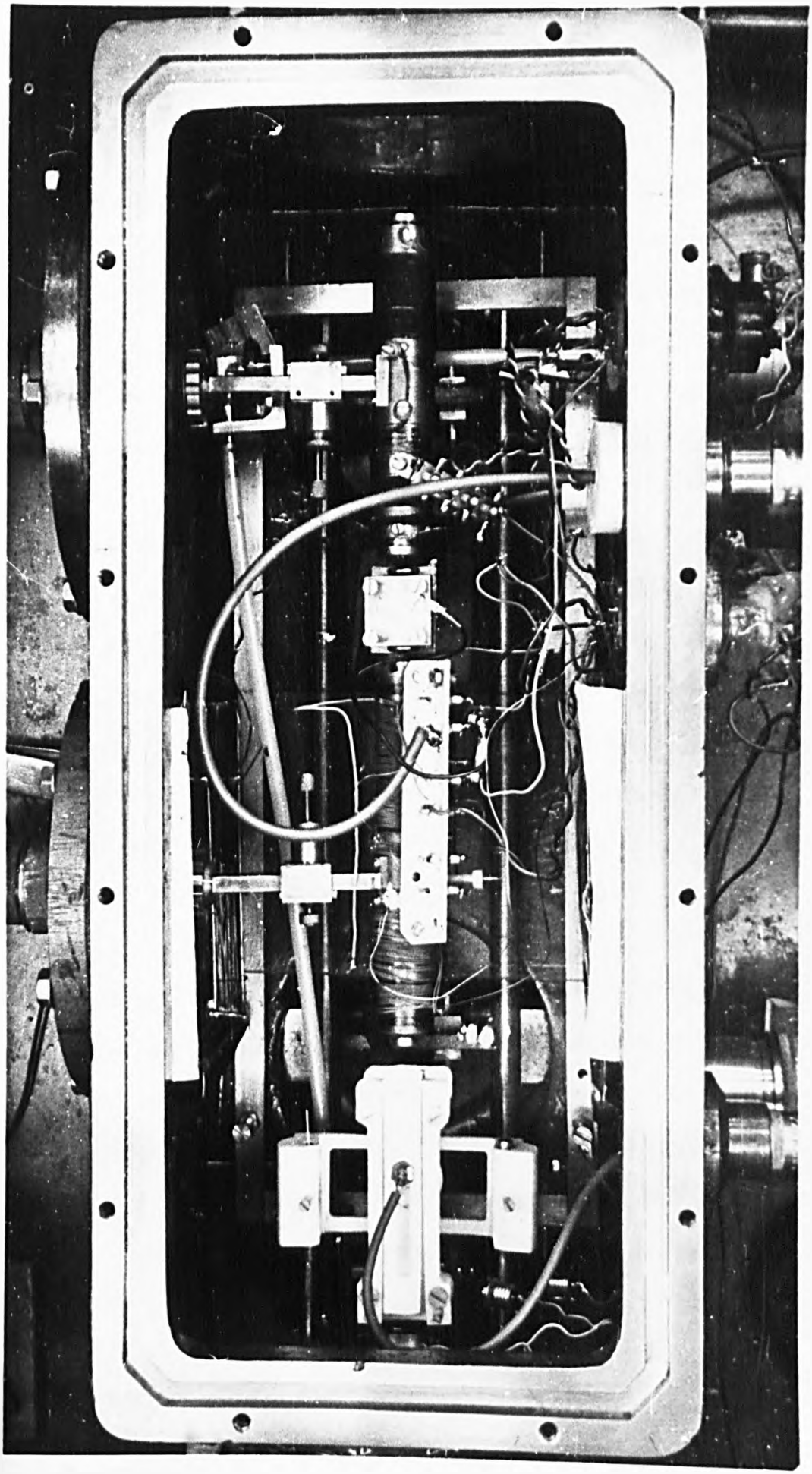

FIGURE 2.3. THE MASER.

polarization studies (Section 2.5.). Both cavities operate in the $E_{010}$ mode, in which the microwave electric field is parallel to the axis of the resonator. The external static magnetic field must therefore be directed perpendicularly to the axis of the first cavity to allow the $\Delta M = \pm 1$ transitions required for Zeeman maser operation. This field is provided by a pair of square coils, 150 mm on a side, mounted inside the vacuum system, and arranged symmetrically about the axis of the first cavity in a near-Helmholtz configuration. The same coils were also used for the g-factor measurements in low fields.

The microwave bridge used for detection of maser oscillation is shown in figure 2.4. This bridge (Hermann and Bonanomi 1956) is capable of displaying both slow variations in oscillation amplitude, using an unswept (i.e. constant frequency) local oscillator, and rapid variations in oscillation amplitude using a swept frequency local oscillator. Variations in oscillation frequency can be observed in principle with this bridge if a very stable oscillator (e.g. another ammonia maser) is used as a reference signal.

For most of the experiments with the Zeeman maser the local oscillator klystron (Elliot-Lytton type 12RK3) was used in an unswept mode, and was detuned by 30 MHz from the maser frequency. The two sigmals were mixed together in a type 1N26C crystal detector and the resulting 30 MHz beat frequency signal was amplified by an intermediate frequency amplifier with a bandwidth of 3 MHz at this centre frequency. Changes in oscillation amplitude produced corresponding changes in the D.C. level of the detected output of the amplifier.

Measurements of the beat mode characteristics at the edge of lock were achieved by using a triangular waveform generator of standard design to vary the magnetic field and to sweep the

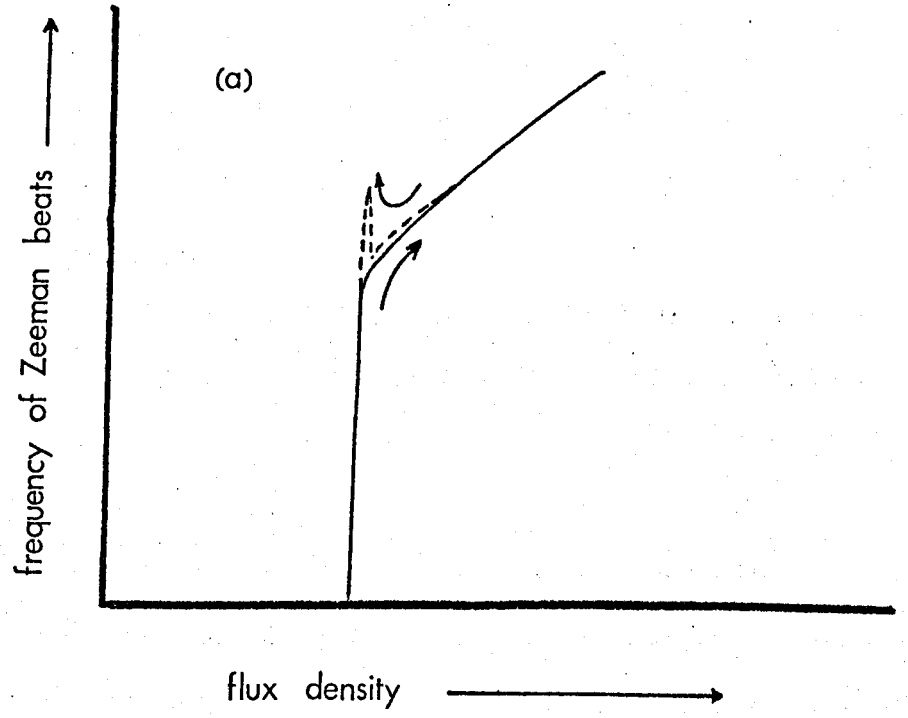


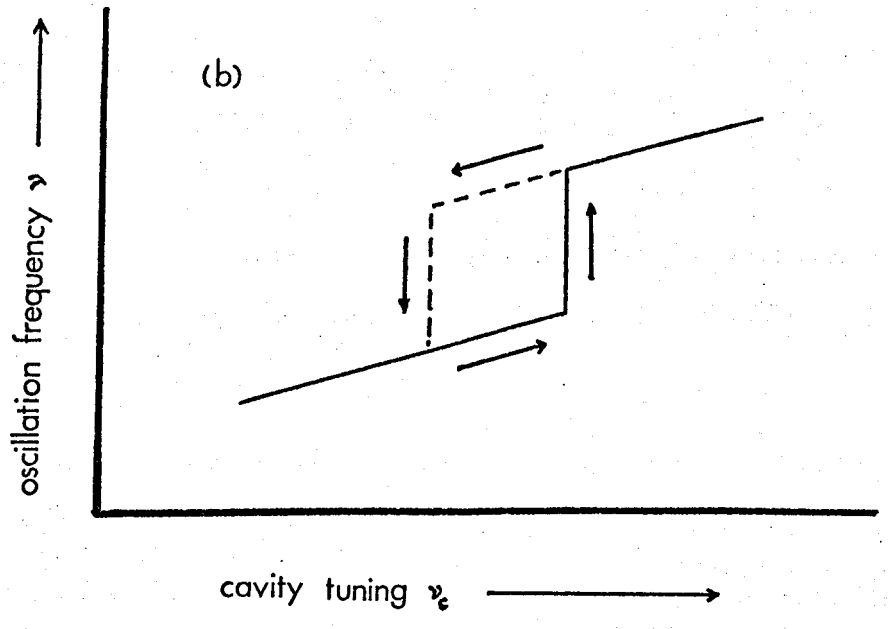


FIGURE 2.5. Sketch of form of hysteresis effects:

(a) in a Zeeman maser with an $E_{010}$ mode cavity.

(b) for a maser using an $E_{01}$ mode cavity (After Becker 1966).

X-channel of an Advance model HR-96 pen recorder. Associated variations in beat frequency near the locking region were plotted simultaneously by connecting the output of a British Physical Laboratories model FM406-C-Mk.II frequency meter/converter to the Y-channel of the pen recorder.

The minimum time required to sweep through the Zeeman maser beat mode was determined by the ratio of the response time of the pen recorder ($< 0.5$ seconds for f.s.d.) to the slewing rate of its input signal following a transition from the synchronous mode to the beat mode of operation. Sweep times of about 20 seconds were found to be quite satisfactory in this respect, but most measurements were taken with a 60 second sweep to reduce any possible instrumental error to a minimum. This was taken as the upper limit to sweep time, because over longer periods slight variations in parameters such as nozzle pressure and cavity tuning made the results obtained invalid.

A typical tracing of the transition from a phase locked double oscillation to beats is shown in figure 2.5.a. for the case when the cavity is tuned to the molecular resonance frequency $\nu_o$.

It will be seen that the transition from the beat mode to the synchronous mode of operation is accompanied by a sudden jump in the beat frequency, although the reverse transition to the beat mode is monotonic in character. This hysteresis phenomenon may be taken as indicating that the two Zeeman components are strongly coupled in small magnetic fields, but become weakly coupled when the Zeeman splitting is comparable to the unperturbed spectral line width.

The degree of coupling between the two Zeeman components is determined by the maximum emission principle, since the final oscillation state must be the one which maximizes the total emission.

However, for a small range of values of magnetic field there may be little difference in output power between the synchronous mode of operation, where the final oscillation level may correspond to excitation beyond the $\pi$-pulse condition for some molecules, and the beat mode, where the oscillation signal from individual Zeeman components may correspond to the same molecules being nearer the $\pi/2$ pulse condition.

In such an inherently unstable situation the final oscillation state may well be decided by the change in the susceptibility of the maser oscillator to the influence of noise, and frequency jumps may thus occur during the transition from the "beat mode" to the competing "synchronous mode", although a transition in the opposite direction will show the hysteresis which arises from this competition.

This hysteresis effect may be compared with a result obtained when an $E_{013}$ mode resonator was used in an ammonia maser operated without a magnetic field (Becker 1966). The presence of three nodes along the axis produces a Doppler splitting of the spectral line into two components with frequency separation $\sim(nv)/(L)$, where n is the number of half-wavelengths along the cavity axis, v is the mean molecular velocity, and L is the length of the resonator. Oscillation is only possible on one or other component by tuning the cavity to one side or the other of the centre of the molecular resonance frequency $\nu_o$. Successive detuning of the resonator from low to high frequencies, and vice versa, is therefore accompanied by sudden changes in frequency as the maser jumps from oscillating on one spectral component to oscillating on the other, as in figure 2.5.b. The frequency hysteresis is explained by Becker as reflecting the limitation in amplitude of the microwave field produced by the molecules.

This limitation in the level of oscillation can produce an

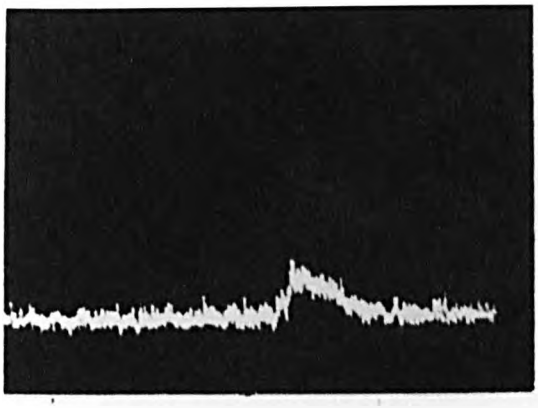

a. large detuning

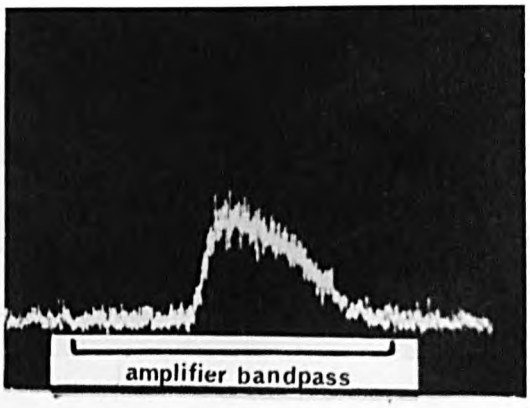


b. reduced detuning

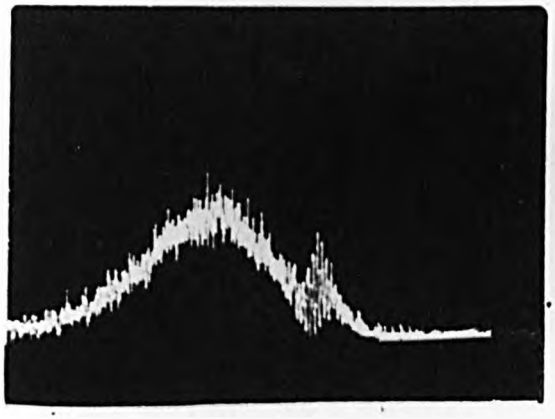

c. near resonance

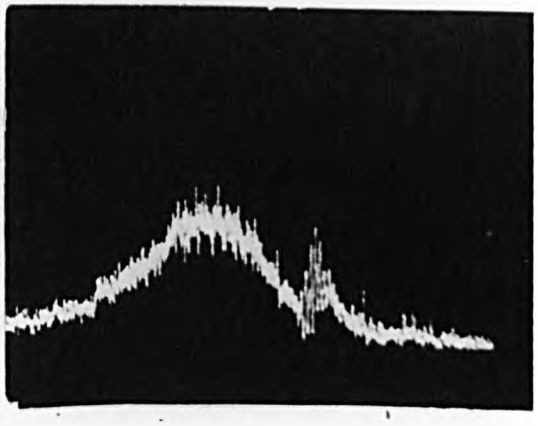

d. nearer resonance

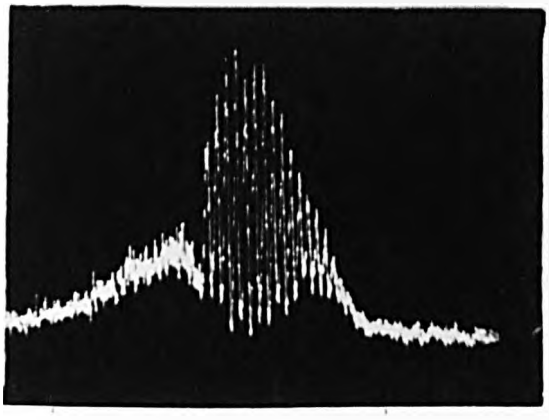

e. beats on resonance

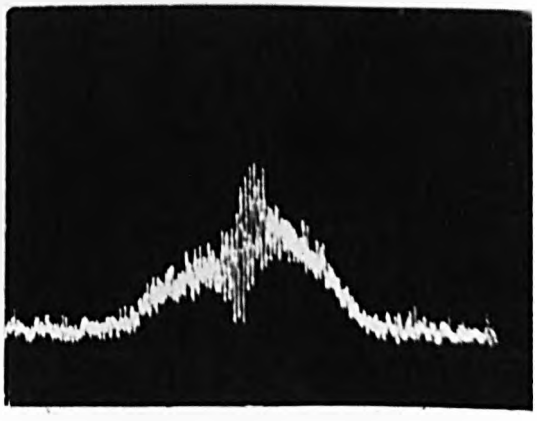

f. past resonance

FIGURE 2.6. EFFECT ON ZEEMAN MASER OF VARIOUS VALUES OF CAVITY DETUNING.

analogous effect in a Zeeman maser if the losses of each component are different. This effect, which may be seen when the maser is operated in a constant magnetic field with an $E_{010}$ mode cavity, is particularly pronounced when the resonator is tuned nearer one line than the other, because the coupling between these components is then reduced.

If the maser oscillates at a constant level at a single frequency, and the klystron power does not vary substantially over the frequency range for which a beat signal may be detected then the detected output will correspond in height to the maser oscillation level and in shape and width to the amplifier bandpass characteristic. A simultaneous double oscillation will appear as a beat signal over the whole of the bandpass.

However, if the local oscillator power is large the VSWR of the crystal detector, and hence the load imposed on the maser cavity by the microwave bridge, may vary with frequency. This may cause the threshold requirements for maser oscillation to vary sufficiently, as the local oscillator klystron is swept, for sudden quenching of a low-level oscillation (in either the single or the double oscillation mode) to occur, and since the maser oscillation is monitored in the time domain, the detected signal will occupy only a portion of the bandpass characteristic, as shown in figures 2.6.a and 2.6.b.

When the cavity is nearly on tune, as in figures 2.6.c. and 2.6.d., this synchronous mode gives way to the Zeeman beat mode for a time, but even when the cavity is tuned to the unperturbed oscillation frequency the frequency-dependent losses are such that Zeeman beats still occupy only a portion of the bandpass.

Section 2.4. The Zeeman maser II - slope of the beat mode.

In preliminary experiments on the Zeeman maser the beat frequency was measured as a function of the field-coil current, and hence

magnetic field, using a frequency counter. The beat frequency was found to vary by as much as 10% over a period of 10 - 20 seconds, precluding accurate measurements of the slope of the beat mode (i.e. the dependence of beat frequency on field).

It might be thought that these fluctuations could be averaged out somewhat by taking several readings of frequency for each value of field. However, large random fluctuations in frequency are found to occur when measurements are taken over a period of minutes, and any results obtained in this manner are therefore invalid. Successive single readings in fact showed that beat frequencies could range from 2 or 3 kHz at 0.2 to 0.3 mT to 11 or 12 kHz at about 0.6 mT. Outside these field values a single oscillation signal was usually observed.

Unfortunately, it is difficult to compare these results with those obtained in previous work on the properties of a Zeeman maser (Logachev et al 1968) since very few experimental details are given in their paper. These workers limit their discussion of experimental technique to the following sentences:

"Experimentally, we observed a biharmonic mode which emerged for fields of 2 - 3 Oe, while the beat frequency was 1 - 2 kHz. For an increase of the magnetic field, the frequency increased to 10 kHz. Further increase of the field led to a decrease in the amplitude of the oscillations to zero."

No mention is made of any experimental investigations into the slope of the beat mode. It is therefore not surprising that they assumed that the slope of the beat frequency could be used to determine the magnitude of the applied magnetic field. This conclusion is definitely not borne out by experiments reported in this thesis, and it must be surmised that any measurements of beat frequency by Logachev were subject to large random errors, as would

be the case if a frequency counter were used.

As explained in Section 2.3. a frequency converter technique allows measurements to be taken in a much shorter time than is possible when using a counter, and therefore reduces the effect of random fluctuations in the beat mode parameters.

Use of this technique of frequency conversion showed that the slope of the beat mode did vary with field, but could also be varied substantially by factors such as the voltage applied to the separator.

Typical tracings of such a variation in slope with separator voltage are shown in figure 2.7. The pressure of gas behind the nozzle was constantly monitored using a Pirani gauge, and maintained within about 5% of its initial value during the course of these measurements. This precaution was necessary because a change in gas pressure was found to have a similar effect to a change in separator voltage.

It should be noted when referring to figure 2.7. that these results, which were obtained in an identical manner to those of Section 2.3., have been re-drawn slightly for clarity, omitting the hysteresis effect which occurs at the edge of lock. It may be seen that both the slope and extent of the beat mode are noticeably greater than when large separator voltages are applied, i.e. when the maser is well above oscillation threshold. This effect is also seen in tracings obtained by varying the gas pressure and keeping the separator voltage constant.

Although the separator voltage and nozzle pressure are major factors in determining the slope of the beat mode , it is also of interest to note that the tuning of the resonator relative to the peak of the unsplit spectral line is of importance. Small variations in the temperature of the resonator may change the beat

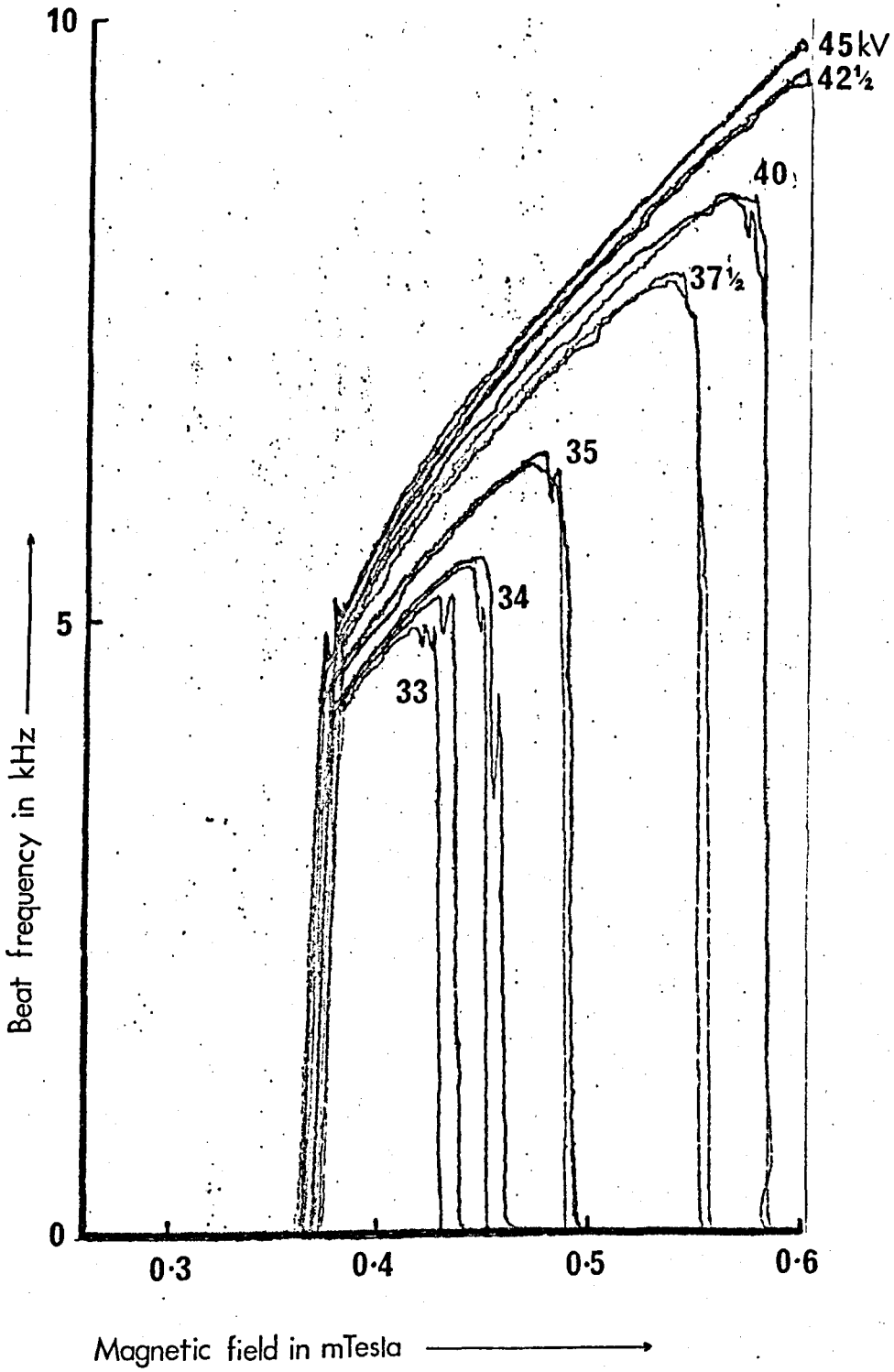


FIGURE 2.7. Variation in slope of beat mode with separator voltage.

frequency by 10% or more, even if other parameters are constant.

In order to interpret these results a satisfactory model of a Zeeman maser must be found. In previous work (Logachev et al 1968) a model of a molecule with $J = \frac{1}{2}$ was used, but such a model can only explain the existence of a beat mode, and is therefore unsatisfactory. This is confirmed later (Section 2.5.) when experiments on the properties of the beam emerging from the Zeeman maser are described.

Nevertheless, it is instructive to consider how the $J = \frac{1}{2}$ model leads to the (erroneous) conclusion that the slope of the beat mode enables the value of the magnetic field to be calculated.

In this model the selection rules $\Delta J = 0, \Delta M = \pm 1$ apply, and there are thus (neglecting frequency pulling effects initially) two possible oscillation frequencies $\nu_+$ and $\nu_-$ which can occur when the spectral line is split, as shown in figure 2.8.

The molecular oscillator, or self-consistent field equations of chapter one must therefore be modified slightly to take account of this. In the unperturbed case the following form of these equations may be used:

$$\ddot{P} + \frac{2\dot{P}}{T} + (\omega_o^2 + T^{-2})P = -2NE\frac{\omega_o}{\hbar}\left|\mu_{12}\right|^2$$

$$\ddot{E} + 4\pi\ddot{P} + \frac{\omega_c}{Q_c}\dot{E} + \omega_c^2 E = 0 \qquad 2.6.$$

$$\dot{N} + \frac{1}{T}(N - N^o) = \frac{2}{\hbar\omega_o}E(\dot{P} + \frac{1}{T}P)$$

where $N^o$ and $N$ are the number of active molecules per unit volume in the absence and presence of the resonator field respectively, $\omega_o$ is the unperturbed resonance frequency (often referred to here as $\nu_o$), $\omega_c$ and $Q_c$ are the frequency and Q-factor of the resonator,

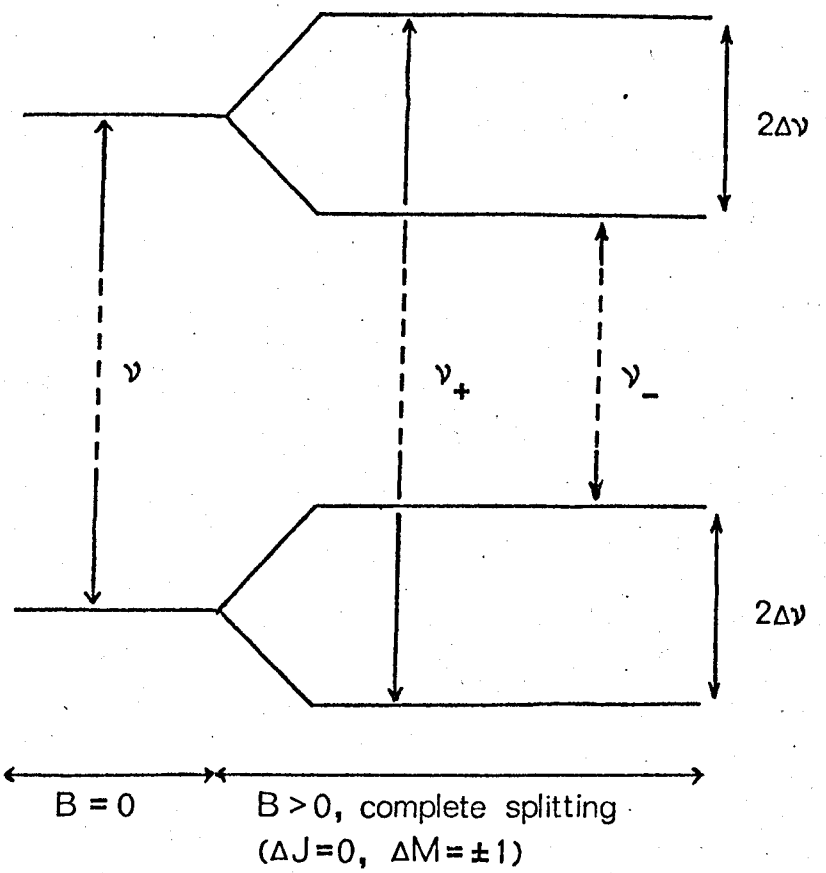


FIGURE **2.8.** The $J = \frac{1}{2}$ model of a Zeeman maser.

T is the average transit time of the molecules through the resonator and $\mu_{12}$ is the dipole matrix element for the transition.

When the line is split by a magnetic field B it would appear that the number of equations required is doubled. However, the two oscillations remain (weakly) coupled by the common radiation field, and the two oscillating polarizations of this model therefore add, reducing the total number of equations required by one:

$$\ddot{P}_{\pm} + \frac{2\dot{P}_{\pm}}{T} + (\omega_{\pm}^2 + T^{-2})P_{\pm} = -2N_{\pm}E\frac{\omega_{\pm}}{\hbar}|\mu_{12}|^2$$

$$\ddot{E} + 4\pi(\ddot{P}_{+} + \ddot{P}_{-}) + \frac{\omega_c}{Q_c}\dot{E} + \omega_c^2 E = 0 \qquad 2.7.$$

$$\dot{N}_{\pm} + \frac{1}{T}(N_{\pm} - N_{\pm}^{o}) = \frac{2}{\hbar\omega_{\pm}}E(\dot{P}_{\pm} + \frac{1}{T}P_{\pm})$$

Here $P_+$ and $P_-$ refer to the oscillating polarizations at the frequencies $\omega_+$ and $\omega_-$, where $\omega_{\pm} = \omega_o \pm 2g\mu_o B\hbar^{-1}$; $N_+$ and $N_-$ are the relative population inversions of the Zeeman sublevels ($N_+^o + N_-^o = 1$); g is the Zeeman splitting factor and $\mu_o$ is the nuclear magneton, $5.05 \times 10^{-27}$ J/T (or $Am^2$).

It is shown in textbooks of Nonlinear Mechanics (e.g. Hayashi 1964) that approximate (variational) solutions to such coupled equations can be found by first making the equations dimensionless and then restricting the oscillator parameters somewhat. Such equations can be further simplified in situations where some of the oscillator parameters fluctuate at a much faster rate than others, and this proviso will be considered in due course.

In all microwave masers two simplifying assumptions may be made immediately:

(i) the effective Q-factor of the spectral line is much greater than the Q-factor of the cavity, which is itself much greater than 1,

$$Q_m >> Q_c >> 1 \qquad 2.8.$$

(ii) any fractional change $\delta_c$ in the tuning of the cavity is also much less than 1,

$$\delta_c \simeq (\omega_c - \omega_o)/\omega_o << 1 \qquad 2.9.$$

In addition, the fractional detuning $\delta_{\pm}$ of the spectral line is small,

$$\delta_{\pm} \simeq (\omega_{\pm} - \omega_o)/\omega_o << 1 \qquad 2.10.$$

Equations 2.7. may be made dimensionless by introducing equivalent quantities for time, electric field and polarization as follows.

The dimensionless quantity representing time, t', may be obtained by combining time t and a frequency, e.g. $t' = \omega_o t$; the electric field may be eliminated by combining the pulsatance $|\mu_{12}|E/\hbar$ and the average transit time T in $x = T|\mu_{12}|E/\hbar$; the polarizations $P_{\pm}$ may be combined with the dipole matrix element $|\mu_{12}|$ to yield a dimensionless quantity $y_{\pm} = P_{\pm}|\mu_{12}|^{-1}$; finally, the line widths of the oscillation and of the cavity may be represented as $h_o = (2Q_M)^{-1} = (\omega_o T)^{-1}$ and as $h_c = \omega_c/2\omega_o Q_c$.

$$\text{Now } \frac{dP}{dt} = \frac{dP}{dt'}\frac{dt'}{dt}, \text{ thus } \dot{P} = \omega_o \frac{dP}{dt'} \text{ and } \ddot{P} = \omega_o^2 \frac{d^2P}{dt'^2} \qquad 2.11.$$

Hence $\dot{P}_{\pm} = \mu_{12}\omega_o \dot{y}_{\pm}$ and $\ddot{P}_{\pm} = \mu_{12}\omega_o^2 \ddot{y}_{\pm}$. Also, $\omega_{\pm} \simeq \omega_o(1 \pm \delta)$. Direct substitution of these quantities into the first of the equations 2.7. therefore gives the following dimensionless equation for the polarization:

$$\mu_{12}\omega_o^2 \ddot{y}_{\pm} + 2\mu_{12}h_o\omega_o^2 \dot{y}_{\pm} + \mu_{12}y_{\pm}(h_o\omega_o)^{-2} + \mu_{12}y_{\pm}\omega_o^2(1 \pm 2\delta + \delta^2) =$$

$$= -2N_{\pm}\mu_{12}x\omega_o^2 h_o \qquad 2.12.$$

To first order, this equation becomes, after a little rearrangement,

$$\ddot{y}_{\pm} + y_{\pm} = -2h_o\dot{y}_{\pm} - 2\delta_{\pm}y_{\pm} - 2h_oxN_{\pm} \qquad 2.13a.$$

Similarly, the second of equations 2.7. is equivalent to

$$(\omega_o^3 h_o \hbar/\mu_{12})\ddot{x} + 4\pi(\mu_{12}\omega_o^2[\ddot{y}_+ + \ddot{y}_-]) + 2h_c(\omega_o^3 h_o\hbar/\mu_{12})\dot{x} +$$

$$+ (\omega_c/\omega_o)^2(\omega_o^3 h_o\hbar/\mu_{12})x = 0$$

or $$2.13b.$$

$$\ddot{x} + x = -2h_c\dot{x} - 2\delta_c x - 2k(\ddot{y}_+ + \ddot{y}_-)$$

where the quantity $(2\pi\mu_{12}^2)/(\omega_o h_o \hbar)$ has been written as k for convenience, and the last of the equations 2.7. yields

$$\omega_o\dot{N}_{\pm} + h_o\omega_o(N_{\pm} - N_{\pm}^o) = (2xh_o\omega_o)/(1+\delta)\dot{y}_{\pm} + (2xh_o^2\omega_o)/(1+\delta)y_{\pm}$$

or $$\dot{N}_{\pm} = -h_oN_{\pm} + h_oN_{\pm}^o + 2xh_o\dot{y}_{\pm} \qquad 2.13c.$$

Similar systems of coupled equations are often used to describe the behaviour of two coupled mechanical or electrical oscillators (Minorsky P.265).

When the frequency difference is small the two classical oscillators will "lock" (synchronize) together, but with a larger frequency difference "beats" occur. (The correspondence between classical and quantum oscillators that is referred to here is not fortuitous, and will be discussed further in sections 2.6. and 2.7.)

The point at which such a system changes from a beat mode to a stable single frequency mode of operation can often be predicted by using the Routh-Hurwitz and the Liapunoff stability criteria (Hayashi 1964), always provided the nonlinearity is small, so that linear equations may be obtained variationally. Briefly, these stability criteria are concerned with the problem of whether or not the stored energy (or analogous quantity) increases when the system

is displaced in any direction from a given "position"; if it does increase then the previous "position" is an equilibrium point.

These criteria have been applied to the $J = \frac{1}{2}$ model of a Zeeman maser by Logachev et al, who have shown that single frequency oscillations will take place when $|\delta_{\pm}| < h_o$, i.e. when the Zeeman splitting is less than the oscillation linewidth.

However, this Zeeman splitting will produce a dip on the line profile, as explained in Section 2.3., and when this dip is large ($|\delta_{\pm}| \gtrsim h_o$) the beat mode will appear.

As previously stated, the slope of the beat mode is found to vary somewhat with field. In the $J = \frac{1}{2}$ model an equation for such a variation may be derived by separating the set of equations 2.13. into "fast" and "slow" components by the method of "stroboscopic averaging" (Hayashi P.24). This method of analysis is acceptable because some of the oscillator parameters fluctuate much more rapidly than others; the slow parameters are considered to be those concerned with the transfer of energy between the molecules and the radiation field (e.g. the decay times), and the fast parameters are those concerned with oscillation period and phase.

Thus, substituting new variables $x = X\cos(t' + \varphi_o)$, $y_{\pm} = Y_{\pm}\cos(t' + \varphi_{\pm})$ into the set of equations 2.13., where $X, Y_{\pm}$, $\varphi_o$ and $\varphi_{\pm}$ vary slowly with time, effectively separates these equations into a set of equations for fast motion and a set for slow motion,

$$-X\dot{\varphi}_o = -\delta_c X + kY_+\cos\Phi_+ + kY_-\cos\Phi_- \qquad 2.14a.$$

$$-\dot{X} = h_c X + kY_+\sin\Phi_+ + kY_-\sin\Phi_- \qquad 2.14b.$$

$$-Y_{\pm}\dot{\varphi}_{\pm} = \pm\delta Y_{\pm} - h_o X N_{\pm}\cos\Phi_{\pm} \qquad 2.14c.$$

$$-\dot{Y}_{\pm} = h_o Y_{\pm} + h_o N_{\pm} X\sin\Phi_{\pm} \qquad 2.14d.$$

$$\dot{N}_{\pm} = -h_o N_{\pm} + h_o N_{\pm}^{o} + h_o Y_{\pm} X \sin \Phi_{\pm} \qquad 2.14e.$$

where $$\varphi_o - \varphi_{\pm} = \Phi_{\pm} \qquad 2.15.$$

The behaviour of the beat mode may be found by considering the way in which the phases of the two oscillations vary. If a new quantity, $\dot{\Phi} = \dot{\varphi}_- - \dot{\varphi}_+$, is now defined, it can be seen from equation 2.14.c. that

$$\dot{\Phi} = -2\delta - h_o X[(Y_+ N_- \cos\Phi_- - Y_- N_+ \cos\Phi_+)/(Y_+ Y_-)] \qquad 2.16.$$

This may be simplfied by first considering equations involving fast fluctuations, assuming for simplicity that $\delta_c = 0$ (zero detuning of cavity).

In this case it will be seen from equation 2.13.b. that these fast variations will be stable if the right hand side of the equation has little effect on the left hand side, i.e. if

$$h_c \dot{x} = -k(\ddot{y}_+ + \ddot{y}_-) \qquad 2.17.$$

then $$\ddot{x} + x = 0 \qquad 2.18.$$

Similarly, the fluctuations in 2.13.a. will be small if

$$\ddot{y}_{\pm} + y_{\pm} = 0 \qquad 2.19.$$

$$h_c x = -k(\ddot{y}_+ + \ddot{y}_-) = k(y_+ + y_-) \qquad 2.20.$$

Differentiation of 2.18. then gives

$$\ddot{x} \ (= -x) = (k/h_c)(\dot{y}_+ + \dot{y}_-) \qquad 2.21.$$

If slow fluctuations are now considered, then equation 2.13.c. may be re-written as

$$h_o N_{\pm} = h_o N_{\pm} - 2XY_{\pm} \cos\varphi_o \sin\varphi_{\pm}(1 + \dot{\varphi}_{\pm}) \qquad 2.22.$$

assuming that $N^o_+ = N^o_-$ (equal intensity of Zeeman components at the moment the molecules enter the cavity).

Following Logachev, therefore, we may substitute equations 2.21. and 2.22. into 2.16., obtaining an equation for relative changes in phase of the beat mode,

$$\dot{\varphi} = -2\delta - 2h_o \sin\Phi[\cos\Phi + \cos(\varphi_1 + \varphi_2)]^{-1} \qquad 2.23.$$

which Logachev has integrated to give the beat frequency $\Omega$, in 2.24.,

$$\Omega = |\omega_1 - \omega_2|(h_o/\delta)(\delta^2/h_o^2 + 1)/[\delta/h_o + \tfrac{2}{\pi}\ln([\tfrac{\delta}{h_o} + 1]/[\tfrac{\delta}{h_o} - 1])]$$

The variation in beat frequency predicted by this equation is shown in figure 2.9., together with that expected in the case of zero coupling. Two typical tracings from figure 2.7. are also shown superimposed on this graph, so that an immediate comparison of the shape of the experimental and the theoretical beat mode characteristics can be made.

It is clear that little reliance can be placed on the theoretical model, especially as it does not predict any hysteresis effects, or any decrease in beat frequency in high fields. Such discrepancies may arise because the basic assumptions of the model (e.g. a constant g factor) are faulty, or it may be that the special case of zero detuning and equal populations considered in the derivation of equation 2.24. has no relevance to situations encountered in practice.

This situation may be clarified by using a second maser cavity to monitor the state of the molecular beam leaving the Zeeman maser cavity, as described in the following section, section 2.5.

Section 2.5. The Zeeman maser III - study of the emergent beam.

In this Section complementary studies of polarization, population and phase in a two cavity Zeeman maser (with both cavities tuned to $\omega_o$) are described. The results of Section 2.4. are then re-examined in the light of the effects found, allowing the necessary features of a Zeeman maser model to be outlined.

Since only the population and the polarization effects are relevant to the previous Section, these will be considered first.

The use of a second cavity, as shown in figure 2.3., permits a simultaneous study of the beat mode and of the polarization received by the molecular beam in the first resonator to be made. This is possible because the second cavity may be regarded as a passive system, coupled to the first cavity solely by the oscillating polarization signal carried by the molecular beam from the first cavity (Basov and Oraevskii 1962). If the polarization is destroyed before it reaches the second cavity (thereby eliminating the molecular "ringing" signal) by an inhomogeneous electric field between the cavities (provided by the electrode system which may be seen in the centre of figure 2.3.) then spectroscopic examination of the beam (by a technique described later) shows that the flux of lower state molecules emerging from the first cavity is amplitude modulated at the beat frequency. Similarly, direct observation in the second cavity of the polarization signal carried by the emergent beam shows that when the first cavity is operated in the beat mode, beats occur simultaneously in the second cavity.

The reason for the existence of polarization beats and population modulation lies in certain aspects of the non-linearities of quantum systems, as may be seen if the polarization of Zeeman lasers in similar situations is considered.

In zero applied magnetic field a single mode laser will operate at a frequency $\omega_o$ with an arbitrary polarization. If there were no locking then a left- and a right-handed circularly polarized mode (at frequencies $\omega_+$ and $\omega_-$, respectively, separated by the atomic Zeeman splitting) would be produced by an applied magnetic field. However, in weak fields the circularly polarized modes have equal frequencies, since frequency locking does occur, and they combine to give an elliptically polarized mode. The mode will only be linearly polarized if the circularly polarized modes have the same amplitude. The plane of polarization has a definite angle to the x-axis and may rotate from zero up to $\pm \pi/4$ with increasing field, as shown in figure 2.10. (after Tomlinson and Fork, 1967). Furthermore, the rotation depends on the laser intensity, cavity anisotropy and detuning. If the magnetic field exceeds a critical value, the linearly polarized mode changes into circularly polarized modes with different frequencies. In higher magnetic fields there may exist a further locking region, in which case the polarization will be linear (or elliptical) once more, rotating with the magnetic field from $-\pi/4$ to $+\pi/4$.

These experiments are carried out by simply analysing the laser beam with a polarizer, although no complementary experiments involving spectroscopic analysis are possible, since there is no second-cavity analogue in lasers. Similarly, the Zeeman maser does not exhibit more than one locking region, because the roles of cavity and molecular linewidths are reversed in the laser case. However, the nonlinear polarization effects observed in Zeeman lasers provide a useful basis for discussion of the Zeeman beam maser results. Thus it may reasonably be argued that the polarizations associated with each maser component will only add linearly if the maser is just above oscillation threshold, for in such a case the molecules

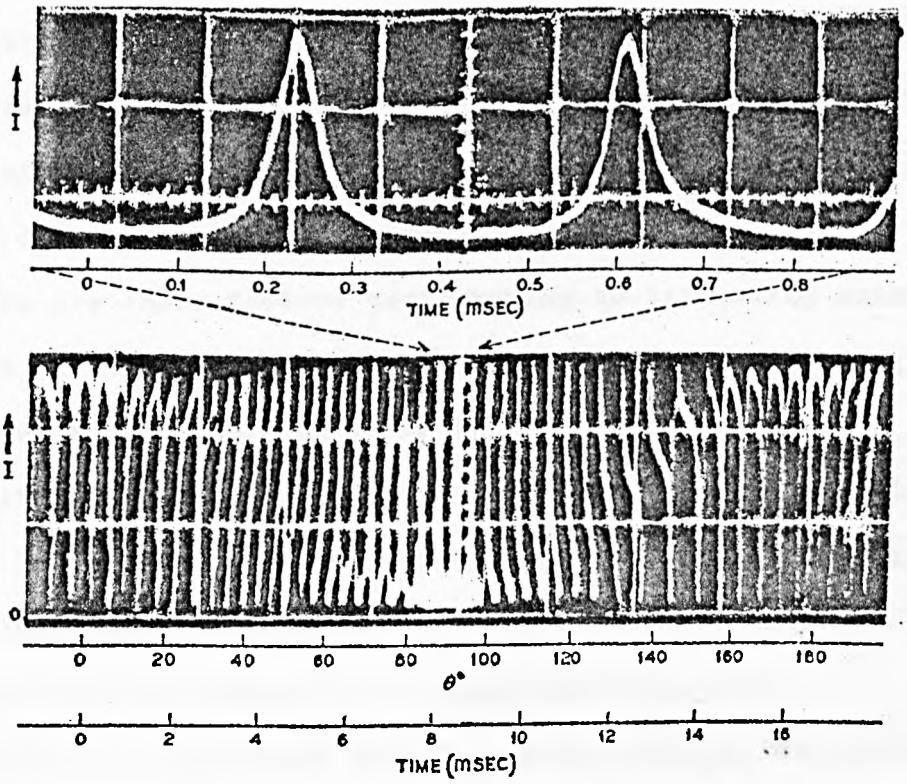


FIGURE 2.10. INTENSITY VARIATIONS IN A ZEEMAN LASER, WHEN OBSERVED THROUGH A ROTATING POLARIZER (After Tomlinson and Fork, 1967).

passing through the first cavity may be considered to experience only a small pulse (e.g. $\pi/4$ excitation) of radiation (Lainé and Bardo 1970). Well above threshold, however, the molecules will experience pulses which are much larger (e.g. $\pi$ or $3\pi/2$), and it cannot be assumed in such a case of partial saturation that the net polarization of the molecular system is equal to the sum of the polarizations associated with each component of the line. Indeed, it is common in laser theory (e.g. Lamb 1964) to take a self-consistent field approach in which terms involving third- (or higher-) order polarizations appear.

There are three factors contributing to saturation which are important in this context: spatial reorientation, scattering and the existence of travelling waves in the resonator.

Spatial reorientation effects arise when individual molecules "rotate" in stray electric or magnetic fields such as may exist between the focuser and the first cavity. Contributions to the net polarization by molecules in a particular $M_J$ state ($M_J = 0, \pm 1, \pm 2, \pm 3$) may therefore vary, causing the amplitude (which depends on the relative orientation of the molecules and the resonator field) or the oscillation frequency to change.

For example, if the spectral line of the working substance is approximately Lorentzian, and consists of two components only in the absence of a magnetic field, it can be shown that the oscillation frequency $\nu$ is given by (Nikitin and Oraevskii 1962) equation 2.25:

$$\nu = \nu_o \left\{ 1 - \frac{Q_c}{Q_m} \frac{\nu_c - \nu_o}{\nu_o} \left[ 1 + 2 \frac{\sum_{n=1}^{2} \left( \frac{I_n \delta_n^2}{1 + s_n^2} \right)}{\sum_{n=1}^{2} I_n/(1 + s_n^2)} \right] + 3 \frac{\sum_{n=1}^{2} \left( \frac{I_n \delta_n^2 (\nu_n - \nu_o)}{1 + s_n^2} \right)}{\sum_{n=1}^{2} I_n/(1 + s_n^2)} \right\}$$

with $\nu_o = (I_1 \nu_1 + I_2 \nu_2)/(I_1 + I_2)$ 2.26.

where $I_1$ and $I_2$ are the intensities of the two components, which are at frequencies $\nu_1$ and $\nu_2$ respectively; $\delta_1$ and $\delta_2$ are the (dimensionless) Zeeman splittings of these two components, and $s_1$ and $s_2$ are factors related to the relative saturation factors of the components. This equation should be compared with equation 2.1., the pulling equation for an undefined power output factor $f(\theta)$.

Thus for small fields (i.e. below the threshold of the beat mode) an ideal Lorentzian line should show a quadratic dependence of oscillation frequency on field if the magnetic tuning method is used. The quadratic dependence would be the result of spectral narrowing of a line consisting of two components of equal strength. If, as a result of spatial reorientation, one transition predominates, however, the relative saturation factors will change, and a linear dependence of oscillation frequency on magnetic field will become apparent, since the effective line centre will tend to be displaced linearly as well as quadratically in such a case.

Although the (3,3) line of ammonia is sometimes considered to consist of only two components, $F_1 = 3$ and $F_1 = 4$, the actual line shape is certainly not Lorentzian, and hence the oscillation frequency is found to depend on the pressure of the molecular beam source and the voltage of the focusing system, since each of these factors can change the number of molecules in a particular energy state. In such a case both a linear and a quadratic dependence of oscillation frequency on magnetic field are found, (as shown by Krupnov, Logachev and Skvortsov 1967), providing further proof that the populations of each $M_J$ state are usually slightly different.

Reorientation effects are well documented in the maser literature (e.g. Basov, Oraevskii et al 1963) but should not be confused with effects due to Majorana-type (non-adiabatic) transitions. The latter effects only occur in situations for which

$$\hbar(\partial\mathcal{H}/\partial t) \gg (W_1 - W_2)^2 \qquad 2.27.$$

where $W_1$ and $W_2$ are the energy levels corresponding to any two $M_J$ states, and $(\partial\mathcal{H}/\partial t)_{12}$ is the matrix element of the time derivative of the Hamiltonian describing the interaction of the molecule with the stray B or E field.

Scattering processes (between molecules, or between molecules and the resonator walls) may also be important, since polarization may be transferred from one sublevel to another in a collision. Indeed, collision processes are known to be a major source of coupling in Zeeman lasers (Tomlinson and Fork 1967).

At first sight it might be thought that the perturbing effect of one wall collision would be sufficient to destroy the polarization carried by a particular molecule. However, this may not be the case with ammonia, since in the experiments described here it has been found that comparatively large polarization signals may be detected in the second cavity even when the angle of tilt between the cavities is such as to ensure that every molecule undergoes at least one wall collision before it leaves the second cavity.

Travelling wave effects will occur if the emission of radiation by the molecules is non-uniform along the length of the cavity, as would be the case if the power level of the maser oscillation varied or if the cavity were more lossy at one end than the other. Thus, just above oscillation threshold very few of the molecules will emit in the first part of the resonator, even if the cavity losses are uniform, and the emitted power will flow in the opposite direction to the beam. Well above threshold the reverse occurs, because most of the molecules then emit in the first part of the resonator.

Although these unbalanced travelling waves only cause a very

small change in the total polarization, and hence in the oscillation frequency (Shimoda et al 1956) this change might possibly be sufficient to favour one mode of oscillation over another at the edge of the beat mode. However, perhaps the polarization change at this point may be discussed more profitably if it is thought of as reflecting changes in all the other oscillator parameters, since these determine the direction of flow of emitted power.

It will be appreciated that polarization beats cannot be considered in isolation, since, as previously mentioned, spectroscopic examination of the depolarized molecular beam emerging from the first cavity shows that the flux of lower state molecules is amplitude modulated at the Zeeman beat frequency.

This result was obtained by first ensuring that the local oscillator (the klystron) was at a frequency approximately 30 MHz away from the maser frequency, and then injecting a 30 MHz signal of suitable amplitude (about 100 mV) into the second, previously unused crystal detector of the microwave bridge, so that a sideband signal very near the maser frequency was produced by nonlinear mixing. This crystal also produced a sideband signal 60 MHz away from the maser line, but this latter signal was not detected by the tuned amplifier used to monitor the maser oscillation.

A slow sweep of the klystron frequency therefore produced a corresponding variation in the frequency of the sideband signal, and if the detection system remained fairly stable the spectral line could be examined.

Unfortunately the short-term stability of the klystron used was insufficient for a detailed examination of the behaviour of the population modulation (variation in amplitude of spectral line components) to be made over the whole of the beat mode (as one complete set of observations), but repeated retuning of the

klystron to the correct frequency showed that the modulation faithfully followed the variation in frequency of the Zeeman beats observed in the first cavity.

It will be remembered from the discussion of equation 2.25. that the populations of the various $M_J$ states are not usually equal, although the total number of molecules in the beam for a given beam flux is constant.

Since this total is constant, the occurence of amplitude modulation may now be explained.

The relative populations of the individual Zeeman components may be considered to be independent in first order, but since the supply of molecules into the cavity is the same if the source parameters are constant, the same pool of molecules must be used to sustain the oscillation. Thus, if the amplitude of one oscillation increases, the other must decrease. When this occurs, the new polarization components will then react back upon the radiation field, (and hence upon the populations), to give a further asymmetry, or nonlinearity, so that the total molecular flux will show increased modulation at the beat frequency.

The various factors (e.g. nozzle pressure and focuser voltage) affecting the beat mode are now seen to arise naturally from the presence of nonlinearities in the molecular system. The main contributions to these nonlinearities, which must be included in any successful Zeeman maser model, are listed below:

1. The asymmetrical line shape (and nonlinear g-factor),
2. The differential losses caused by the anisotropic distribution of the microwave electric field,
3. The differential losses caused by cavity detuning,
4. Spatial reorientation processes.

These will all tend to produce slight differences in the 2F+1

sublevel populations, which are important since they are responsible for the elliptical character of the oscillating polarization, for the differential saturation effects and for the non-sinusoidal appearance of the beats observed (figure 2.23. shows this point clearly).

When a successful model has been developed, second-order processes involving the transfer of polarization from one level to another (e.g. quadrupole transitions, where $\Delta M_J = \pm 2$, scattering, and travelling wave effects) should be evaluated.

It is interesting to note that not one of these four nonlinearities was considered by Logachev et al when they derived equation 2.24., the equation for the slope of the beat mode of a $J = \frac{1}{2}$ Zeeman maser, and thereby concluded (erroneously) that measurement of this slope would enable the value of the magnetic field to be calculated.

However, even with such nonlinearities a technique does exist for tuning the cavity of a Zeeman beam maser to minimize asymmetries. This technique is analogous to the phase modulation method employed for precise tuning of two-cavity ammonia beam masers (Veselago et al 1965) or nuclear maser magnetometers (Krause and Laine 1968). In such two-cavity systems the second cavity is coupled to the first solely by the polarized maser molecules. Upon entering the second cavity, therefore, the molecules will radiate at the same frequency $\nu$ as the polarizing signal in the first cavity, although the relative phase of the signals in the two cavities will depend on (a) the frequency difference between $\nu$, the frequency of the oscillating signal in the first cavity, and $\nu_0$, the centre frequency of the spectral line, as well as (b) the distance between the resonators.

If either the frequency difference $|\nu - \nu_0|$ (which is a function of the relative saturation, and hence of oscillation amplitude) or

the distance between cavities is modulated, therefore, the phase of the signals in the two cavities (relative to $\nu_o$) will also be modulated, unless $\nu = \nu_o$, when the phase modulation will vanish, showing that the maser cavity is on tune. This condition of zero phase shift may be thought of as analogous to that obtained in Ramsey-type separated field experiments (Ramsey 1956), since in both cases the molecules experience the Fourier equivalent of an oscillating field which is successively on, off, and on again. It should be noted that the variation in phase, $\Delta\psi$, or phase angle, $\Delta\varphi$, achieved by the various modulation methods (e.g. amplitude modulation, as proposed by Oraevskii and Uspenskii 1969) is usually very small. In the case of a modulation $\Delta\ell$ in the physical separation of the cavities $\Delta\psi$ will be given by the formula (Veselago et al 1965):

$$\Delta\psi = 2\pi(\nu - \nu_o)(\Delta\ell/\bar{v}) \qquad 2.28.$$

where $\bar{v}$ is the average molecular velocity, and if $\Delta\ell$ = 100 mm, $\bar{v} = 5 \times 10^2$ m/se and $(\nu - \nu_0) = 10^{-10}\,\nu_0$, then the approximate change in phase angle $\Delta\varphi$ will be about $0.01^\circ$. In the case of the Zeeman ammonia beam maser, however, a very large change in relative phase angle (e.g. $180^\circ$) may be achieved by simply altering the value of the applied magnetic field.

An equivalent equation to 2.28 for the Zeeman Maser case may be derived quite readily, as follows. If the square-law detection is assumed, then the signal $A_1$ detected from the first cavity in the beat mode will be given by:

$$A_1(t) \simeq A_o\cos([\omega_1 + \omega_2]t) + A_o\cos([\omega_1 - \omega_2]t) \qquad 2.29.$$

where $A_o = A_{\omega_1} + A_{\omega_2}$, the amplitudes of the two oscillations at frequencies $\omega_1$ and $\omega_2$, where $\omega_1 > \omega_0 > \omega_2$.

The signal arising in the second cavity after a time of flight T between the cavities is not simply given by

$$A_2 \propto \cos([\omega_1 + \omega_2][t + T]) + \cos([\omega_1 - \omega_2][t + T]) \qquad 2.30.$$

however, because, as previously discussed, the phase of each oscillation (at $\omega_1$ and at $\omega_2$) is changed by an amount $\Delta\omega_{1,2}\,T$ relative to the first cavity, where $\Delta\omega_{1,2} = \omega_{1,2} - \omega_0$ and $\omega_1 > \omega_0 > \omega_2$, assuming that the maser cavity is tuned to $\omega_0$.

Thus the detected signal from the second cavity will be given by

$$A_2(t + T) = kA_o[\cos([\omega_1 + \omega_2]t) + \cos([\omega_1 - \omega_2]t + 2\Delta\omega T) \qquad 2.32.$$

supposing $\Delta\omega_1 T \simeq \Delta\omega_2 T = \Delta\omega T$, so that the phase difference between the beat signals in the two cavities will be

$$\Delta\phi = 2\Delta\omega T \qquad 2.33.$$

Increasing the magnetic field will thus give a phase change of

$$[(\omega_1' - \omega_1) - (\omega_2' - \omega_2)]T = \Delta\phi' \qquad 2.34.$$

where $\omega_1'$ and $\omega_2'$ are the frequencies resulting from this increase in field.

In one experiment (figure 2.11.) the magnetic field was doubled in value, from ~0.4 mT to ~0.8 mT, while the beat frequency increased by approximately 5 kHz (from ~6.5 kHz to ~11.5 kHz). A relative phase change of $\pi$ was observed between the beat signal in the first cavity and the corresponding signal in the second cavity when the cavities were geometrically 30 mm apart, so that the cavity fields were perhaps 40 or 50 mm apart. While such a large change in phase is rather outside the scope of the above analysis, it is interesting to note that the mean time of flight T between the cavities is given

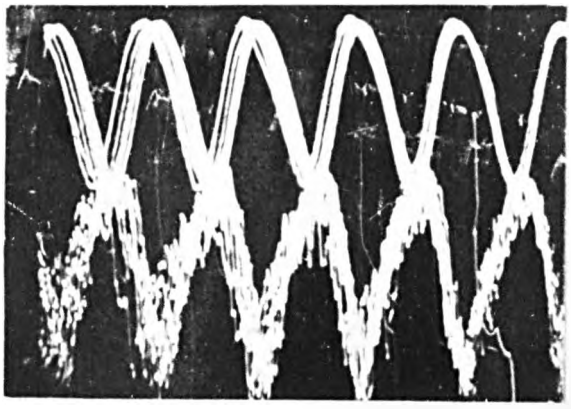

(a) 0.4 mT; beats at about $6\frac{1}{2}$ kHz.

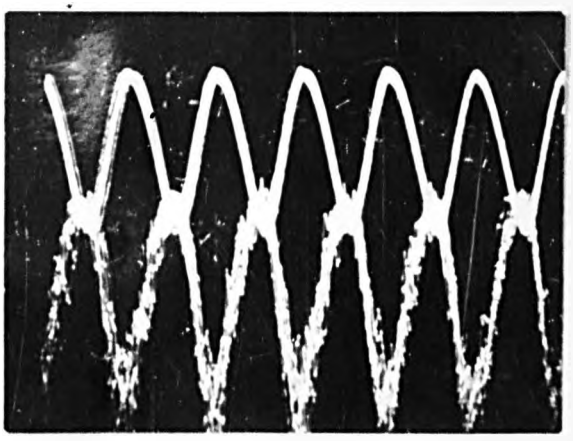

(b) 0.45 mT; lower trace is $C_2$ signal .

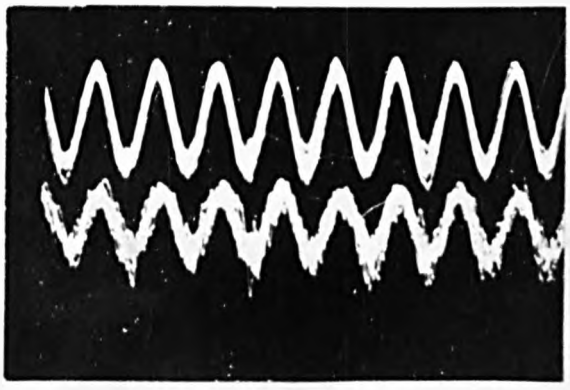

(c) 0.8 mT; beats at about $11\frac{1}{2}$ kHz.

FIGURE 2.11. Variation in relative phase of Zeeman components in a two-cavity Zeeman maser.

by 2.34. as approximately 100 $\mu$sec, in order of magnitude agreement with the value of 60 $\mu$sec obtained if a mean molecular velocity of $5 \times 10^2$ m/s is assumed.

This phase shift, which need only be small if field modulation and lock-in detection are used, will be a minimum when the changes in $\omega_1$ and $\omega_2$ are nearly symmetrical. Such a minimum will be observed when the first cavity is tuned to minimize the effects of the asymmetrical line shape and the nonlinear g-factors.

In effect, therefore, the field modulation technique provides a simple method of tuning a Zeeman maser.

Section 2.6. The van der Pol model.

In this section some aspects of the connection between classical and quantum oscillators are examined, and a short derivation of the van der Pol equation of classical physics is given.

In the semiclassical or heuristic approach taken in chapter One to derive the molecular oscillator equations, (equation 2.6.), the electromagnetic field was treated classically, but the active medium was treated quantum mechanically. To connect the treatments the dynamics of the motion of the molecules making up the active medium had to be described by equations referring to averages which were quantum mechanical and statistical in nature.

In a purely classical treatment of the motion of an atom of mass m and charge e (e.g. by linear dispersion theory) the polarization equation would be of the form

$$\ddot{P} + \frac{2}{T_2}\dot{P} + \omega^2 P = (e^2/m)E\cos\nu t \qquad 2.35.$$

The polarization of the atom thus acts as a harmonic oscillator of frequency $\nu$ driven by an electric field E through a constant coupling coefficient. This is directly analogous to the case of a simple pendulum of mass m and length a undergoing small amplitude

forced vibrations when given a charge e and placed in an electric field E cos $\nu t$.

In this case the equation for the case of undamped motion is

$$\ddot{x} + \omega^2 x = \frac{eE}{m} \cos \nu t \qquad 2.36.$$

No saturation is allowed for in either harmonic oscillator equation since the respective coupling coefficients are constant. Such equations cannot therefore be used to describe the dynamics of a self-oscillating system. A useful phenomenological model applicable to both classical and quantum oscillators may be derived by considering the role played by nonlinearity and by noise in such systems, however.

The essential features of any self-oscillating system are (i) that the oscillations, once started, will be sustained, and (ii) that some saturation mechanism exists, which limits the maximum amplitude of the oscillations.

The saturation arises from the nonlinear response of the individual oscillators which make up the medium, although it has been shown that the quantum aspects of this nonlinearity need not be introduced to explain the essential features of quantum oscillators (Borenstein and Lamb 1972). This may be seen by considering the mechanical model previously described. If such a pendulum undergoes large amplitude forced oscillations the equation of motion must be written as a non-autonomous equation:

$$\ddot{x} + a\omega^2 \sin\left(\frac{x}{a}\right) = \frac{eE}{m} \cos \nu t \qquad 2.37.$$

where $\omega$ is the small amplitude resonant frequency, or, expanding $\sin\left(\frac{x}{a}\right)$ to third order,

$$\ddot{x} + \omega^2 x - \frac{1}{6}\left(\frac{\omega}{a}\right)^2 x^3 = \frac{eE}{m} \cos \nu t \qquad 2.38.$$

The period of the resulting anharmonic pendulum oscillations is then given by the formula:

$$T(x) = T(0)[1 + \frac{x^2}{16}], \text{ with } T(0) = 2\pi\sqrt{(a/g)} \qquad 2.39.$$

Equation 2.38. is a particular case of Duffing's equation, which is generally written as:

$$\ddot{x} + ax + k\dot{x} + cx^3 = f(t) \qquad 2.40.$$

where damping is represented by the term in $\dot{x}$.

The similarity of the behaviour of an ensemble of these classical systems and an ensemble of the molecules used in a quantum oscillator is readily appreciated if a one-dimensional "beam" of classical anharmonic oscillators is sent through a resonant radiation field (a cavity tuned to $\omega$) with a velocity v, as shown in figure 2.12.

Upon entering the cavity the phase of some oscillators may be such that they lose energy, while others may gain energy. Those that gain energy from the field will go out of resonance, however, since the period of oscillations is amplitude dependent, while those that initially lose energy come closer to resonance, thus losing more energy. In the calculations of Borenstein and Lamb it is shown that a continuous stream of such Duffing oscillators can transfer energy <u>to</u> the cavity field under certain conditions, and the way in which the cavity field oscillations then build up is not substantially different from that obtained using a simple quantum mechanical model.

The nonlinearities of the oscillators therefore allow both the strength and the phase of the (polarization) - (driving field) interaction to vary. This nonlinear coupling is also introduced in the semiclassical approach of equation 2.6, in which the quantum

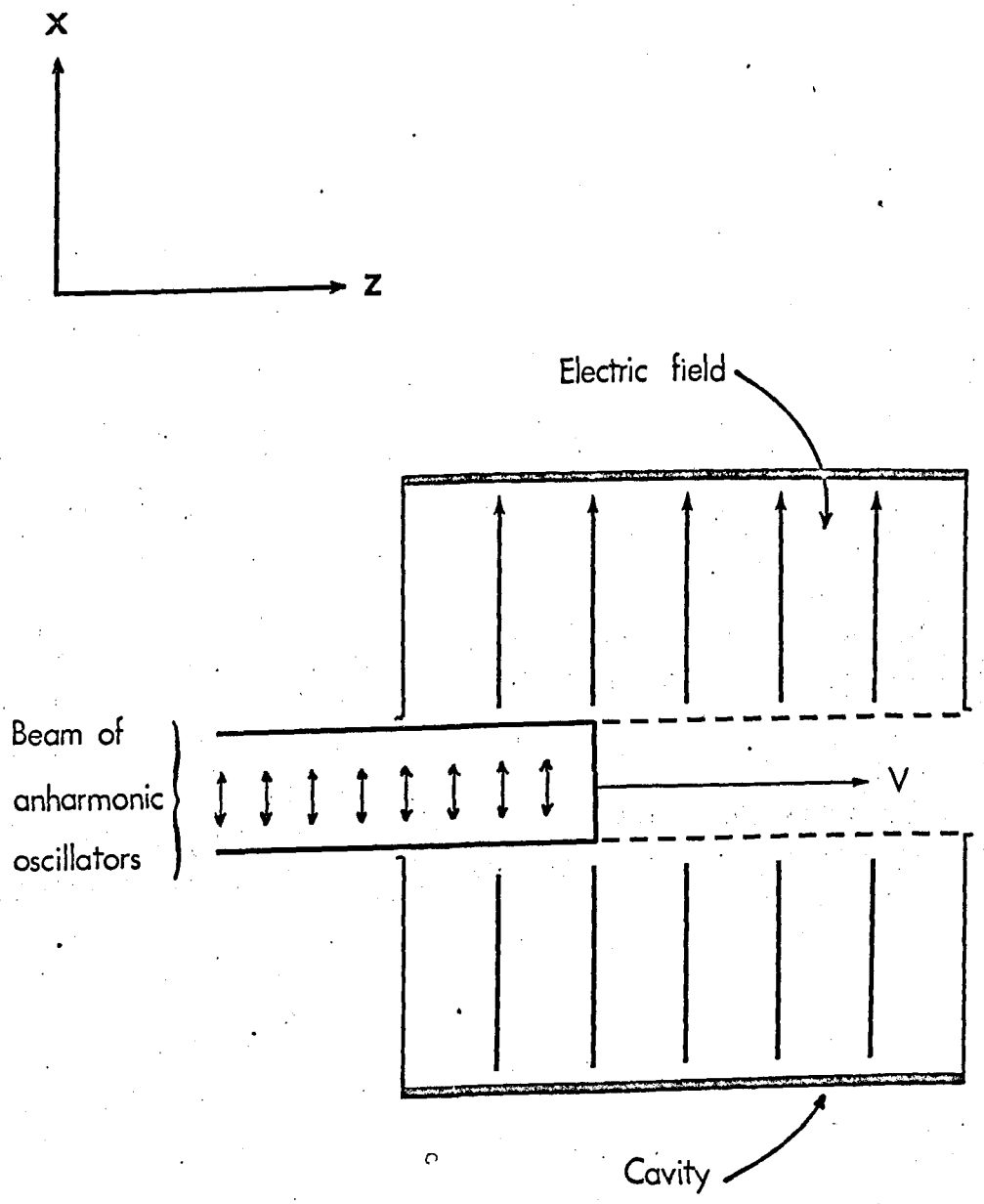


FIGURE 2.12. A classical model of a beam maser

(After Borenstein and Lamb 1972).

analogue of equation 2.35., is obtained:

$$\ddot{P} + \frac{2}{T_2}\dot{P} + \omega^2 P = -2\nu\mu_{12}^2 E(N_2 - N_1)/\hbar \qquad 2.41.$$

In this equation the classical factor $e^2/m$ has been replaced by a quantum mechanical factor.

The classical model of a quantum oscillator just described consists of many Duffing (non-autonomous) oscillators, but eventually stabilizes at a steady oscillation amplitude, and therefore becomes an autonomous system. This is because the driving force, which may be thought of as being rather noisy, will only fluctuate by a small amount at this stage, and is therefore effectively constant for most purposes. The equation of motion for such a system will then be of the form:

$$\ddot{x} + x = \mu f(\dot{x},x) \qquad 2.42.$$

where $\mu$ is a constant parameter which characterizes the degree of (variable) damping, necessary for saturation to occur.

This model of a quantum oscillator is thus of general interest, since a similar equation governs the behaviour of many triode oscillators (Lax and Louisell 1969). The coincidence is not fortuitous, however, because a formal equivalence between the triode oscillator and quantum oscillators does exist. This may not be immediately obvious, since classical systems operate in the limit of very large quantum numbers, but a brief resumé of the relevant quantum mechanical concepts will elucidate the matter.

The essential mathematical difference between classical and quantum systems is the algebra obeyed, since quantum mechanical variables do not necessarily commute, and hence the order in which they are written is important. It is possible to order these operators (in the Heisenberg picture) so that a correspondence

between a quantum system and an equivalent "classical" system is set up, allowing the stochastic problem (statistical behaviour of the ensemble) to be separated from the quantum problem. This is the procedure taken in numerous papers on the quantum mechanical theory of radiation damping (e.g. Gordon 1967). A simple picture of the damping process is thereby readily obtained, since the Heisenberg equations of motion for the operators of the system have the same form as the equations of motion for a classical damped system subject to fluctuating forces (the Langevin equations encountered in the theory of such processes as Brownian motion).

These fluctuating forces are of fundamental importance in quantum oscillators, since they represent the effect of noise on such an oscillator, and therefore determine the final oscillation state reached, as well as the phase and amplitude fluctuations of the oscillator. In the maser these forces represent thermal noise and the noise of the pumping process (e.g. the random injection of molecules into the ammonia maser cavity), but in the optical region spontaneous emission noise will predominate. In the case of a single-mode homogeneously broadened laser such considerations show that the stochastic problem of determining the behaviour of the oscillator may be approached in the following stages (Lax and Louisell 1969):

(i) quantum mechanics is used to describe the atoms in the active medium, and classical electromagnetic theory to describe the radiation field,

(ii) a random polarization term is added to represent the effect of noise,

(iii) quantized field theory is used to describe the subsequent build-up of the radiation field.

If the rotating-wave approximation of paramagnetic resonance

is used in this analysis, the result is the operator equivalent of a classical van der Pol type equation such as equation 2.43., which governs the behaviour of the oscillator shown in figure 2.13.

$$\ddot{x} - \mu(1 - x^2)\dot{x} + x = 0 \qquad 2.43.$$

The analysis of this circuit made by van der Pol is somewhat lengthy, but a short, non-rigorous derivation of this equation will suffice to show how noise and saturation processes in such a classical system are related to similar processes in quantum oscillators.

Denoting the operator $\frac{d}{dt}$ by D for convenience, and employing a notation for currents and voltages which is made clear in the figure, then the following set of equations may be written down immediately:

$$\begin{aligned} LDi &= Ri_r = (CD)^{-1} i_c \\ i_a &= i + i_r + i_c \\ v_g &= MDi - E_g \\ v_a &= E - LDi \end{aligned} \qquad 2.44.$$

To a good approximation the characteristics of triode valves are given by the formula (Terman 1946):

$$i_a = \phi(v_a + \mu v_g) \qquad 2.45.$$

where $\mu$ is the amplification factor of the valve. Figure 2.13. shows that such a characteristic has nearly the same shape as the <u>symmetric</u> part of the cubic equation, ($y = ax - bx^3$), <u>between</u> operating points such as A and B.

Obtaining equations for $i_a$ from equations 2.44. and 2.45. and equating them produces the following equation in i:

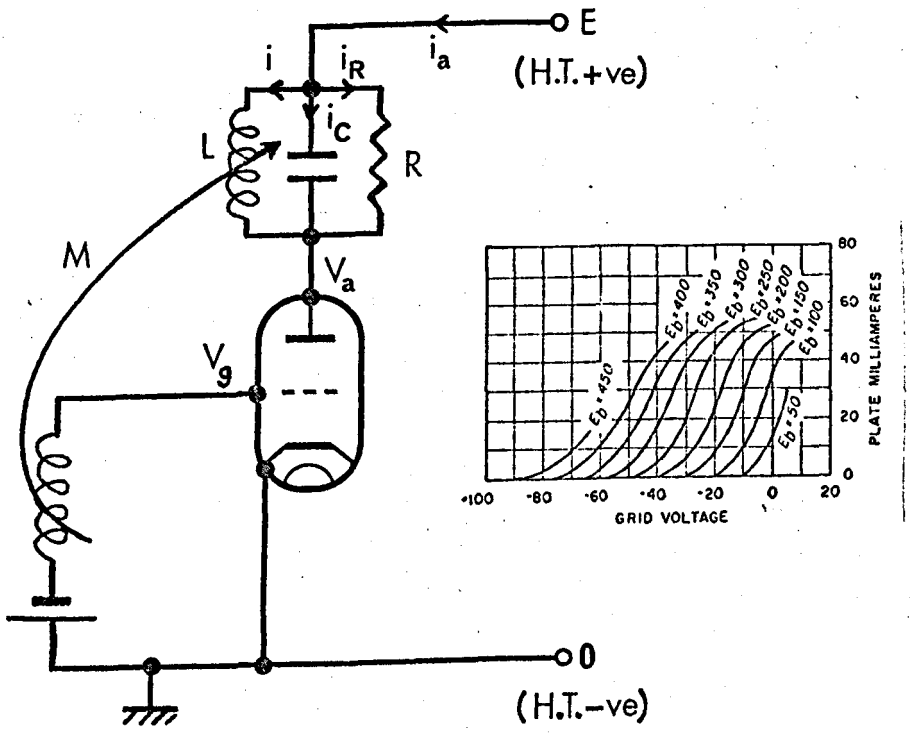


FIGURE **2.13.** A simple van der Pol oscillator

(Inset : valve characteristic, after Terman 1946).

$$(LCD^2 + \frac{L}{R}D + 1)i = \phi(E - \mu E_g + [\mu M - L]Di) \qquad 2.46.$$

Suppose that the valve is operated near the point of inflexion I, $(x_1, y_1)$, so that the characteristic may be replaced by a cubic curve whose origin has been displaced to this point. Then if the grid bias is adjusted until $E - \mu E_g = x_1$ this method gives

$$\phi(x) - y_1 = a(x - x_1) - b(x - x_1)^3 \qquad 2.47.$$

and $$\phi(x_1 + [\mu M - L]Di) = y_1 + a(\mu M - L)Di - b(\mu M - L)^3(Di)^3 \qquad 2.48.$$

or $$\phi(x_1 + [\mu M - L]Di) = y_1 + \alpha Di - \beta(Di)^3, \qquad 2.49.$$

where $\alpha = a(\mu M - L)$ and $\beta = b(\mu M - L)^3$ .

Equation 2.46. may now be written as

$$LCD^2 i + (\frac{L}{R} - \alpha) Di + \beta (Di)^3 + i = y_1 \qquad 2.50.$$

or, changing the variable to $i = y_1 + k$,

$$LC\ddot{k} + (\frac{L}{R} - \alpha)\dot{k} + \beta \dot{k}^3 + k = 0 \qquad 2.51.$$

In this equation k represents the oscillating part of the current through L, since $y_1$ is the steady current which flows under nonoscillatory conditions. This equation completely describes the way in which the circuit oscillates, but is not recognizable as being equivalent to equation 2.43. unless a change of both dependent and independent variables is introduced:

Let $k = w\sqrt{(LC\gamma/3\beta)}$ , $t = \sqrt{(LC)}\tau$ , and $\frac{L}{R} - \alpha = -\gamma$ 2.52.

Then $$\ddot{w} - \varepsilon(\dot{w} - \frac{1}{3}\dot{w}^3) + w = 0 \qquad 2.53.$$

where $\varepsilon = \gamma/\sqrt{LC}$ and differentiation has been carried out with respect to $\tau$.

Substituting $x = \dot{w}$ and differentiating once more produces equation 2.43., the van der Pol equation for the amplitude of oscillations in the tank circuit. Amplitude limiting is provided by the term which is quadratic in x, and arises from the non-linearity in the valve characteristic.

An oscillator which obeys an identical type of equation can be made by placing the tank circuit in the grid. In this case shot noise can be minimized by making the quality factor of the tank circuit very high. This allows the feedback coupling M to be very small and the parallel resistance of the tank circuit to be much larger than the noise resistance of the tube.

The resonant character of the nonlinear response of atoms and molecules makes a model of the maser slightly more complicated than that of valve oscillations. However, figure 2.14., shows the circuit of an ideal van der Pol oscillator, incorporating a "noiseless" valve with a negative slope, which represents a maser oscillator (Grivet and Blaquiere 1963). Alternatively, one may modify the scheme of figure 2.13. to include two or more simple oscillators, so that the complete system can exhibit oscillation at more than one frequency, as in lasers or Zeeman masers.

In conclusion, it may be said that any circuit model of a quantum oscillator must consider the roles played by noise and by saturation, and must also obey a van der Pol type of equation.

Section 2.7. Oscillation quenching and frequency locking in classical and quantum oscillators.

The first part of this section gives a qualitative explanation of the difference between oscillation quenching and oscillation phase-locking in coupled oscillators, while the second part is

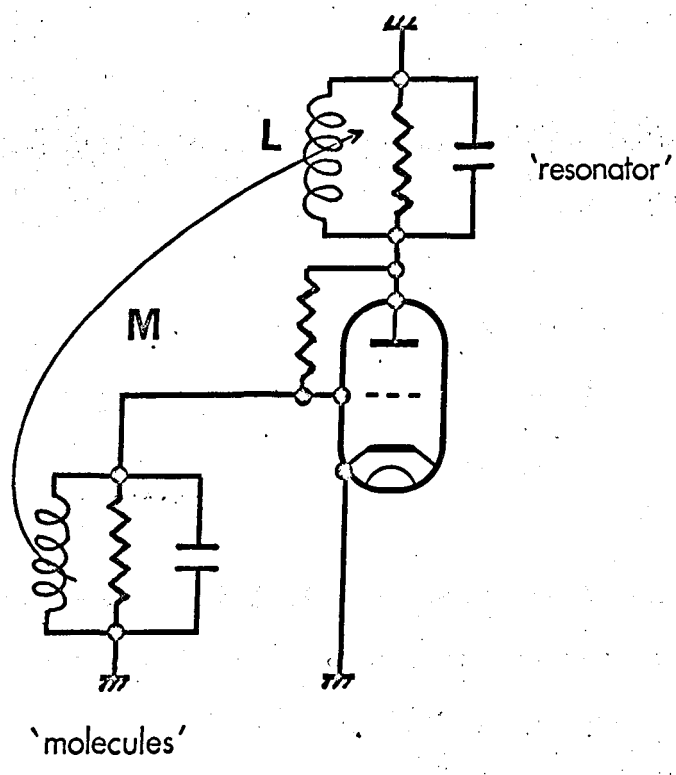


FIGURE 2.14. An electronic model of a maser

(After Grivet and Blaquière 1963).

concerned with the quantitative aspects of locking in quantum oscillators.

Elementary texts on nonlinear mechanics (e.g. Jones 1961) often deal with the concepts of "quenching" and "phase-locking" by stating that a weak periodic force applied to a linear system will produce a forced oscillation with the same period as the applied force and phase-locked to it. With a nonlinear system whose free oscillation is of the self-excited type the periodic force will reduce the amplitude of the self-excited oscillations while also producing a beat signal. Such texts then state if the periodic force is much larger it may well extinguish, or quench, the self-excited oscillations.

This interpretation of oscillation entrainment should be compared with that in a typical statement made in connection with an experiment on the injection-locking of one laser by another (Tang and Statz 1967):

"When there is an injected signal (first laser) at a frequency $\omega_o + \delta\omega$ (close to $\omega_o$) one expects that the injected signal will be amplified at the expense of the oscillator output at $\omega_o$ (second laser). Physically, when the injected signal is so high that the increase in the signal at $\omega_o + \delta\omega$ due to amplification becomes higher than the output of the free-running oscillator at $\omega_o$, one expects further that the oscillation at $\omega_o$ will be quenched and the laser output becomes phase-locked to the injected signal at $\omega_o + \delta\omega$."

Perusal of the literature on oscillation entrainment will show that the terms "quenching" and "locking" are often used as loosely as this. In fact, three modes of entrainment can be distinguished: oscillation quenching, phase-locking and asynchronous quenching (Minorsky 1947).

Quenching (suppression of the free oscillation by the forced oscillation) is a form of entrainment which can be achieved for any frequency deviation, provided that a forcing function of the required magnitude is applied. If the frequency deviation is of the order of several oscillator bandwidths and the magnitude of the forcing function is slightly smaller than that required for quenching, then the phenomenon known as asynchronous quenching (synchronization at large values of the detuning parameter) may be observed. On the other hand, if the detuning and the external forcing function are both sufficiently small there is a frequency band for which the free oscillation exists but is phase-locked by the driving frequency. It should be noted here that the natural frequency of a system can also be entrained in a kind of quasi phase-locking process whenever the driving frequency is an integral multiple (higher harmonic) or sub-multiple (sub-harmonic) of the natural frequency.

Such phenomena are observed in all fields of Science, although the differences between the various types of entrainment are not widely appreciated, perhaps because phase-locked oscillators are often operated with large injected signals and are therefore partially quenched. Thus, oscillation quenching is only seen clearly in the ammonia beam maser when a strong saturating signal is injected at, or near, the molecular resonance frequency (Lainé 1967). If this saturating signal is swept rapidly through the maser emission line, using the sideband technique of section 2.5., the beat between the injected signal and the free maser oscillation, (shown in the wings of figure 2.15.), is found to give way to a stimulated emission signal, observed under quenched oscillation conditions, whenever the sideband signal is within the linewidth of the maser oscillation. With careful adjustment of the microwave bridge pronounced wiggles may be seen, following the rapid

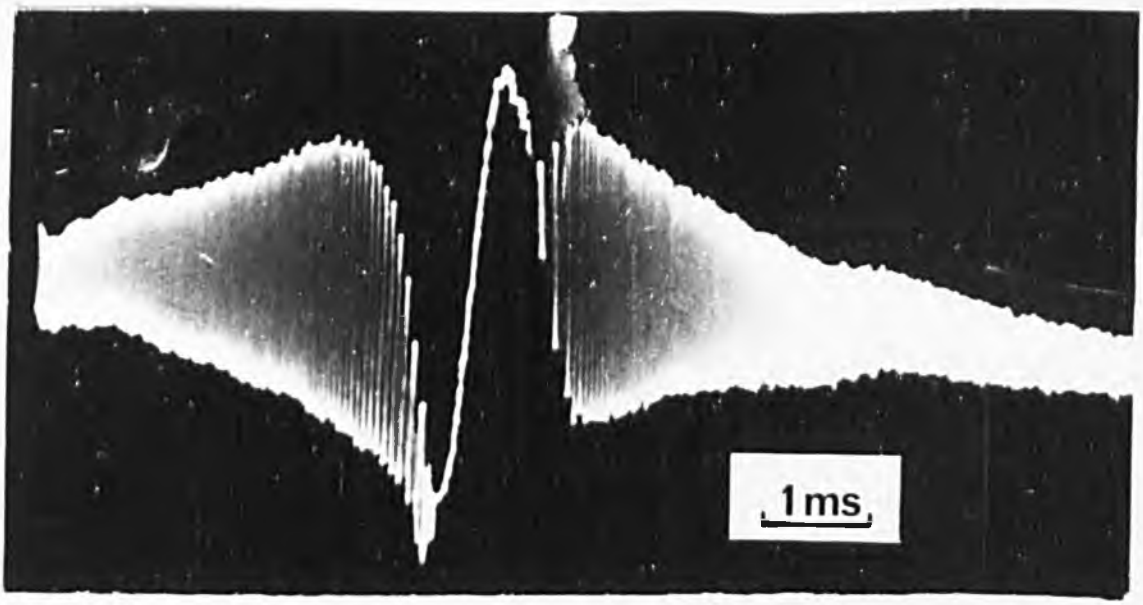


FIGURE **2.15** Oscillation quenching in an ammonia maser.

passage through the line which produces the stimulated emission signal, indicating that the free oscillation builds up from the low-level driven oscillation signal which remains after the quenching process. Increasing the level of injected signal completely suppresses the maser oscillation, so that only stimulated emission is observed from the main line, whereas a considerable decrease in the level of injected signal may conceivably give rise to phase-locking when the sideband signal is instantaneously at the frequency of the free maser oscillation. Asynchronous quenching can easily be observed with the same experimental system if a relatively narrow frequency sweep is used and the maser is operated under strong oscillation conditions. If the beat frequency is of the order of 10 kHz before and after the region of phase-locking, a series of narrow pulses are seen, as shown in figure 2.16. These oscillation spikes are of relatively large amplitude, as would be expected if they are the result of a repetitive perturbation. Further evidence for this interpretation is provided by close examination of an expanded trace. It is then seen that the spiking repetition frequency follows the beat frequency. A similar effect appears on television screens whenever one of the sweep synchronization controls is altered, causing the picture to jerk. This phenomenon is also met with in acoustics, (Minorsky states that Lord Rayleigh was the first to remark on this), where it is termed "periodic pulling", rather than asynchronous quenching. Lord Rayleigh apparently experimented with two electrically driven tuning forks of slightly different frequencies, "coupled" by an acoustic resonator, and observed irregular relative phase variations which he termed "snapping beats", because the phase changed slowly at one part of the beat cycle and quickly at the opposite part. With reduced coupling the tuning forks oscillated independently, as does

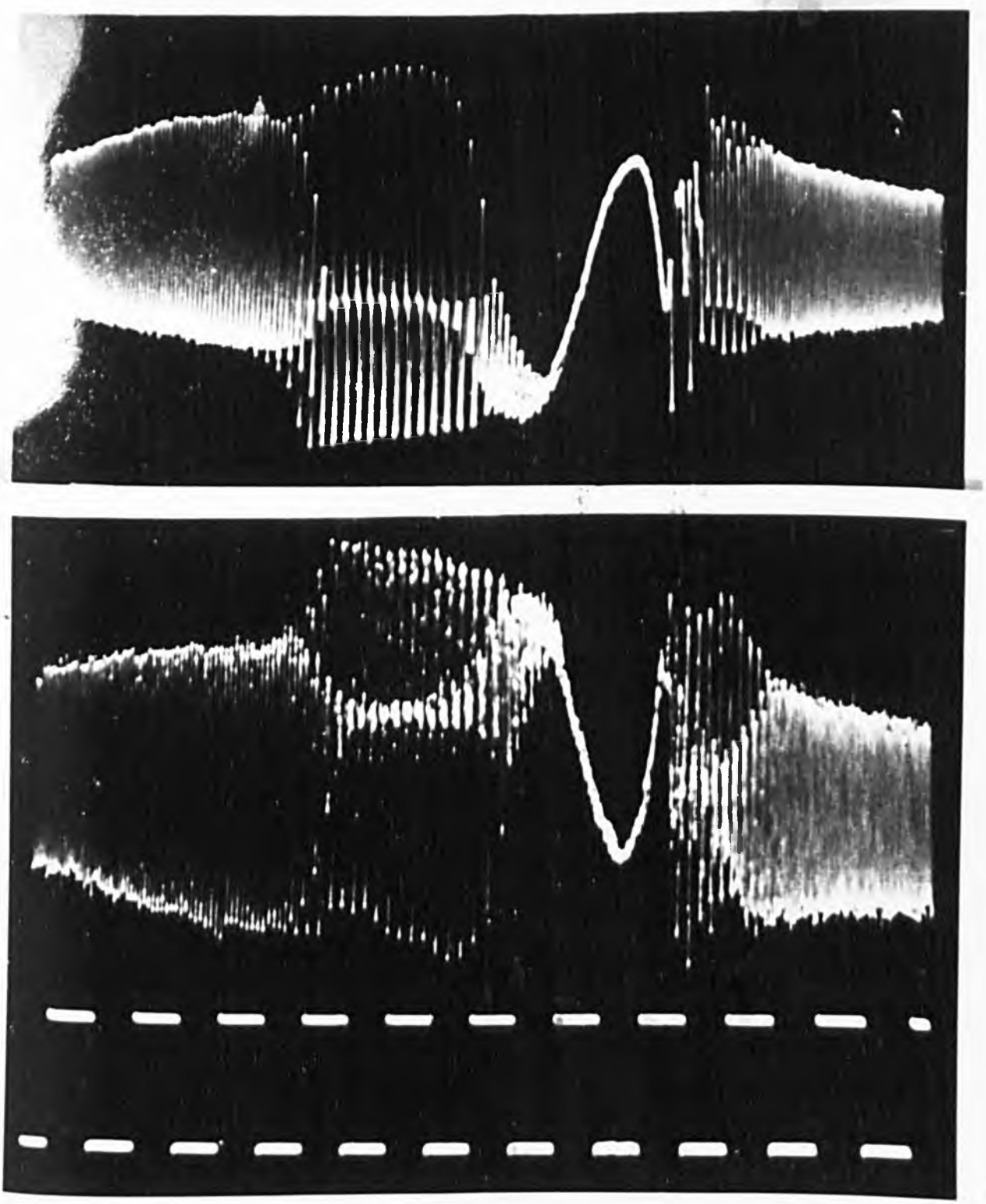

FIGURE 2.16. Asynchronous quenching effects in an ammonia maser.

the above ammonia maser at lower levels of applied signal.

The qualitative aspects of such entrainment phenomena have also been demonstrated by using a simple mechanical model - a pendulum, suspended in a viscous fluid inside a container which rotates clockwise at the uncoupled beat frequency, $\Delta\omega_o$ (Adler 1946). If the viscosity of the liquid is very large, it may be assumed to follow the rotation of the drum completely, so that if the vertical direction is taken as representing the phase of the impressed signal the position of the pendulum will indicate the relative phase of the oscillator "grid voltage". At low drum speeds the pendulum will be locked, coming to rest at a definite angle to the vertical; if disturbed slightly, the pendulum will come slowly back to this position. As the drum speed rises the vertical angle made by the pendulum will increase, until at a certain critical speed the pendulum will be vertical. "Snapping beats" (asynchronous quenching) will then ensue if the drum accelerates slightly, so that the pendulum gradually rotates, going down very quickly and up very slowly. Clearly, subsequent increases in drum speed will cause the pendulum to rotate at frequencies closer and closer to $\Delta\omega_o$.

However, this model does not show whether such frequency fluctuations mirror corresponding fluctuations in amplitude, and figure 2.16. only gives information on variations in amplitude, not frequency. An electronic analogue of the injection-locked maser was therefore constructed, as shown in figure 2.17. This system used a Z-modulation technique to display amplitude and phase fluctuations simultaneously, with the results shown in figure 2.18. The two oscillators used (Farnell Instruments type LFM2) had "SYNC" sockets which permitted direct injection of a locking signal into the Wien bridge circuit upon which these oscillators were based.

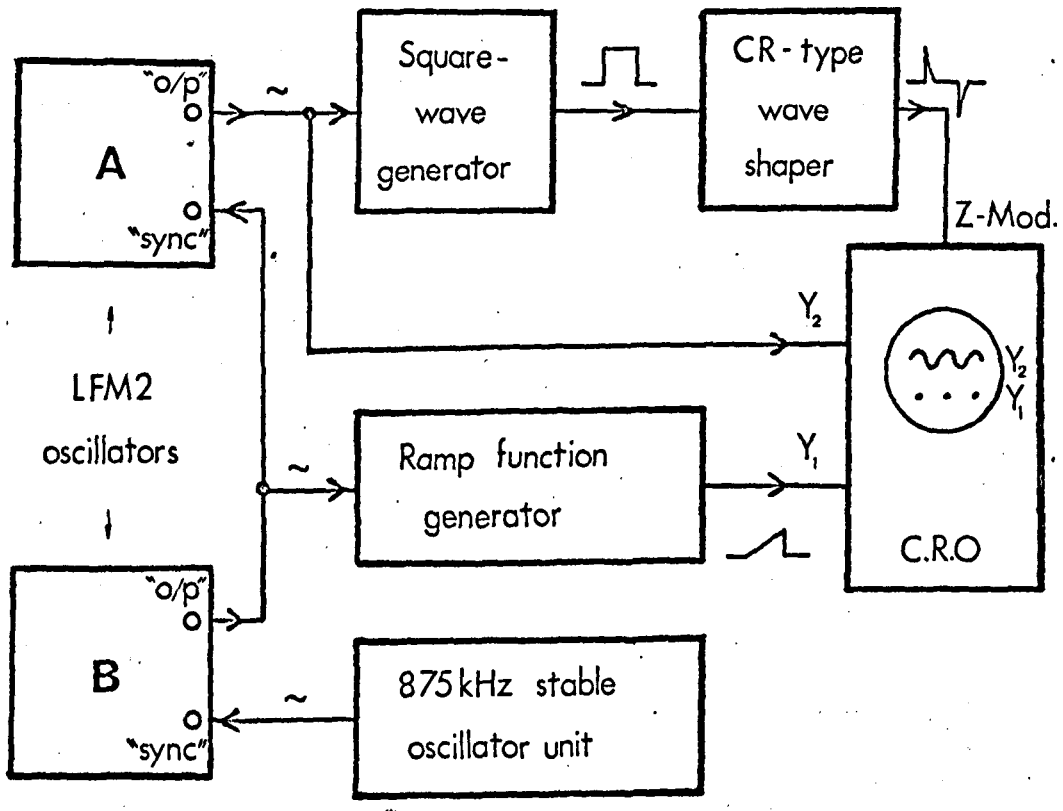


FIGURE 2.17. An electronic analogue of an injection-locked maser.

It should be noted here that in their unlocked state the Farnell oscillators were particularly prone to sudden changes in centre frequency, because the oscillators were rather temperature dependent.

Oscillator A was adjusted to a frequency (875 kHz) where it could be phase-locked to a suitably buffered signal derived from a crystal oscillator, (HCD Research, type 70), and was then used to provide the forcing signal for oscillator B. When oscillator B was set to oscillate at or very near the same nominal frequency (875 kHz) locking could be readily achieved, even with very weak injected signals ( ~10 mV). With larger frequency deviations ( ~1 kHz) the value of the forcing function required to produce complete synchronization was usually considerably greater (several Volts), reflecting the filtering effect of the Wien bridge circuit in the oscillator. Sometimes, however, the frequency jitter produced by slight fluctuations in temperature would suddenly reduce the deviation sufficiently for locking to occur with weaker injected signals. Slightly lower levels of injected signal produced the amplitude fluctuations shown in figure 2.18., which may be interpreted as reflecting the unstable nature of the transition from a phase-locked to a quenched state. The repetition rate of such fluctuations also depends to some extent on the time constant involved in the amplitude control mechanism and the "time constant" involved in the locking process. To be consistent with definitions of "time constants" for amplitude transients, locking time is defined here to be the time required for the phase between the locking signal and the oscillator being locked to reach $\frac{1}{e}$ ($\theta t$), where $\theta t$ is the phase change necessary for locking to occur. Under some conditions the phase transient will be approximately exponential in shape, so that this general definition of locking time will be similar to that for an amplitude transient. It will

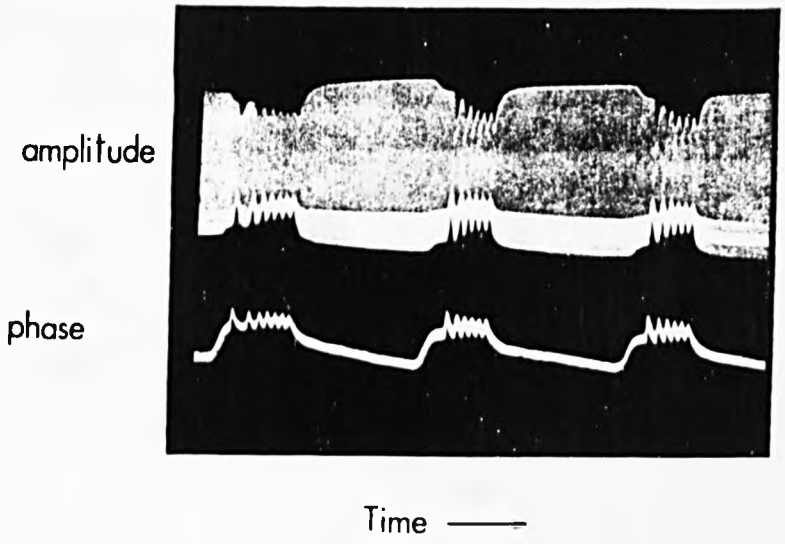


FIGURE **2.18.** Simultaneous amplitude and phase transients observed with the system of coupled oscillators shown in figure 2.17.

be seen from figure 2.18. that the amplitude fluctuations of oscillator B were always accompanied by phase fluctuations, showing that the amplitude variations mirrored corresponding changes in oscillation frequency.

These phase fluctuations were monitored by using an intensity-modulation technique (Schlesinger 1949). A ramp generator (driven by oscillator A, at 875 kHz) was used to provide a reference signal, and the brilliance of the resulting trace (viewed on an oscilloscope) was modulated by applying short (100 nsec) 60 Volt pulses to the Z-modulation socket of the oscilloscope (Telequipment type D53). These pulses were derived from the output of oscillator B by using several stages of electronic amplification, buffering and limiting. Thus, when the frequencies of the two oscillators were identical the same point on each ramp waveform appeared brighter, so that at a slow sweep rate a horizontal bright line, composed of many dots, appeared to be superimposed on the display. When the two frequencies were slightly different this line traced out the resulting variations in relative phase, producing in this way the phase transients of figure 2.18. It should perhaps be noted here that the existence of such amplitude and phase transients in coupled electronic oscillators does not appear to be well known.

A frequency multiplier unit (from ~5 MHz to the maser frequency) based upon a stable crystal oscillator (HCD Research, type 35) was constructed in an attempt to quantify the results of figure 2.16., but the derived signal was too noisy for this to be achieved. The only synchronization effect seen was similar in shape to the amplitude transient of figure 2.18., but even this effect proved impossible to reproduce.

In summary, therefore, we may say that the qualitative aspects of the three main types of oscillation entrainment (oscillation

quenching, phase-locking and asynchronous quenching) have been adequately described, although no quantitative results have been obtained by the author. However, a brief review of other work on the quantitative aspects of entrainment will suffice to show that the van der Pol model of a quantum oscillator also applies to the locking regime.

When a forcing signal of amplitude $E_1$ and frequency $\omega$ is injected into the van der Pol oscillator shown in figure 2.13., the resulting system is then described by a modified form of equation 2.43:

$$\ddot{x} - \mu(1 - x^2)\dot{x} + x = E_1 \sin\omega t \qquad 2.54.$$

It can easily be shown that this oscillator will be phase-locked to the injected signal if the following conditions holds (van der Pol 1934):

$$\frac{E_1}{E} \geqslant \frac{\sqrt{2}\, Q\, \Delta\omega_o}{\omega_o} \qquad 2.55.$$

where E is the amplitude of the signal fed back to the grid (normally equal to the total grid voltage), Q is the quality factor of the tuned circuit, and $\Delta\omega_o$ is the difference in frequency of the free oscillation (at $\omega_o$) and the injected signal (at $\omega$).

However, a similar formula has been derived for the oscillator shown in figure 2.19., (an Adler type oscillator), which incorporates a factor of 2, rather than $\sqrt{2}$, in the locking equation 2.55 (Adler 1946). This numerical factor might seem trivial at first sight, but should not be ignored, since the presence of the additional element in the feedback circuit (the combination of $C_T$ and $R_T$) could well make the equation of motion for this circuit different from that of a van der Pol oscillator. It is therefore surprising that many workers in the laser field (e.g. Tang and Statz 1967) ignored this factor and assumed that their results

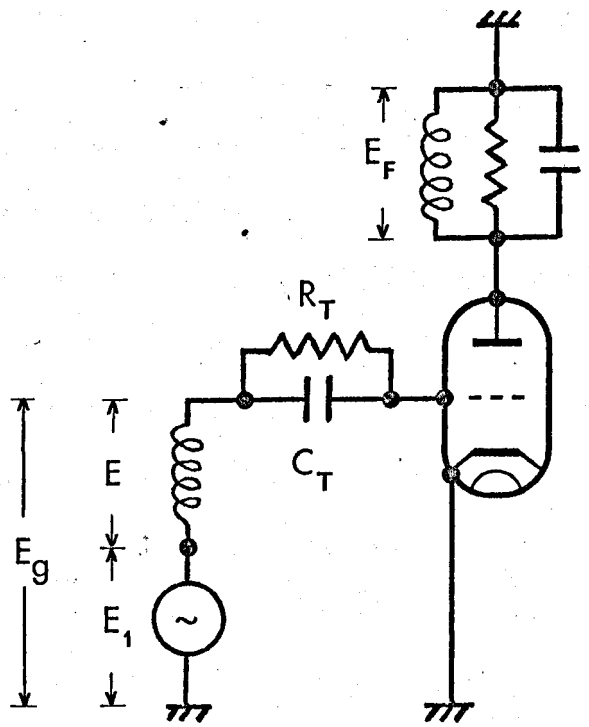


FIGURE **2.19.** A simple Adler oscillator (Adler 1946)

should be compared with the electronic Adler model. This view may still be held by some, since a recent review of laser mode locking (Allen and Jones 1971) states that the Adler analysis of the quantitative aspects of locking is directly applicable to lasers. However, consideration of early work in the maser field (Oraevskii 1963) and recent work on lasers (Wang 1972) shows that the conditions for phase-locking in quantum oscillators are in fact the same as those derived by van der Pol for electronic oscillators.

The numerical discrepancy in the Adler model of locking results from two approximations made by Adler: (i) all frequencies involved were near the centre of the "resonator" pass band, so that the phase lag (or lead) of E changed linearly with oscillation frequency, and (ii) E was independent of oscillator gain or saturation. These assumptions are not necessarily true for quantum oscillators.

In conclusion, it should be noted that in elegant analogue computer experiments simulating frequency entrainment in van der Pol oscillators (Dewan and Lashinsky 1969) curves were obtained which showed the onset of asynchronous quenching (figure 2.20). The spiky nature of these curves invites comparison with figure 2.16., which, this thesis claimed previously, is an example of asynchronous quenching under swept frequency conditions.

Such phenomena are indeed complicated, and should therefore be carefully distinguished from phenomena which only involve variations in amplitude, such as the spiking instabilities, exhibited by certain RC oscillators, shown in figure 2.21. (Oliver 1960).

Section 2.8. Loss modulation in ammonia masers.

This section reports the observation of various loss-modulation effects in ammonia masers, and relates them to corresponding processes in lasers.

The technique of loss modulation is well known to workers in

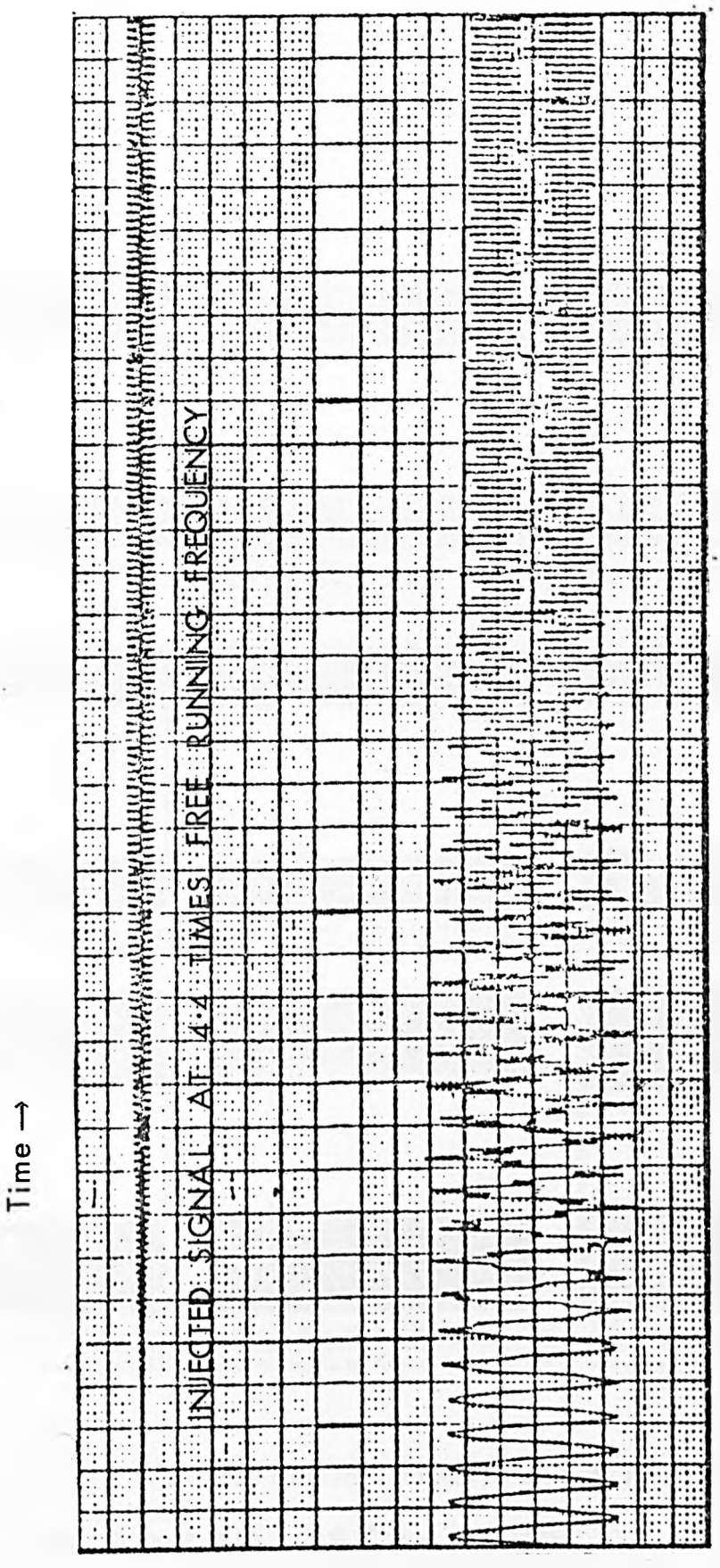


FIGURE 2.20. COMPUTER SIMULATION OF ASYNCHRONOUS QUENCHING (After Dewan and Lashinsky, 1969 ).

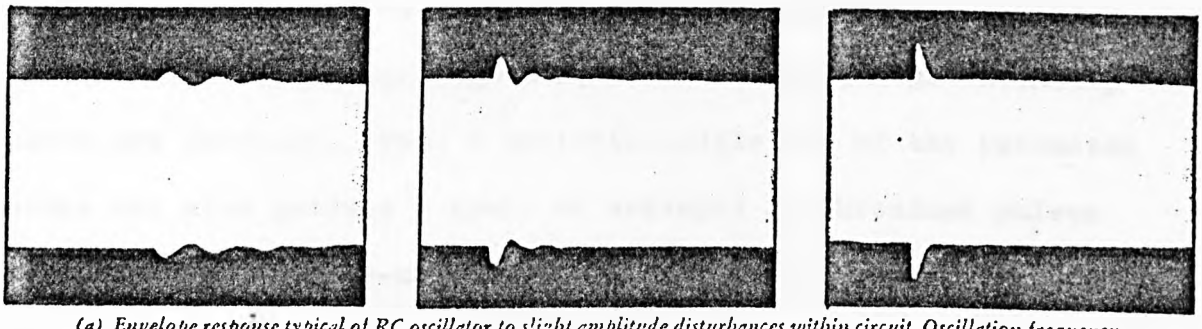

*(a) Envelope response typical of RC oscillator to slight amplitude disturbances within circuit. Oscillation frequency is 100 cps (left), 1 kc (middle), and 10 kc (right). Sweep times are 200, 100, and 50 millisec/cm, respectively. Oscillator distortion is 66 db below oscillation level.*

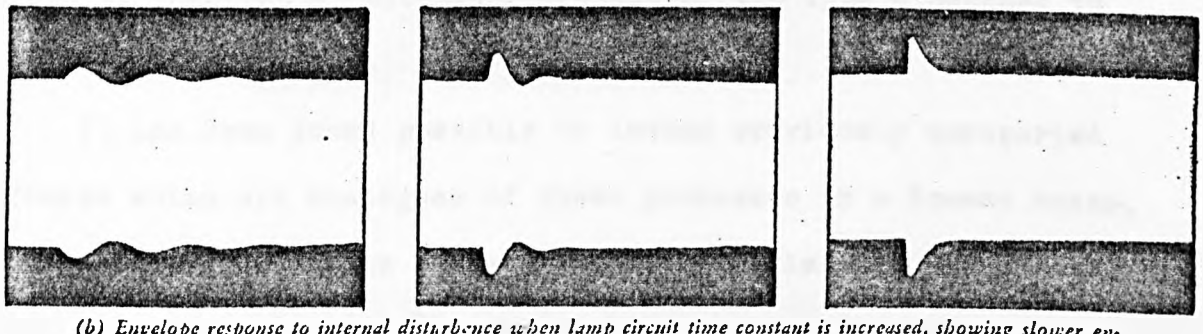

*(b) Envelope response to internal disturbance when lamp circuit time constant is increased, showing slower envelope transients. Distortion, sweep times, and oscillator frequencies are same as in (a).*

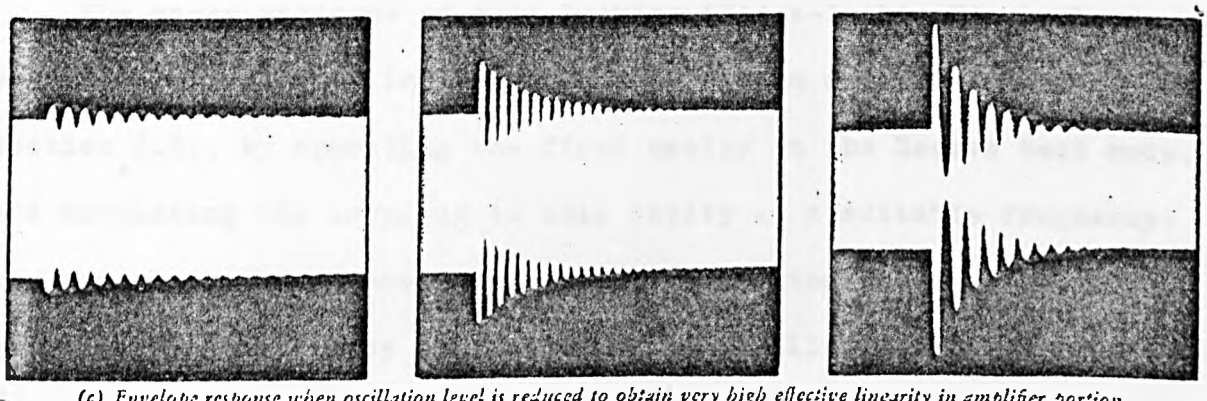

*(c) Envelope response when oscillation level is reduced to obtain very high effective linearity in amplifier portion of circuit. Distortion is about 90 db below oscillation level. Sweep times are 1 sec/cm (left), 500 millisec/cm (middle), and 100 millisec/cm (right). Oscillator frequencies are same as in (a).*

FIGURE 2.21. AMPLITUDE FLUCTUATIONS IN RC LAMP - CONTROLLED OSCILLATORS (After Oliver, 1960).

the laser field, who commonly use it to produce ultrashort pulses from multimode laser oscillators (Allen and Jones 1971). In such work the modulator, which may be a Kerr cell or an ultrasonic diffraction grating, is driven at a frequency corresponding to the axial mode spacing. The sidebands produced then lock the phases of the oscillating modes together, so that short, high intensity pulses are produced. Such a periodic modulation of the resonator losses can also produce a train of undamped synchronized pulses ("spikes") in a single-mode laser (De Maria et al 1963), although this situation should be distinguished from the mode-locked case, since it involves a "settling" process of the type discussed in the following chapter.

It has been found possible to induce previously unreported effects which are analogues of these processes in a Zeeman maser, and to generate a train of large-amplitude pulses in the same maser when it was operated without an applied magnetic field.

The maser analogue of mode-locking ("line-locking") may be obtained very readily in the two cavity system described in section 2.5., by operating the first cavity in the Zeeman beat mode, and modulating the coupling to this cavity at a suitable frequency; the second cavity is used, as before, to monitor the oscillating polarization carried by the molecular beam, allowing the effects of this modulation to be studied. Without such modulation the Zeeman maser is free running, and the beat frequency will vary about some mean value in a random manner.

If the cavity loading is then modulated at the frequency of the prevailing Zeeman beats, or at one third of this frequency, the sidebands produced will cause the two oscillations to maintain this frequency separation, even if the strength of the applied magnetic field is varied by 5% or 10%. However, with larger changes

(a)

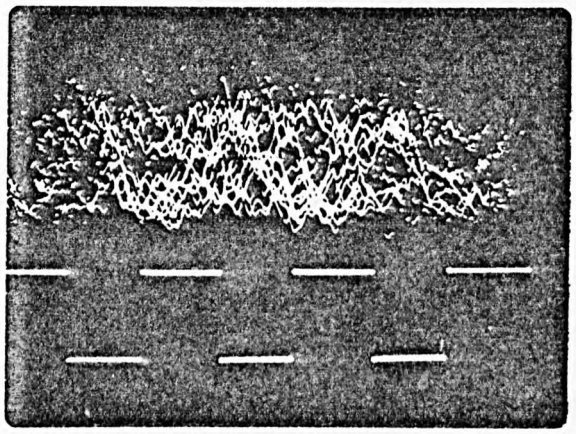

(b)

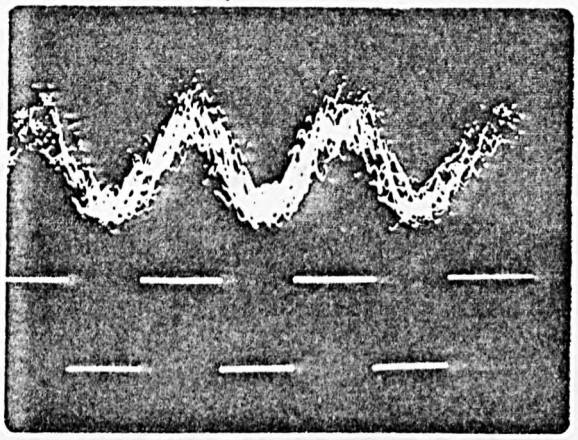

FIGURE 2.22. Zeeman maser analogue of mode-locking: (a) free-running signal (b) Zeeman beats synchronized with applied modulation signal.

in the operating parameters the beat frequency will change abruptly, indicating a transition to an "unlocked" state (figure 2.22.). This effect may therefore be thought of as the Zeeman maser analogue of mode-locking. In practice, the impedance presented to the first cavity was varied by applying specially shaped pulses, derived from a squarewave generator, to a waveguide switch (Philco-Ford type PS 6521), so that square-wave modulation of the impedance coupled to the first cavity was obtained. In the "ON" state this switching unit allowed the free passage of microwaves from the cavity to a matching unit in the waveguide system, whereas in the "OFF" state the switch acted as a 20 db attenuator. It should be noted here that a mechanical arrangement for obtaining impedance modulation in masers has been reported previously (Lainé and Smith 1966).

Amplitude modulation has also been achieved in lasers (Landman and Marantz 1969) and ammonia masers (Bardo and Lainé 1971) by means of intra-cavity Stark broadening. This "molecular Q-switching" technique, which is considered in more detail in the following chapter, may be used in the Zeeman maser to produce a "quasi line-lock" effect, as shown in figure 2.23. The spectral line is normally slightly Stark broadened in this experiment, to suppress the beat mode and leave only a single oscillation. It is thus only when the Stark voltage is removed that the double oscillation shown in the centre of this figure can take place. If the Stark voltage is repeatedly applied and then removed, the subsequent build up of the beat mode will therefore be synchronized to the trailing edge of each pulse, so that the beat mode may be thought of as "quasi line-locked" to the broadening mechanism. The results shown in figure 2.23. were obtained by applying a 50 volt 400 Hz square wave to an electrode mounted within the resonant cavity, in

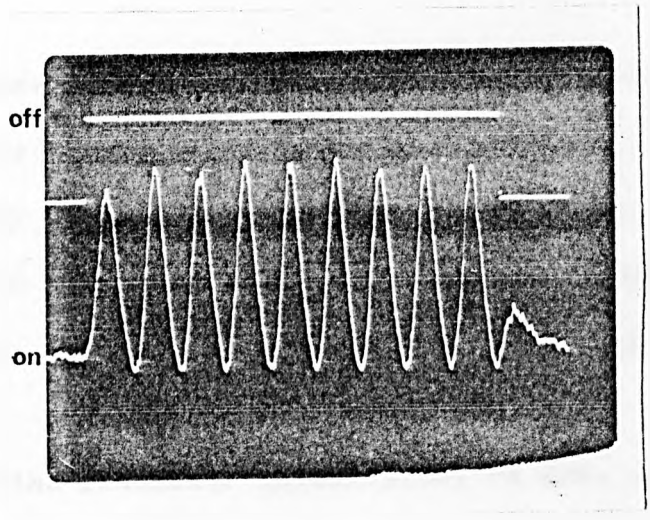


FIGURE 2.23. 'Line-locking' of Zeeman beats to a perturbation from a Stark probe.

the manner of Bardo and Lainé.

When the same maser is operated under strong oscillation conditions, and without an applied magnetic field, this modulation technique can be used to generate a train of undamped synchronized pulses, similar in appearance to those shown in figure 2.22.

Such pulsations are considered in considerably greater detail in the next chapter, but it should be noted here that the peak power output of the maser, under such pulsating conditions, can be almost a factor of two greater than the continuous wave power level.

These continuous pulsations can be obtained by applying large amplitude square waves (~200 volts) to the Stark electrode at a frequency which is the same as the characteristic frequency (~8 to 10 kHz under strong oscillation conditions) of the transients which are observed in the "settling" process preceding the steady state.

If the resonator losses could be modulated by a large amount at this frequency a similar effect would doubtless be observed, but the coupling of the waveguide switch to the cavity was insufficient to give such a range of modulation. However, the pulsations observed here by line-modulation are identical in nature to those which have been obtained in single mode loss-modulated lasers (De Maria et al 1963), confirming the theory of Morozov and Oraevskii (1966).

References

Adler R., (1946), Proc. IRE, 34, 351-7.

Allen L. and Jones D. G. C., (1971), Prog. in Optics 9, 180-234.

Bardo W. S. and Lainé D. C., (1969), Electron. Lett. 5, 688-9.

Bardo W. S. and Lainé D. C., (1971), J. Phys. D. (Applied Physics), 4, L42-44.

Barnes J. A., Allan D. W. and Wainwright A. E., (1962), IRE Trans. Instr. 1, 26-30.

Basov N. G. and Oraevskii A. N., (1962), Sov. Phys.-JETP, 15 1062-66.

Basov N. G., Oraevskii A. N. et al, (1964), Sov. Phys.-JETP, 18, 1211-7.

Becker G., (1966), Z. Angew. Phys., 20, 398-402.

Borenstein M. and Lamb Jr., W. E., (1972), Phys. Rev. A 5, 1298-1311.

De Maria A. J. et al, (1963), J. Appl. Phys. 34, 453, (1963).

Dewan E. M. and Lashinsky H., (1969) IEEE AC-14, 212-4

Gordon J. P., Zeiger H. J. and Townes C. H. (1955), Phys. Rev. 99, 1264-74.

Gordon J. P., (1967), Phys. Rev. 161, 367.

Grivet P. A. and Blaquiere A., (1963), Proc. Symp. Opt. Masers, Ed. J. Fox (New York: Polytechnic Press), 69-93.

Hayashi C., (1964), Nonlinear Oscillations in Physical Systems, McGraw Hill (publ.) New York, 1964.

Hellwig H., (1966), Z. Angew. Phys. 21, 250-5.

Herrmann J. and Bonanomi J., (1956), Helv. Phys. Acta., 29, 225-7.

Jen C. K., (1948), Phys. Rev. 74, 1396-1406.

Jones D. S. (1961), "Electrical and Mechanical Oscillations", Routledge and Kegan Paul (publ.), London.

Krupnov A. F., Logachev V. A. and Skvortsov V. A., (1967), Izv. Vyssh. Uch. Zav. Radiofiz., 10, 1689-95.

Lainé D. C. and Smith A. L. S., (1966), Proc. IEEE J. Quantum Electron 2, 399-408.

Lainé D. C., (1967), Electron. Lett, 3, 454-5.

Lainé D. C. and Bardo W., (1970), J. Phys. B. 3, L23-4.

Lamb Jr., W. E., (1964), Phys. Rev. 134A, 1429-50.

Landman A. and Marantz H., (1969), Proc. IEEE J. Quantum Electron 5, 330.

Lax M. and Louisell W. H., (1969), Phys. Rev. 185, 568.

Logachev V. A., Morozov V. N. et al, (1968), Radio Engng. Electron. Phys., 13, 1764-70.

Minorsky N., (1947), "Introduction to non-linear mechanics", J. W. Edwards Inc. (Publ.)., Ann Arbor, Mich.

Morozov V. N. and Oraeskii A. N., (1966), Soviet Radiophysics 9, 423-5.

Nikitin V. V. and Oraevskii A. N., (1962), Radio Engng. Electron, Phys., 7, 814-20.

Oliver B., (19600, Hewlett-Packard J., 11, 1-8.

Oraevskii A. N., (1964), "Molecular Generators", Nauka (publ.), Moscow.

Oraevskii A. N., and Uspenskii A. V., (1969), Radio Engng. Electron. Phys., 14, 806-8.

van der Pol B., (1934), Proc. IRE, 22, 1051-86.

Ramsey N. F., (1956), "Molecular Beams", O.U.P. (publ.)., Oxford.

Sargent III, M., Lamb Jr., W. E. and Fork R. L. (1967), Phys. Rev. 164, 436-449.

Schlesinger K., (1949), Electronics 22, 112-7.

Shimoda K., Wang T. C. and Townes C. H., (1956), Phys. Rev. 102, 1308-21.

Shimoda K., (1957), J. Phys. Soc. Japan 12, 1006-1016.

Shimoda K., (1961), J. Phys. Soc. Japan 16, 2270-2282.

Stenholm S. and Lamb Jr., W. E. (1969), Phys. Rev. 181, 618.

Stover H. L., and Steier W. H., Appl. Phys. Lett. 8, 91, (1966).

Tang C. L. and Statz H., (1967), J. Appl. Phys. 38, 2963-8.

Terman F. E., (1946), "Radio Engineering", McGraw Hill (publ.), New York.

Tomlinson W. J. and Fork R. L., (1967), Phys. Rev. 164, 466-483.

Veselago V. G., Oraevskii A. N., et al, (1965), Sov. Phys.-JETP Letters, 2, 49-50.

Wang C. C. (1972), J. Appl. Phys. 43, 158-9.

# CHAPTER THREE

## Superradiance and related effects in masers.

### Section 3.1. Introduction.

In this chapter, which is mainly concerned with various damping phenomena observed in the ammonia maser, the nature of the molecule-radiation field interaction is considered explicitly rather than implicitly as in the preceding chapter.

Much of the discussion is of general applicability, however, since many similarities exist between transient effects observed in maser and in laser oscillators. Thus, in the first section it is concluded, after a review of the literature which exists on the various pulsation effects that have been observed in quantum oscillators, that self-induced radiation-damping type instabilities ("spiking") should result in an ammonia maser if the level of excitation is high enough. Such an excitation level can perhaps be achieved by using a short, cryogenically-cooled cavity together with a supersonic ~~effuser~~ nozzle.

The following section investigates the relationship between radiation damping in quantum oscillators and the phenomenon of superradiance observed in passive systems, using the concept of "cooperation", or correlation between emitted wave-trains (Dicke 1954). A detailed description is then given of the way in which oscillations build up in an ammonia maser following various types of perturbation, and the superradiant amplitude transients observed by the author in these experiments are compared with those which occur in other systems.

The remainder of the experimental work described in this chapter is concerned with transient effects of a slightly different nature which have only been seen so far is an ammonia maser: those which appear after the oscillating maser has been partially quenched

by the presence of an inhomogeneous Stark field inside the cavity ("Stark" transients), and those which appear in the second cavity of a two-cavity maser when the oscillating polarization carried by the beam is suddenly perturbed by the application or removal of an inhomogeneous Stark field between the cavities ("polarization" transients).

The work on Stark transients is of particular interest, since the present study of the dynamic behaviour of an oscillating maser following the application of a Stark field can be compared in some ways with work which has recently been carried out on passive molecular systems using a Stark-field switching technique (Brewer and Shoemaker 1972). In such ensembles, which are pumped by a coherent source (laser), a large number of effects analogous to those observed in nuclear magnetic resonance have thereby been observed in the infrared region of the spectrum, and previously unknown phenomena such as two-photon superradiance have also been reported (Shoemaker and Brewer 1972). The present case is somewhat more complicated, because of the active nature of oscillating systems, but several models of maser Stark transients are presented and compared.

These transients may be contrasted with the other Stark-field induced effect, that of polarization transients, which may perhaps be thought of as less fundamental, in that they can be interpreted as reflecting, in the time domain, changes in the level $A(C_2)$ of the signal from the second cavity due to spatial reorientation by a time-varying (square-wave) inter-cavity field V. These changes are very similar to those previously observed by plotting $A(C_2)$ against V under steady-state conditions (Basov et al 1964).

The final section of this chapter summarizes these investigations, and gives suggestions for further work on the quantitative aspects of the molecule-radiation field interaction in a beam maser.

Section 3.2. Pulsating conditions in quantum oscillators: a critical review.

The spikes observed in quantum oscillators are very well known, but a complete explanation of such pulsation phenomena has not been forthcoming, despite considerable theoretical and experimental effort.

This section re-examines this general area of physics, and considers the conditions necessary for continuous, self-induced, spiking-type pulsations to occur in an ammonia maser.

Several types of pulsation may occur in quantum oscillators: mode-locked pulsing (DiDomenico 1964), self-pulsing (e.g. Smith 1967), and spiking (e.g. Collins et al 1960). However, only the spiking pulsations are not well understood. Both mode-locking and self-pulsing only occur in multimode lasers, whereas spiking is observed in many types of quantum oscillators, ranging from ruby microwave masers (figure 3.1a) to Q-multiplied systems, such as optically-pumped magnetometers. Mode-locking has been considered previously (section 2.8), and self-pulsing is an extension of this, in that it relates to situations in which modes may lock together without an external force, as shown in figure 3.1b.

The spiking phenomenon is particularly evident in non-Q-switched solid state lasers, which commonly produce a random train of pulses of a few hundred nanoseconds duration, each pulse profile being different. Occasionally, however, a regular pattern of damped, modulated, or even continuous pulsations is observed.

The models which have been advanced by various workers in their attempts to explain the characteristics of the spiking regime are considered below, but it should be noted that the efforts of these workers have not, as yet, met with success.

The first analysis of spiking (Statz and deMars 1960) derived phenomenological rate equations for laser oscillators: one equation

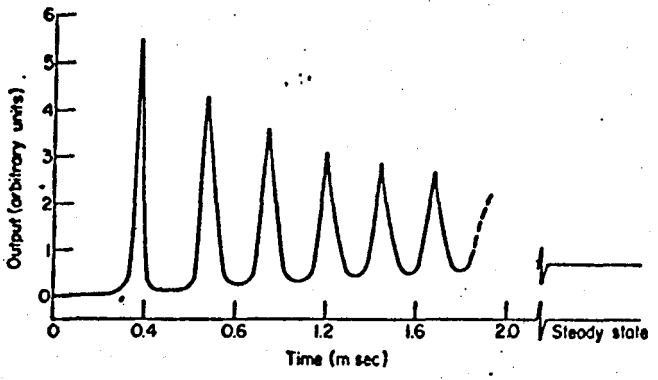


(a) *Experimentally observed energy output from ruby maser*

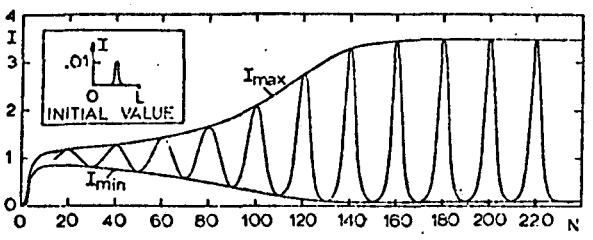


(b) The transient buildup of the intensity from a small Gaussian disturbance as a function of the time $t=NL/c$ in the instable region $\lambda=15$, $L=2\pi c/(3.2\gamma_\perp)$, $\gamma_\parallel=\frac{1}{2}\gamma_\perp$, and $\kappa=\frac{1}{10}\gamma_\perp$. The initial values are given by $E(x,0)=0.1\exp[-100(x/L-\frac{1}{2})^2]$; $P(x,0)=0$, $\sigma(x,0)=\lambda+1$. Only every 20th pulse is shown with a width 20 times the actual width.

## FIGURE 3.1. Transients in quantum oscillators:

(a) spiking pulsations in ruby (After Statz and deMars 1960);

(b) self pulsing in a multimode laser (After Risken and Nummedal 1968).

represented the time evolution of the difference in populations of the energy levels of the material, and the other (which was derived from the principle of conservation of energy) represented fluctuations in the radiation field. It will be appreciated that when a change of two (in the number of atoms or molecules in a particular energy level) occurs in the population difference equation, this is associated with the creation or annihilation of one photon. These workers concluded that regular damped spiking in pulse-excited lasers is a manifestation of either relaxation oscillations or an amplitude stabilization process with a time constant which is long in comparison with the duration of the excitation. Similar settling processes occur in van der Pol oscillators, as shown in figure 3.2. However, it has been shown (Sinnet 1962) that the rate equations do not have a stable limit cycle, (or isolated periodic solution), and thus the undamped spiking seen in solid state lasers should not occur, according to a rate-equation analysis.

In maser oscillators the cavity resonance width is broader than the molecular linewidths ($T_1^{-1}$ and $T_2^{-1}$). The rate equations in this case can be derived by using a simplified version of the so-called "reaction-field" principle (Anderson 1957), but then differ from those obtained for the laser in two respects (Tang 1963). First, the way in which the energy density of the radiation field varies with time is governed by the molecular time constant, $T_2$, rather than the cavity lifetime, $\tau_c$. Second, the driving term in the population equation, which determines the rate of decay of the excess population, is directly proportional to the energy density in the maser cavity, rather than to the product of this with the excess population, as in the laser rate equations. As a result, the population of the upper maser level could become less than that of the lower maser level in some transient approach to a steady state.

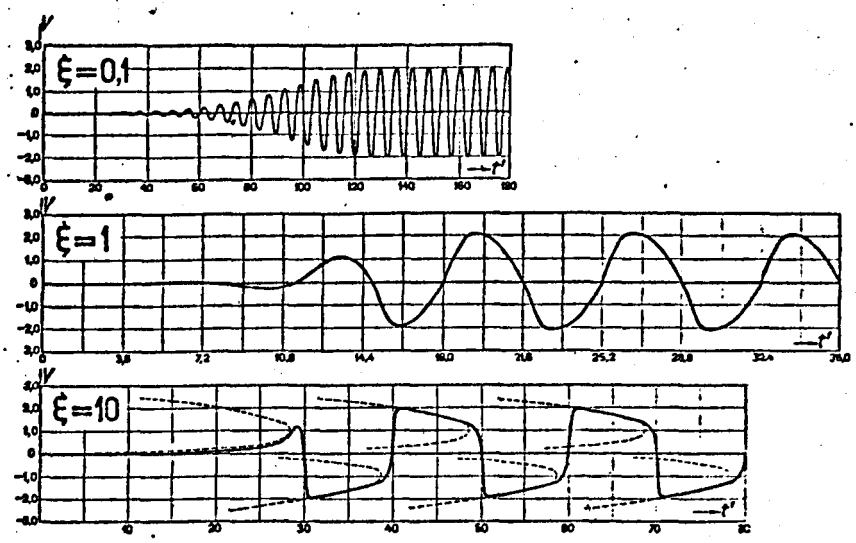


**FIGURE 3.2. Settling processes in electronic oscillators.** *Relaxation oscillations ensue from an initial small perturbation when* $\xi$ *(the nonlinearity) is large; when* $\xi$ *is small the build-up takes many cycles.* (After van der Pol 1934).

However, both sets of rate equations predict that the oscillations will eventually stabilize, unless additional terms are added, when undamped transient solutions can be obtained. Several such modifications have been suggested by various workers, but no physical justification of the additional terms appears possible.

Another model which seems popular is concerned with mode interactions in multimode systems. Such systems can either be free-running, in which case beats will be observed between modes, (e.g. Davidenko et al 1969), or self-pulsed, although it has recently been shown that self-pulsing is very rarely achieved in solid-state lasers (Bambini and Vallauri 1971). It is interesting to note that under certain conditions (non-Q-switched operation) the spikes from Nd: glass and ruby lasers have a regular picosecond sub-structure (Shapiro et al 1968), showing how complicated mode interactions can be. However, the "mode-interaction" model does not seem generally tenable, as spiking has been seen in single-mode lasers (Dzhibladze et al 1969).

There remain several other models, certain aspects of which, taken together, may provide a more apt description of the spiking process. These models are concerned with (i) the effects of spatial inhomogeneities and inhomogeneous broadening, (ii) noise, and (iii) nonlinearities due to radiation damping.

Clearly, any spatial inhomogeneities in the pumping power or in the loss characteristics of a system will modulate the amplification factor and quality factor, and if such modulation is large, the subsequent oscillations may be discontinuous. This factor is of great importance in multimode lasers since both the transverse and lateral mode structure will be affected by inhomogeneities. Any modulation which results may be reduced or eliminated by selecting a more symmetrical arrangement of modes or a more

homogeneous region of the active medium with the aid of an aperture introduced into the resonator.

It should be noted here that, according to some workers (e.g. Bennett 1962), instabilities could still arise in a spatially homogeneous system if the spectral line were inhomogeneously broadened, since "hole burning" might cause different portions of the line to emit at different times. The spikes produced by such a process could have an asymmetric profile, (due to the difference there would undoubtedly be between the time constants for buildup and decay of oscillation in such a system), whereas spikes commonly observed are often symmetrical. Inhomogeneous broadening does not, therefore, appear to be as important a factor in spiking as the effects of spatial inhomogeneities.

Random spike generation is found to develop into c.w. oscillation in mode-selected lasers when the medium is moved relative to the resonator mirrors (Livshits et al 1966). Such an observation shows the connection between spiking and noise, since spiking ceases when those fluctuations due to spatial inhomogeneities are themselves modulated by the motion of the medium. If the pumping is treated stochastically, it can be shown that the stabilization processes have a fluctuating character, even in a single mode laser, so that a noisy source can cause large amplitude fluctuations about the equilibrium position (Haken 1966).

However, the application of classical stability criteria to an appropriately linearized set of quantum mechanical oscillator equations shows that an unstable region of operation can occur in both simple beam maser oscillators (Khaldre and Khokhlov 1958) and more complicated systems, even when the random nature of the pumping process is ignored. Thus, spiking type behaviour should be observed in a three-level single-mode laser whenever the excitation level

is sufficient for the following conditions (Haken 1966) to obtain:

$$\gamma_{32} + \omega_{32} + \tfrac{1}{2}\omega_{21} - \varkappa < 0 \qquad 3.1.$$

and

$$\varkappa > \omega_{32} \qquad 3.2.$$

where $\gamma_{32}$ is the halfwidth of the transition from levels 3 to 2, $\omega_{ij}$ is the incoherent transition rate from levels i to j, and $\varkappa$ is the cavity halfwidth. If these conditions can be satisfied, the radiation field intensity will be high enough for significant non-linearities, due to reaction field effects, to appear. Since $\varkappa$ is almost always less than $\gamma_{32}$ in solid state lasers, however, the oscillation pulsations produced in three-level systems such as ruby cannot be due to radiation damping effects.

In the case of two-level quantum oscillators both semiclassical (e.g. Singer and Wang 1961) and quantum electrodynamic (Bevensee 1963) approaches have shown that oscillation pulsations of this type are theoretically possible, provided the number of molecules lost by coherent radiation processes exceeds the supply of upper state molecules. However, this requirement does not appear to be satisfied by the majority of two-level oscillators, since the field-matter interaction time $\tau_R$ is usually much longer that the characteristic coherence-loss time $T_2$ of the atoms or the photon lifetime $\tau_c$ in the resonator.

Cooperative, or "superradiant" (Dicke 1954) effects in the radiative decay of an atomic ensemble can only arise when a large correlation exists between individual atoms. In such a case the emitted radiation can be anomalously intense, in the sense that the radiated intensity can be proportional to the square of the number $N_c$ of atoms participating, where $N_c$ is not the total number of excited atoms, N, but is the cooperation number, defined in equation

3.5.

It is interesting to note that this situation cannot usually arise in lasers, since the polarization relaxes faster than the field and $\tau_R > \tau_c$. Thus, $T_2$ ranges from about $10^{-12}$ sec to $10^{-10}$ sec in solid state lasers to about $10^{-8}$ sec in gas lasers, while $\tau_R$ is usually longer than $10^{-6}$ sec; the field therefore persists after the original polarization or correlation driving it has decayed, since the corresponding value for $\tau_c$ is typically $10^{-8}$ sec.

In masers, however, the field relaxes at a much faster rate than the molecular variables ($\tau_c < T_2$), so that a large radiation field will rapidly damp to the value generated by the polarization at that instant. If the value of either the molecular flux or the resonator quality factor is then made much greater than the value required to sustain oscillation, so that the condition $\tau_R < \tau_c$ is realized, a self-induced periodic transfer of energy, from the molecular system to the radiation field, and back again, will occur (Uspenskii 1963).

Although such a superradiant effect has been observed in a self-oscillating rubidium magnetometer which incorporated electronic Q-multiplication (Bloom 1962), masers operated without artificial Q-enhancement have not yet shown this behaviour, since it is difficult to satisfy the condition $\tau_R < \tau_c$, or, equivalently,

$$\frac{4\pi\mu_{12}^2 N Q_c}{\hbar} > \frac{\omega_o}{2Q_c} \qquad 3.3.$$

where the usual definition of $\tau_R$ is assumed (e.g. Feynman et al 1957).

In the case of an ammonia maser operated on a 3,3 transition with an $E_{010}$ mode cavity, the maximum possible resonator Q is approximately 10,000 at room temperature (Shimoda et al 1956), so that

before continuous pulsations can occur a molecular flux which is perhaps a factor of one hundred times greater than the oscillation threshold value for this cavity Q is required (Basov et al 1966).

This requirement, which has not yet been satisfied, is quite stringent, but may perhaps be met by first cooling the resonator, to reduce wall losses, and then using supersonic beam techniques, to produce an intense, narrow, molecular beam.

As indicated in chapter one, $\tau_c$ may be increased by a factor of nearly two by cooling the $E_{010}$ mode cavity to a temperature near 100 K. It is estimated by the author that little advantage can be gained by further cooling, because of the anomalous skin effect. Furthermore, it has been found that the operation time of such a maser is much reduced by cryogenically cooling the cavity, since any ammonia which condenses detunes the cavity and sometimes broadens the spectral line (via induced charges).

However, although the operation time is short, self-induced pulsations should occur in a strongly oscillating maser which uses a cooled cavity, provided a molecular flux which is 20 to 30 times the normal starting flux (oscillation threshold value) can be generated.

It is interesting to note that it is advisable to use a <u>short</u> cavity to reduce the resulting scattering; although the time of flight is then shorter, and the starting flux is increased, (since for maser oscillations $\tau_R \leqslant T_2$), equation 3.3 shows that the value of molecular flux required for the onset of pulsations is <u>unaffected</u> provided $T_2 \gg \tau_c$.

In summary, since all the models of oscillation pulsations have now been considered, the following regimes of quantum fluctuations may be distinguished:

(i) In the case of low-level excitation of single- or multi-mode

systems, the stabilization process may be characterized by large amplitude fluctuations when the pumping source is noisy.

(ii) Above threshold, the spatial inhomogeneities which commonly occur in lasers modulate their emission characteristics; these inhomogeneities may be so gross that the subsequent oscillations are discontinuous, and "spikes" are observed.

(iii) Simultaneous oscillations at two or more frequencies may produce self-modulation.

(iv) Quantum oscillators which do not exhibit such amplitude modulation, such as ammonia masers operated with a cavity tuned to the centre of the spectral line, may become unstable ("spike") when the radiation field intensity is sufficient for cooperative effects to magnify subsequent fluctuations and therefore make them anomalously large.

It is considered that the large-amplitude pulsations commonly observed in lasers may be explained as due to a combination of the second and the third of these effects.

Section 3.3. Superradiant oscillation transients.

In the first part of this section, a brief outline is given of the way in which the phenomenon of superradiance, well-known in passive systems, is related to radiation damping in quantum oscillators. The techniques by which superradiant amplitude transients can be induced in the ammonia maser are then described in some detail, and an analysis is given of the results obtained using these techniques.

In recent years it has proved possible to prepare large numbers of atoms or molecules in a state which is characterized by a large induced dipole moment. The time evolution of such a state is then determined to a large extent by radiation damping (e.g. Bloom 1957), since the molecules, being bathed in a common radiation field, experience a high degree of coupling, or "correlation", which makes $\tau$, the spontaneous emission lifetime for the system, smaller, by a factor $N_c$, than $T_1$, the spontaneous emission lifetime for a single molecule:

$$\tau = T_1 / N_c \equiv \tau_R \qquad 3.4.$$

where $N_c$, the "cooperation number", may be taken as representing the total number of molecules participating in the emission process. Furthermore, application of the principle of radiation reaction shows that the radiated power in such a cooperative process is proportional to $N_c^2$. Any system which exhibits such a cooperative decay is therefore said to be "superradiant", (Dicke 1954), since the correlation associated with an induced dipole moment produces an enhancement of the spontaneous emission rate.

However, the actual radiation rate can be considerably smaller than that calculated by Dicke (for geometrically small systems), since the size and shape of the sample will modify the enhancement

factor. If $N_c$ molecules are confined in a cylindrical container, such as an $E_{010}$ mode resonator, the radiation from an individual molecule can only extend over all $N_c$ molecules when no molecules are further apart than the coherence length $c\tau$. The cross-sectional area of a cavity of this length must then be of the order of $\lambda^2$, so that this self-consistent argument gives the cooperation number for this container to be

$$N_c = (\lambda^2 c T_1 N / V)^{\frac{1}{2}} \qquad 3.5.$$

where $\lambda$ is the wavelength and c is the velocity of the emitted radiation, since $N_c$ is given by the number of molecules in this volume, and there are N/V molecules per unit volume. It is clear that the cooperation number $N_c$ can be very different from the total number N of available atoms, so that the "coherence volume" $V_c$ ($= N_c V/N$) will generally be smaller than the sample volume in the optical region, comparable with it in the microwave region, and much larger in the case of low-frequency systems (such as n.m.r. flow masers). In general, therefore, it can be said that the emission of radiation from a molecular ensemble is similar to that encountered in the study of arrays of classical oscillators (e.g. Stratton 1941).

Clearly, the self-consistent-field approach generally taken to derive the equations of motion for a macroscopic system such as a quantum oscillator means that radiation damping effects are implicitly considered in any subsequent discussion, since the radiation-reaction field has been included automatically in the total radiation field. However, section 3.2. shows that marked superradiant effects are rarely present in quantum oscillators, since the radiation damping time, although shorter than $T_1$, is usually longer than the other characteristic relaxation times. The phenomenon of superradiance, or cooperative decay, is therefore only

normally associated with those effects, such as optical nutation (Hocker and Tang 1969) and radiative echoes (e.g. Oraevskii 1967), which are the result of an external perturbation on a passive system, since cooperative superradiant decay can only be more important than independent incoherent decay when a system is characterized by a large net microscopic dipole moment, or, equivalently, when the geometrical representation (Feynmann et al 1957) described in chapter one is used, by a super Bloch vector (Stroud et al 1972), whose components, the N individual Bloch vectors, are initially aligned or nearly aligned.

Thus, in the case of pulse-excitation of a small molecular assembly, "tipped" through an angle $\theta$, (using magnetic resonance terminology, appropriate to a geometrical interpretation), each molecule is left in a coherent superposition of its upper and lower states, where, according to Dicke, the parameter $\theta$ also has the significance that $\sin^2\frac{1}{2}\theta$ is the probability that the molecule has been left in its upper state.

It will be appreciated that the only nontrivial cases of interest are those for which $2\pi > \theta > 0$, since when $\theta$ is an even multiple of $\pi$ each of the two-level molecules is left in its ground state, and does not radiate. Also, semiclassically, a system of molecules prepared exactly in its upper state is metastable, and therefore never radiates, since radiation is only possible when the system has a non-zero dipole moment. Suppose, therefore, that the tipping angle is such that the induced polarization is large, and the radiation damping time $\tau_R$ is less than the dephasing time $T_2$. The initial decay will then be proportional to the total number of excited atoms, but as the polarization decays further, collective effects cause the radiation rate to rise quickly to a peak value, which is greater than the incoherent rate. A monotonic decay of

the energy of the assembly then occurs, with a half-life which is approximately equal to the time $t_o$ originally taken for the radiation intensity to rise to its "delayed peak" value. In this sense, therefore, the motion of the super Bloch vector following the pulse is analogous to the time evolution of a suitably prepared classical system of N identical magnets, precessing in a strong homogeneous magnetic field $B_o$ with the same polar angle $\theta$, but initially out of phase (i.e. having different azimuthal angles), since in both cases the radiated power I(t) is nonmonotonic, and shows a $\text{sech}^2$ dependence on time (Bloom 1956):

$$I(t) \propto \text{sech}^2\left[(t - t_o)/\tau\right] \qquad 3.6.$$

This delayed surge of power shows that after the assembly has been put into a superradiant state, oscillation builds up to a point where relaxation effects predominate. Since the criterion for a system to oscillate is that losses (e.g. relaxation mechanisms) are compensated for by the presence of a source of energy, it will be appreciated that the cooperative decay mechanism responsible for the delayed peak phenomenon in passive systems is fundamental to the operation of quantum oscillators. The delayed peak can therefore be seen in masers by the technique of interrupting, in a time $t_s$, the process of replenishment of atoms or molecules in the upper energy level, and then tipping the system through a suitable angle, in a time $t_p$ which satisfies the following criteria:

$$T_1 \geqslant T_2 > \tau_R \gg (t_p + t_s) > \tau_c \qquad 3.7.$$

where the tipping angle depends on the dipole moment $\mu_{12}$ and the pulse amplitude $E_{rf}$ at the transition frequency $\omega_o$:

$$\theta = \mu_{12} E_{rf} t_p \qquad 3.8.$$

Unfortunately, mechanical considerations make it difficult to interrupt the flow of molecules sufficiently quickly ($t_s < 100$ microseconds) to see this effect in an ammonia beam maser, but the delayed peak experiment has been carried out successfully on n.m.r. flow masers (Bender and Driscoll 1958), hydrogen masers (Brousseau and Vanier 1971), and, as shown in figure 3.3., rubidium masers (Vanier 1968). In such experiemnts the detected signal which follows the pulse is found to have both the hyperbolic-secant profile, which characterizes superradiant emission, and the expected dependence of $t_o$ on phase angle (see, e.g. Greifinger and Birnbaum 1959).

However, it is a relatively easy matter to apply some form of step perturbation, in a time $\tau_s < T_2$, to the ammonia maser, thereby inducing a superradiant oscillation transient (following the removal of the perturbation), provided $\tau_R < T_2 \leq T_1$. Such transients, (which are related to the process of a periodic transfer of energy between the molecules and the radiation field, discussed in section 3.2.), have been observed to occur in both maser and solid state laser oscillators, and, besides providing a direct method of determining the degree to which the oscillation condition is over fulfilled, are of practical interest for fast switching in computers (Basov et al 1969). A detailed study of the dynamic behaviour of the ammonia maser is therefore of considerable interest, since the results obtained are relevant to the phenomena of transient processes in quantum oscillators in general.

Accordingly, several techniques for changing the oscillation level in a beam maser in such a way as to induce oscillation transients will be described:

(a) observation of the establishment of oscillations following the sudden removal of a high-level signal at, or near $\omega_o$, which normally acts by saturation broadening to quench the maser

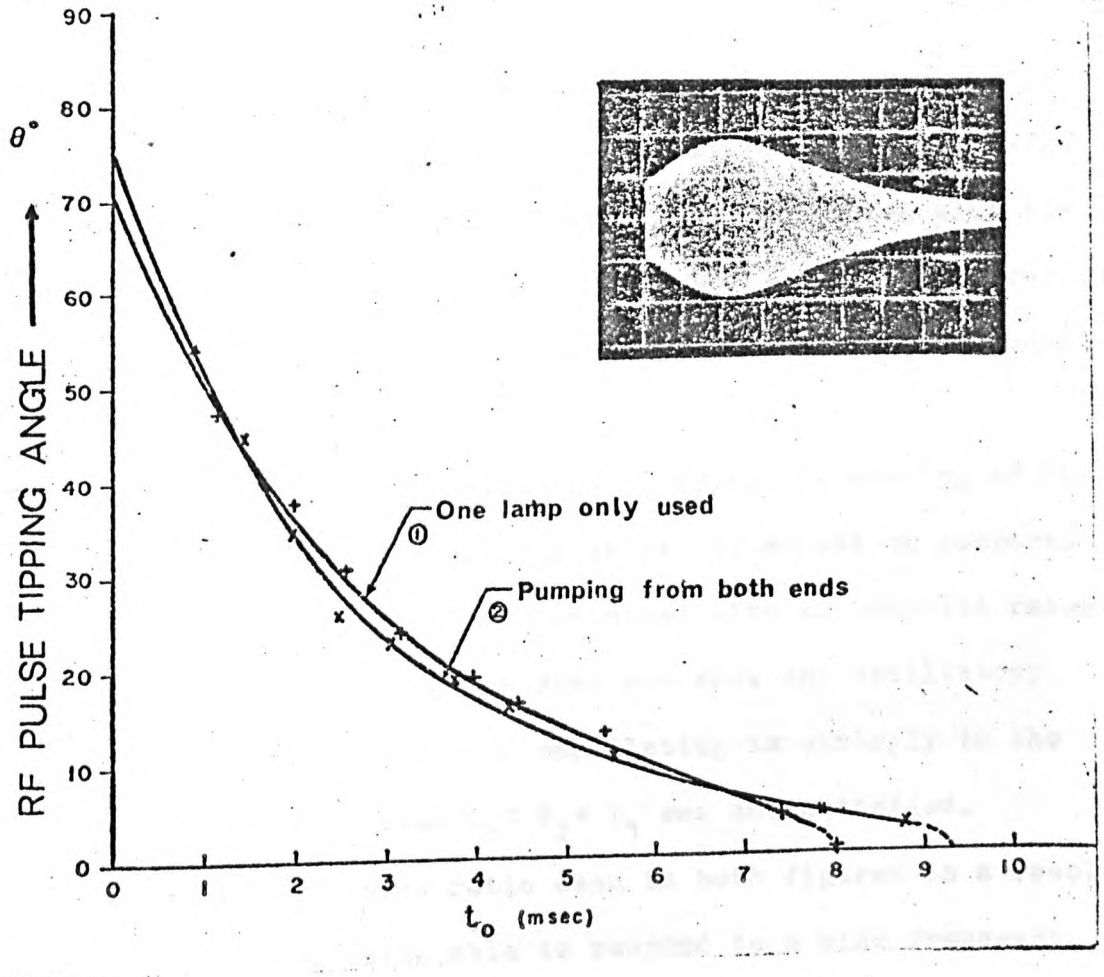


**FIGURE 3.3. Delayed peak in Rb maser** ( After Vanier 1968).

oscillation when injected into the maser resonator (Lainé and Bardo 1971);

(b) an alternative method of molecular Q-switching, involving Stark (or Zeeman) line broadening (Alsop et al 1957);

(c) the technique of suddenly altering the rate at which molecules in particular energy levels are supplied (Grasyuk and Oraevskii 1964);

(d) the cavity loss-modulation method, commonly known as "Q-spoiling".

Typical oscillation transients obtained with the first method can be seen on the right hand side of the stimulated emission signal in figure 3.4. The amplitude fluctuations associated with the build-up process only appear with a high beam flux, and their period decreases (to ~100 μseconds in this case) as the amplitude of oscillation is increased.

This result, which was obtained using cryogenic cooling of the resonator (to ~100 K), to enhance the cavity Q, should be compared with that of figure 2.5., which was obtained with an uncooled resonator and a lower beam flux, and so does not show any oscillatory behaviour, since the maser was not oscillating as strongly in the latter case, and the condition $\tau_R < T_2 < T_1$ was not satisfied.

The poor signal-to-noise ratio seen in both figures is a result of the detection system being able to respond to a wide frequency spectrum; the large bandwidth is necessary to display the envelope of the beats between the maser oscillation and the frequency-swept quenching signal without a large degree of instrumental attenuation occurring during the establishment process. Nevertheless, it will be seen that this method, which may be regarded as one form of molecular Q-switching, since it relies on saturation broadening of the spectral line, provides qualitative confirmation of the existence of transient pulsations accompanying oscillation build-up.

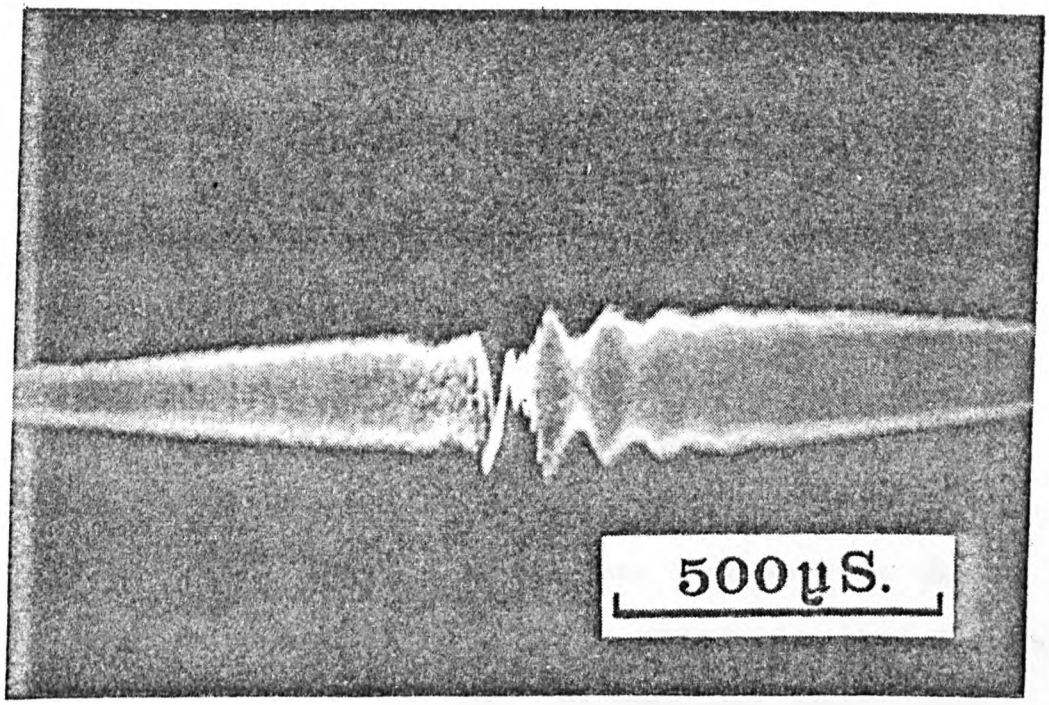


FIGURE 3.4. Oscillation transient following quenching by saturation broadening.

However, the presence of an injected signal at, or near $\omega_o$, together with the concommitant rapid variations in beat frequency associated with this method, preclude any investigations of the manner in which the phase of the oscillations might vary during an amplitude transient.

These difficulties do not arise when a step-function perturbation involving Stark (or Zeeman) line broadening is used to vary the oscillation level, since any transient signals must necessarily always be within the linewidth of the maser oscillator, and therefore only narrow-band detection (~50 kHz) need be employed to display the damped transients observed during the oscillation build-up process, This technique also allows simultaneous investigation of the phase transient expected from theory (Grasyuk and Oraevskii 1964), provided a stable reference signal is available.

In practice, Stark broadening is to be preferred to Zeeman broadening in investigations of these amplitude transients, since, from Lenz's law, an $E_{010}$ mode cavity of the type commonly used in ammonia masers, being equivalent to a one-turn coil, makes the condition $\tau_s \ll T_2$ impossible to satisfy, and machining such a cavity into a hair-pin configuration (Grigor'yants and Mazurov 1968), while allowing faster switching speeds, tends to increase cavity losses.

The Stark field can be applied across the electrically insulated halves of a cavity split longitudinally, as in experiments on the noise properties of masers (Alsop et al 1957), so that all molecules within the cavity can be subjected to approximately the same degree of Stark broadening, or it can be applied more locally, between the cavity and one or more insulated wire probes inserted into the cavity perpendicular to the cavity electric field vector (Bardo and Lainé 1971, Shakov 1969), although this latter method

requires larger quenching voltages (600 - 1000 volts, as against 50 volts with a split cavity). Both methods are described here; however, previous investigators have only used the probe technique, presumably because a split cavity with the necessary high Q-factor is difficult to fabricate.

Preliminary experiments on Stark switching with a single probe showed that if the focuser voltage was less than about 30 kV, then complete switching of the oscillation of the single-beam maser previously described could be achieved quite readily with 400 V applied to the probe.

However, the region of inhomogeneous field near the probe could not be extended sufficiently to quench the maser completely when it was operated with a greater degree of excitation, since the probe insulations tended to break down at potentials above about 600 V. Although this could be circumvented to some extent by the use of more probes, at the very highest levels of excitation even three probes proved insufficient for 100% switching.

Permanent records of the amplitude transients observed were obtained by using a Brookdeal model 415 Box-car detector, operated in the signal-averaging mode, to drive an Advance X-Y-T plotter. As in the case of the Zeeman maser, 1 second proved the optimum recording speed. With a pulse repetition rate of 500 Hz this meant that the number of transients contributing to each pen-recording was in excess of 100.

A family typical amplitude transients, obtained in this way at focuser voltages of from 15kV to 27 kV, in 1kV steps, using a single probe is shown in figure 3.5. The voltage pulse applied to the probe had an amplitude of -400 V, a width of 1 msec, and a p.r.f. of 500 Hz. The probe, which was made from P.T.F.E. - coated silver wire, 0.09 mm in diameter, was mounted halfway along the

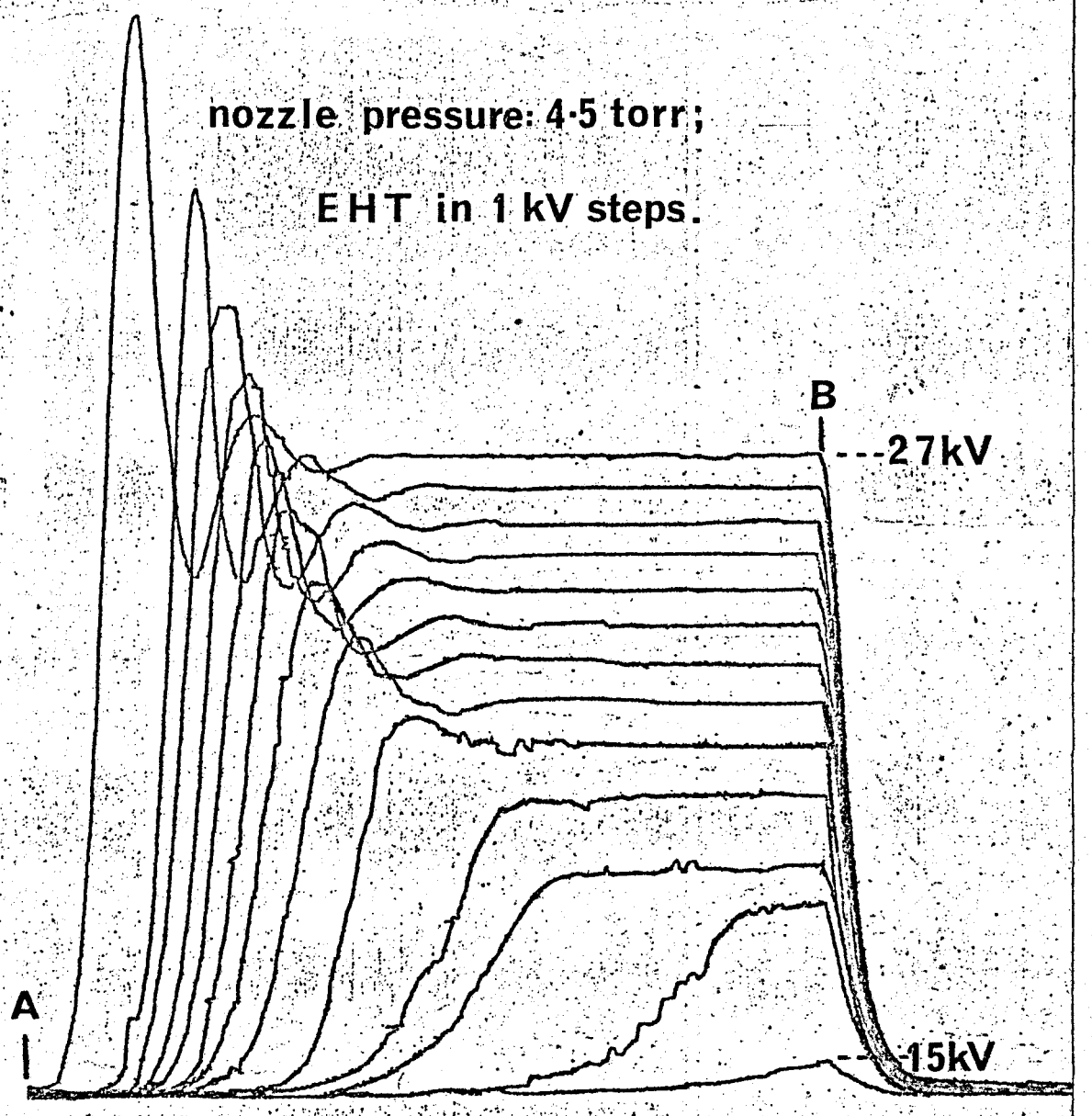


FIGURE 3.5. Maser oscillation amplitude transients following oscillation quenching by means of a Stark probe in the resonator, alternately at 0V(A) and -400V(B).

length of the cavity almost opposite the coupling hole, and extended across nine-tenths of the cavity diameter. It was insulated by means of a fine glass sheath, which projected a distance of a few mm into the cavity interior. The combination of metal probe and dielectric sheath was somewhat propitious, since it did not appear to degrade the cavity Q appreciably from its high initial value of 8000 - 9000, and also had little detuning effect on the cavity. Furthermore, the probe was of fairly low capacitance ($\sim$20 pF), and so could be driven easily by the specially constructed transistor unit used, since this was capable of driving capacitative loads of up to 1000 pF with large ($\sim$600 V) fast rise-time ($\sim$200 nsec) pulses.

It will be seen that the maser does not begin to oscillate immediately the quenching voltage has been removed from the probe, even though the self-excitation condition may be exceeded by a large factor in a steady-state situation. This dead time, $T_m$, which is the time that elapses before maser oscillations are detected, has been termed the "time of silence" in the literature, and has been shown theoretically to depend on both the intrinsic noise of the combination of maser and detection system and the time $\tau_f$ taken before the source can supply sufficient numbers of upper state molecules to the cavity to exceed the threshold condition (Oraevskii 1964):

$$T_m = \tau_f \left[ 1 + \ln (\beta/(\beta - 1)) \right] + \left[ T_1/(\beta - 1) \right] \ln(A_n^2/\varkappa A_i^2) \qquad 3.9.$$

where $A_n$ is the amplitude of the receiver noise, $A_i$ is the initial amplitude of the cavity radiation field, $\varkappa$ is the output coupling constant of the resonator, and $\beta$, which is of the order of $T_2/\tau_R$, is a parameter related to the degree of excitation of the maser.

Since it was not known how the self-excitation parameter $\beta$ depended on the amplitude of the steady-state oscillations which

were monitored during the experiment, it is difficult to make a quantitative comparison of the experimental results of figure 3.5 (shown graphically in figure 3.6) with the predictions of this equation.

Nevertheless, the decrease seen in the time of silence when increasing the focuser voltage may be interpreted qualitatively by considering the relationship which exists between the quenching voltage and the state of the emergent beam. If it is assumed that the majority of molecules entering the resonator are in the upper state, then the power delivered to the radiation field will depend on the probability of a downward transition occuring during the passage through the cavity. Since this transition probability will be modified as shown in figure 3.7. by the presence of a Stark field, it will be appreciated that the dead time will only be a minimum when the Stark field is intense enough to shift the emission lines by perhaps several tens of MHz, thereby reducing the correlation between the molecules and the radiation field substantially, so that the radiation field is nearly in the vacuum state.

Removal of the Stark field would then leave the complete system in a metastable state, allowing a comparison to be made between the predictions of Quantum Electrodynamics and Semiclassical radiation theory regarding superradiant effects (e.g. Stroud et al 1972).

Unfortunately, such a Stark field cannot be produced with the experimental arrangement described here, and thus the time of silence will be a function of the focuser voltage, as shown, if the Stark voltage is fixed. This follows because the efficiency of the sorting system, and hence the steady-state oscillation level and the self-excitation parameter, also depends on the focuser voltage, so that at high focuser voltages the maser will be quenched less effectively, the initial radiation field will have a higher value, and the time

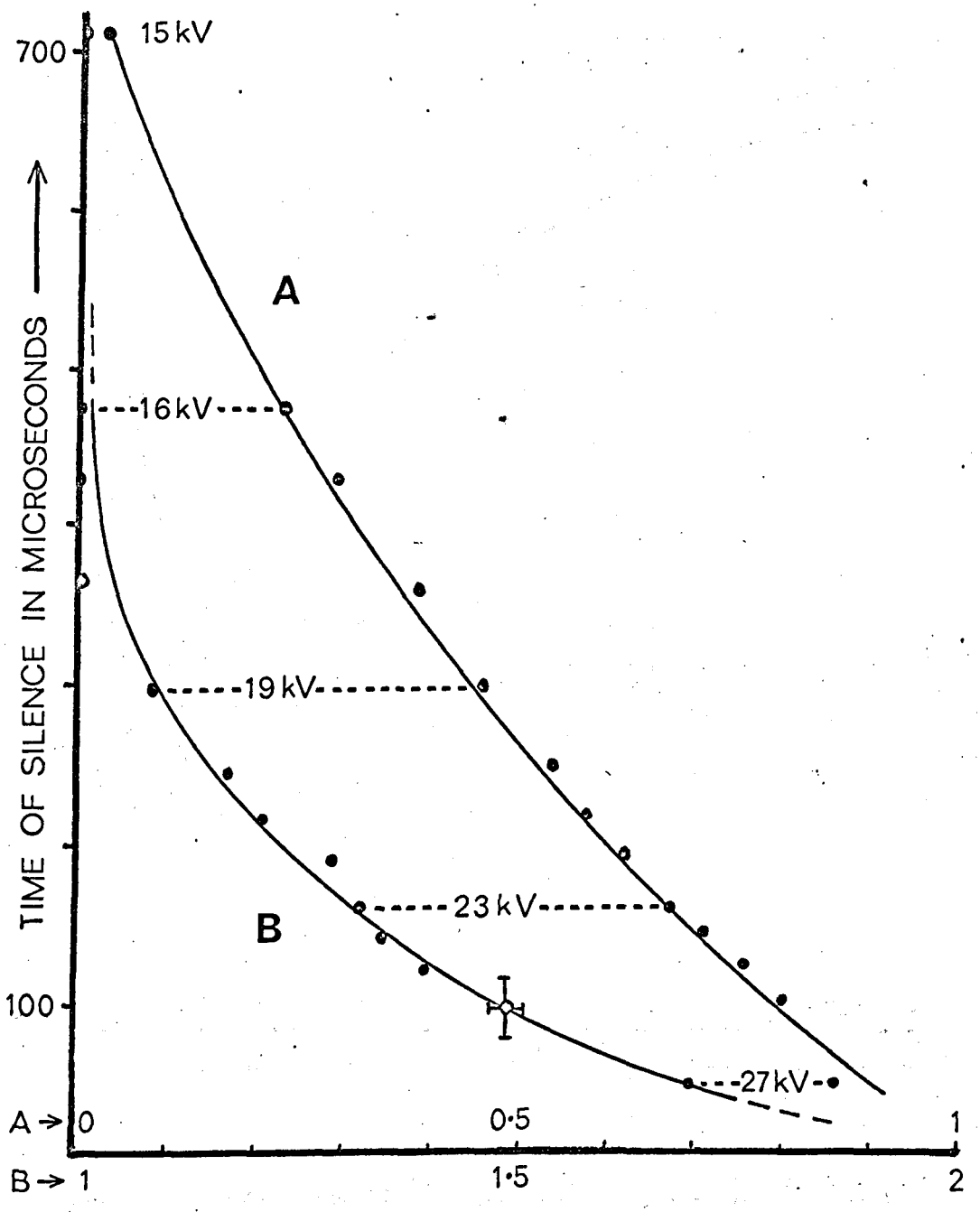


**FIGURE 3.6.** Time of silence vs normalized steady-state amplitude in relative units (A) and ratio of peak output to steady state output (B).

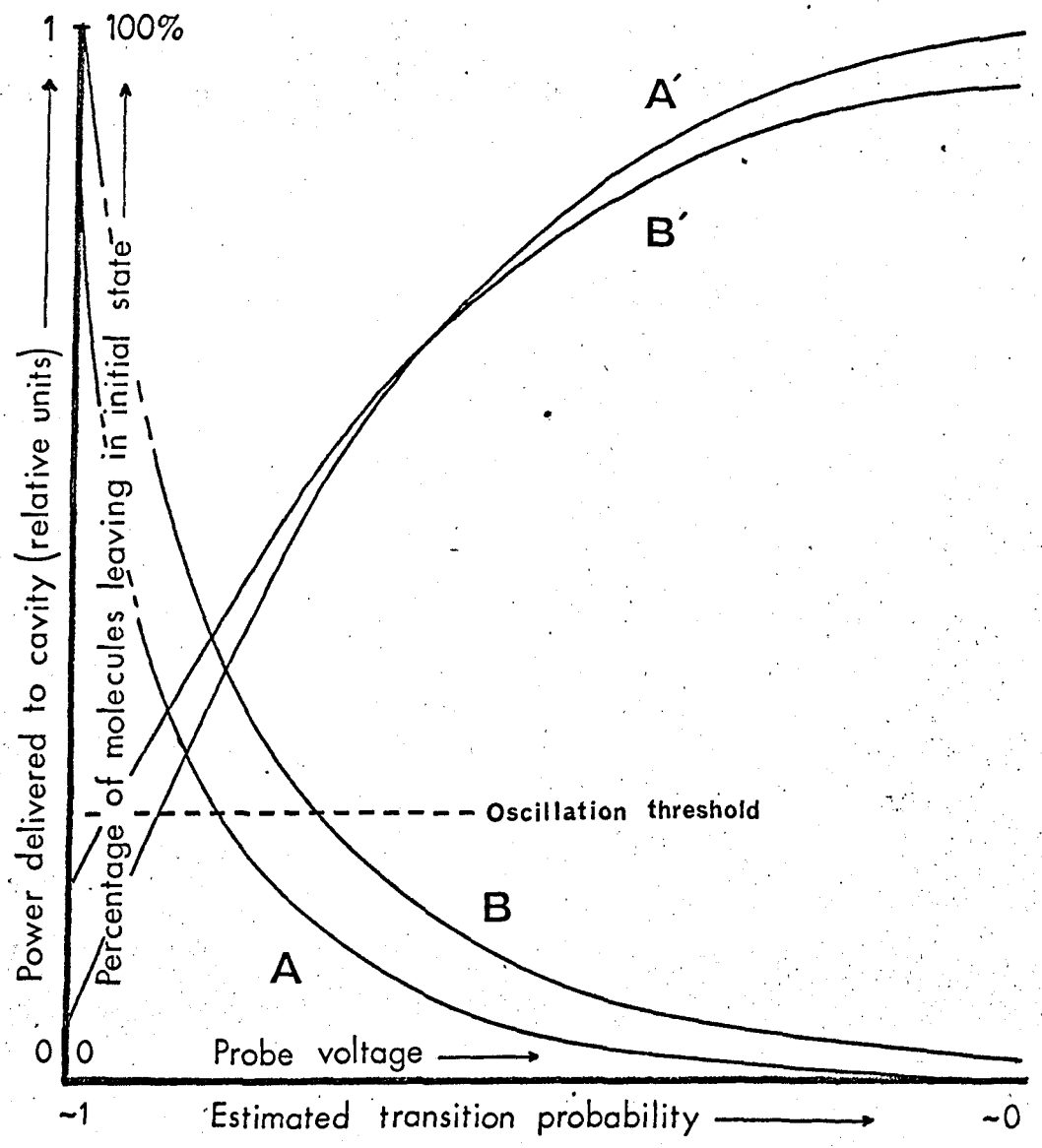


FIGURE 3.7. Model of changes induced in a maser by a central Stark probe: A,B relate to oscillation level and A´,B´ to concommitant state populations.

of silence will be reduced accordingly.

Furthermore, since in the moving frame of reference of the molecules the average time for a transition in the radiation field is a function of distance, it can be argued that the excitation parameter, and hence the time of silence, should also depend on the position of the Stark probe, as the associated region of inhomogeneous field is very localized. That this is in fact the case is shown by experiments on the change in steady-state oscillation level with Stark voltage, using two additional probes of a similar construction to the first, placed symmetrically about the central probe and approximately 40 mm from it.

Comparison of the maser oscillation level with all probes at 0 V and then with each probe in turn at -200 V showed a decrease in maser output analogous to the one previously observed with the middle probe when the quenching voltage was applied to the probe nearest the focuser, but revealed that the Stark field caused a decrease in oscillation level at low focuser voltages and an increase at high focuser voltages when the last probe was used, as shown in figure 3.8. These results can be correlated with the travelling wave effects discussed in chapter 2, since such waves are a consequence of the non-uniform emission of radiation by molecules along the length of the cavity. It will be remembered that when the maser oscillates weakly, most emission takes place in the last part of the cavity. In this case, the emitted power therefore flows from the exit region towards the focuser, in the opposite direction to the beam.

However, power flows in the same direction as the molecules at high amplitudes of oscillation, since the emission then occurs predominantly in the first part of the resonator, and molecules in the last part of the resonator will be in an absorptive state.

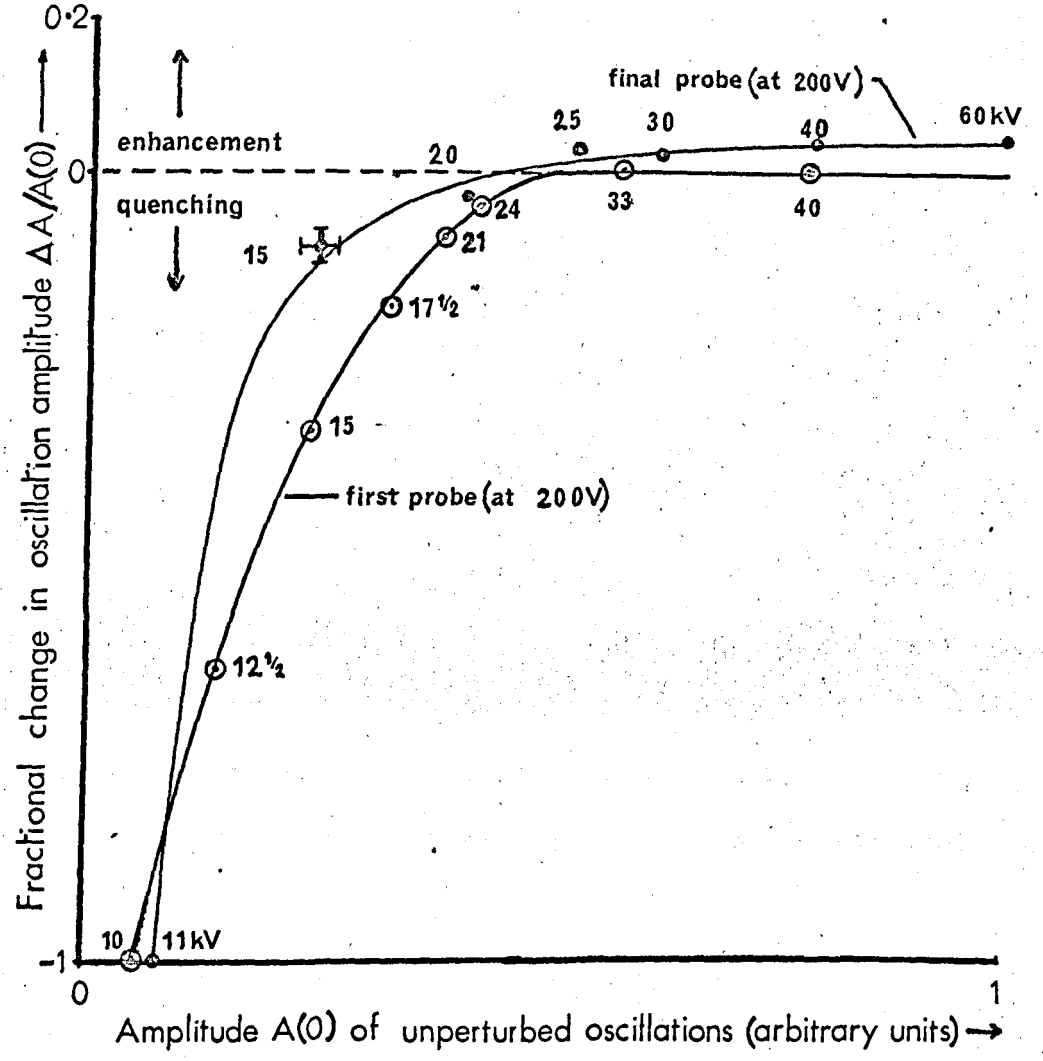


**FIGURE 3.8. Quenching action of Stark probes.**

The final probe will therefore tend to reduce the emitted power at low focuser voltages, by reducing the transition probability in this region of the cavity, and increase the emitted power at higher voltages by reducing the probability of energy absorption by molecules about to leave the cavity.

This modification of the transition probability can change the character of the amplitude transients considerably when combinations of probes are used, as shown in figures 3.9 - 3.12. It will be seen that both the enhancement (with increasing excitation) of the speed with which oscillations build up (relative to the transit time $T_1$) and the radiation-damping - induced overshoot effect were most marked when, as in figure 3.12, a combination of probes which included the middle probe was used, since, for the range of excitation employed, a central Stark field always reduced the transition probability at $\nu_o$. When, as in figure 3.11, this probe was not used, the quenching effect was insufficient to keep the maser below oscillation threshold at high levels of excitation, and therefore the effects of radiation damping were less apparent, since the relative change in oscillation level (following the removal of the Stark field) was smaller.

Furthermore, when three probes were used, so that maser oscillations were completely quenched for all but the very highest levels of excitation achieved, the maser remained below threshold for a time longer than that observed when quenching (at lower excitation levels) with only the centre probe. However, once the threshold condition was satisfied, the subsequent build-up process was noticeably faster than in the single-probe case. In addition the ratio of the (peak : steady-state) amplitudes of oscillation came close to two (this being a limiting value, associated with the situation where all molecules make a transition to the lower state

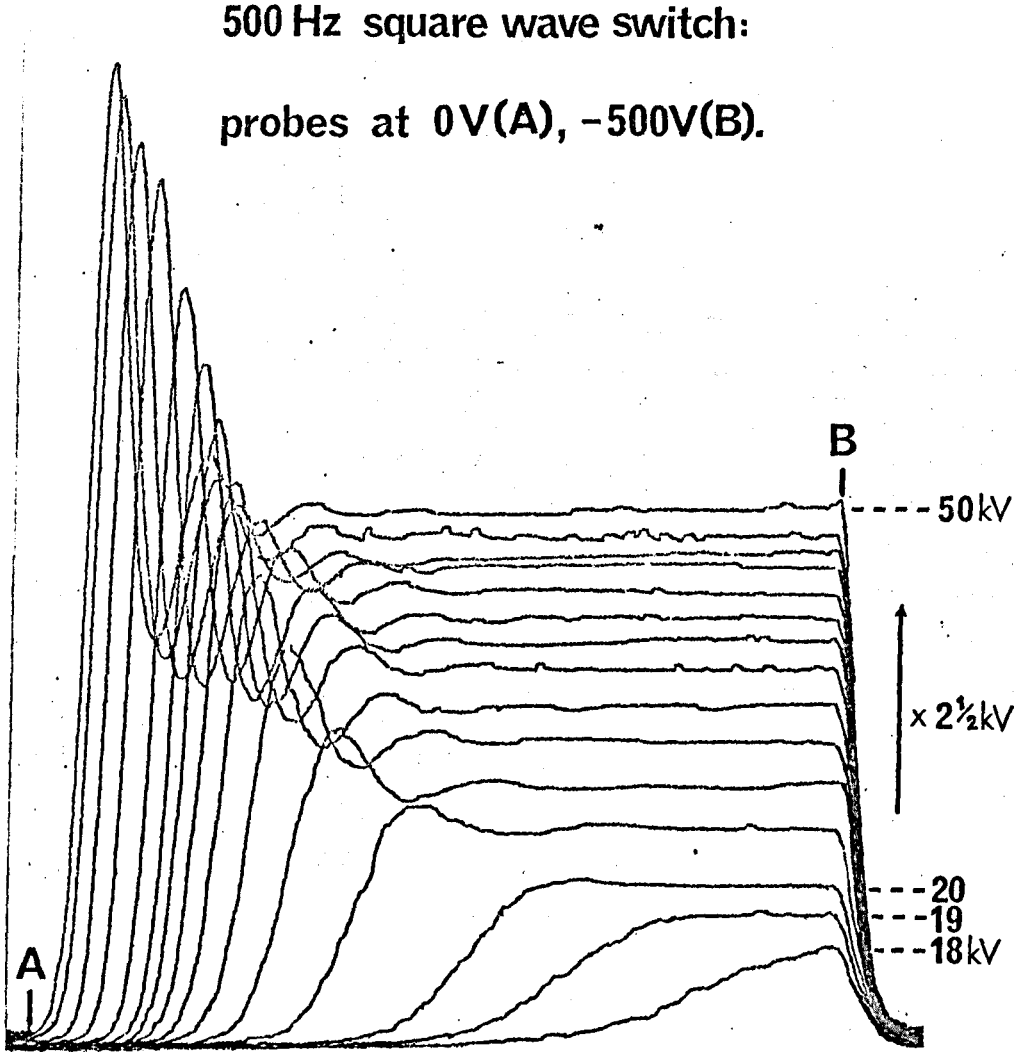


FIGURE 3.9. Maser oscillation amplitude transients obtained by using Stark probes 1 and 2 together.

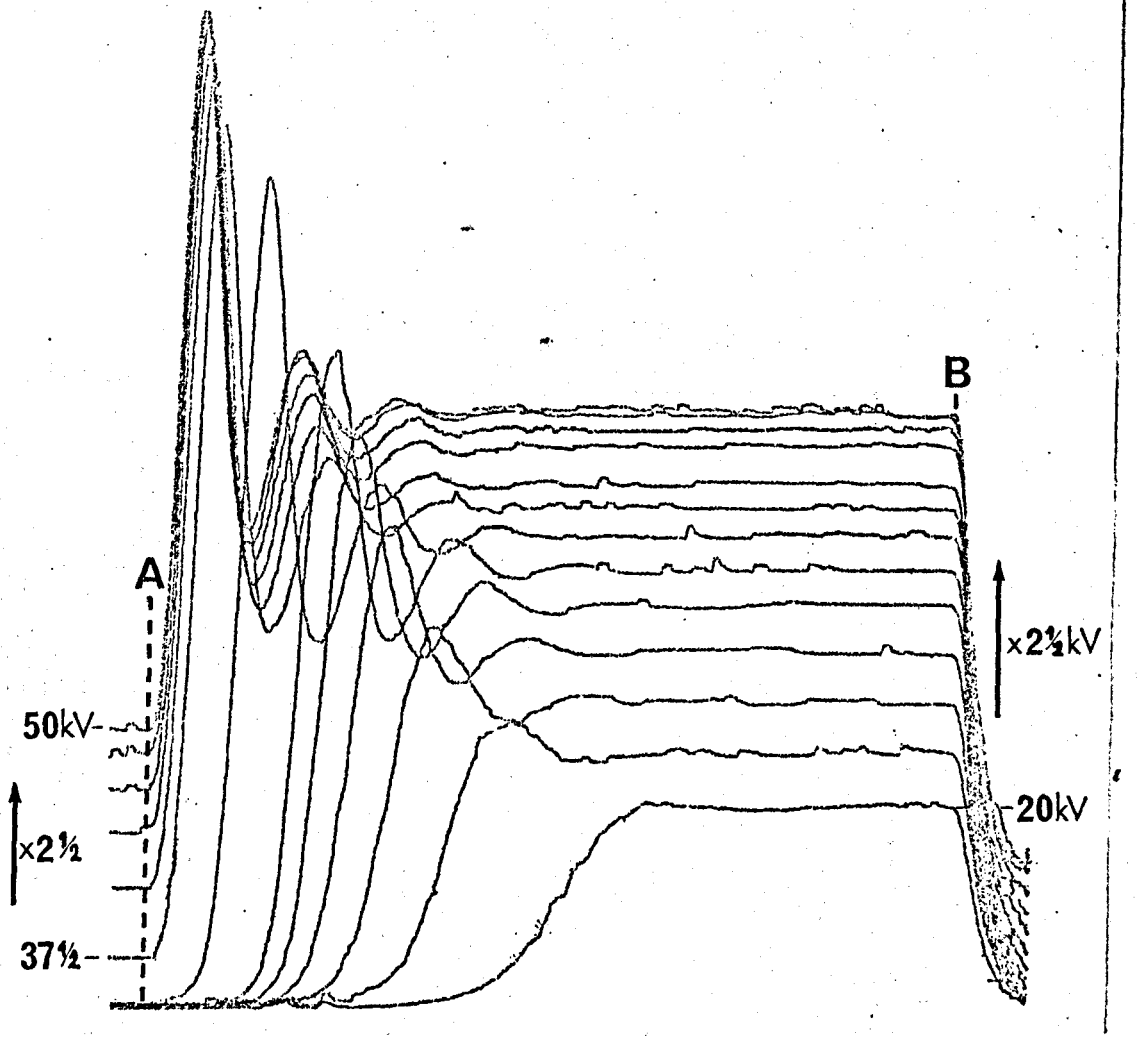


FIGURE 3.10. Transients with probes 2 and 3.

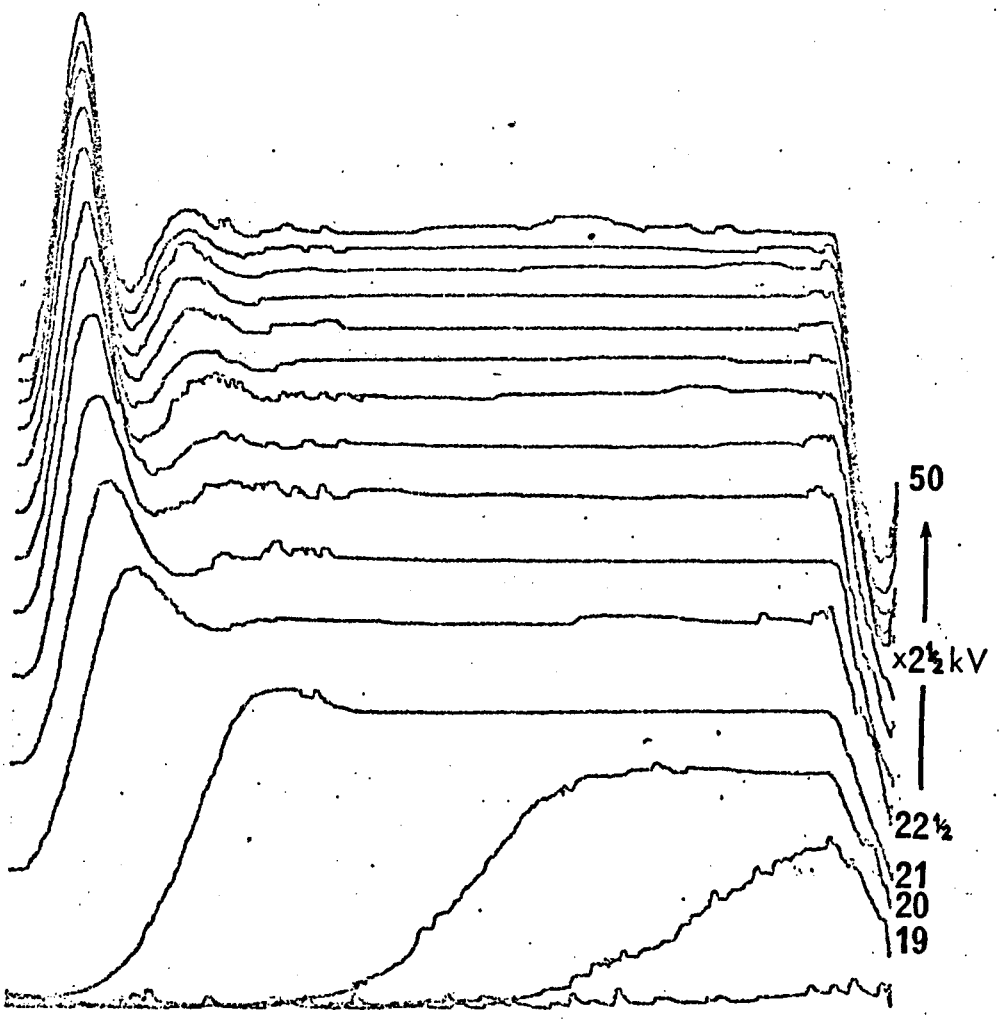


Figure 3.11. Amplitude transients obtained when both the first and last probes were fed with with a 500 volt square-wave at 500 Hz.

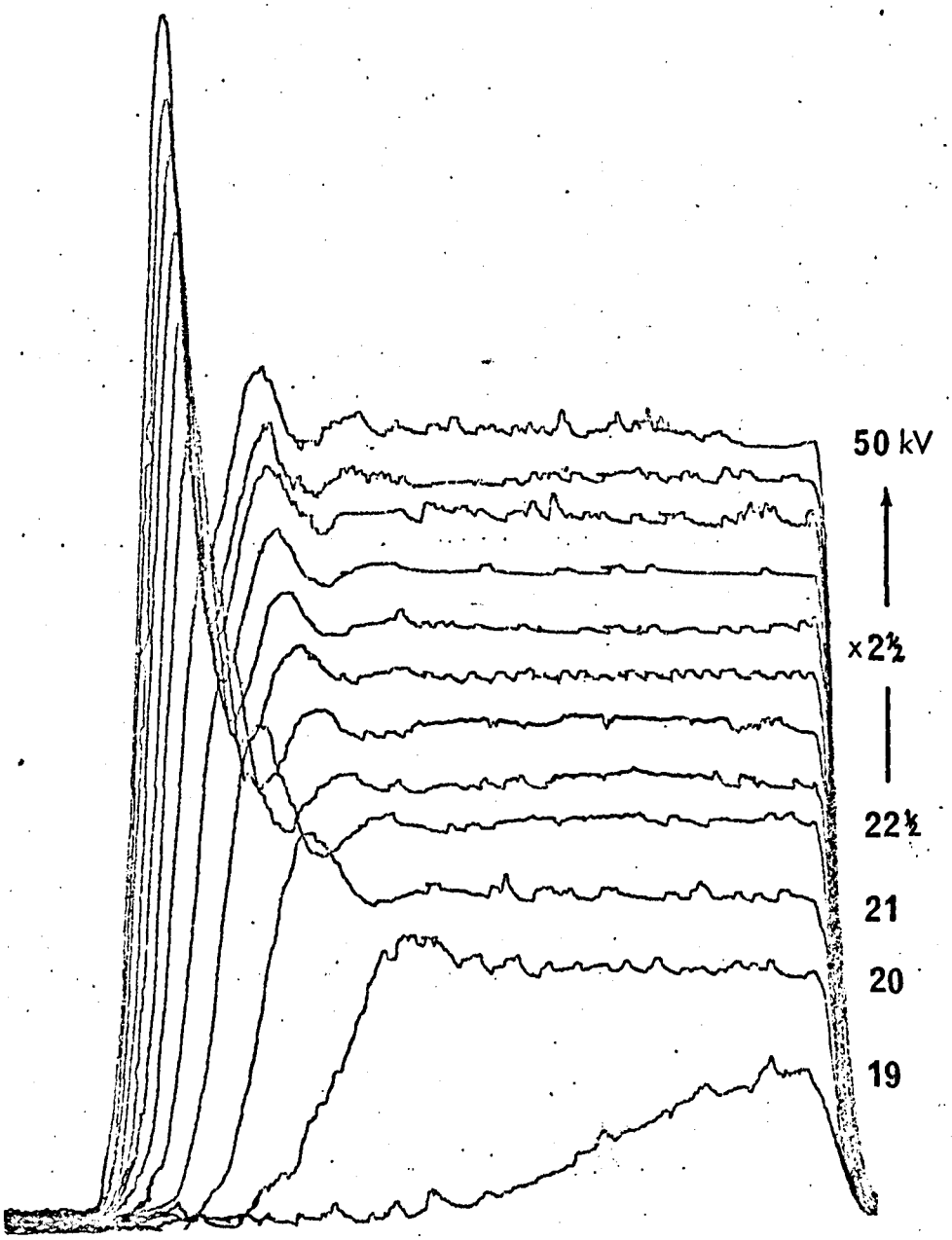


Figure 3.12. Amplitude transients obtained when all three probes were fed with a 500 volt square-wave at 500 Hz.

in a time less than $T_1$ or $T_2$).

Both these observations are in accordance with previous comments regarding relative changes in oscillation level. It will be seen that this increase in the time of silence when three probes are used conflicts with the predictions of equation 3.9. This disagreement with theory may be reconciled by introducing an additional term, which takes into account the effect of preparing the system in a "mixed" initial state (preparatory to removing the quenching perturbation).

The author considers that this state-mixing would arise whenever a perturbation of a localized nature is used for quenching a beam maser, since the response of individual molecules to the radiation field would vary as a consequence during their time of flight through the cavity. This would imply that while the Stark probes might reduce the value of the cavity radiation field at any one frequency near the unperturbed oscillation frequency $\nu_o$ below the level required for maser oscillation at that frequency, the field could still be sufficient to cause many downward transitions at frequencies within a few kHz of $\nu_o$, although molecules which emitted energy at one frequency might well absorb energy at a different frequency. The increase in the stimulated emission rate at frequencies other than $\nu_o$ would therefore tend to reduce the difference between the total number of upper-state molecules in the cavity and the total number of lower-state molecules in the cavity at the instant of removal of the quenching perturbation.

Thus, if the population excess available for the build-up process at this instant were to be much lower than the value associated with preparation in a near-metastable state (i.e. one where very few downward transitions occurred with the perturbation "on"), the time required for the system to come above the threshold

of oscillation could be substantially greater than the simple time-of-silence of equation 3.9.

However, since at high excitations the correlation between individual molecules increases very rapidly once the threshold condition is satisfied, such a reduction in the initial population excess would not affect the superradiant character of the build-up process to any great extent.

These results may be compared with the amplitude transients of figure 3.13, which were obtained with a split cavity. This cavity had been drilled to take a single, centrally placed Stark probe, opposite the coupling hole, and then split longitudinally on a milling machine, (with the aid of a 1 mm slot cutter) so that one half held the Stark probe and the other half the coupling section, with its attached waveguide. The two halves, which were isolated by strips of Paxolin, 1 mm thick, inserted between each machined edge, were held together by aluminium clamps. Considerable care was taken to ensure accurate alignment of the two halves prior to re-assembly, but even so the inherent degradation in cavity quality factor produced by the machining process meant that the oscillation threshold condition was perhaps twice as difficult to satisfy as with an unsplit cavity. The cavity insulation used set a limit of the order of 100 volts to the maximum Stark voltage that could be applied across the two halves, but since the Stark field acted along the whole length of the cavity, 50 volt pulses produced sufficient broadening to give complete quenching of the maser oscillations for the range of excitation used.

It will be seen that the time of silence obtained with the split cavity is nearly the same as that observed in the three-probe case. This is perhaps a consequence of the low values of Stark field available in the split cavity experiments, since some degree of

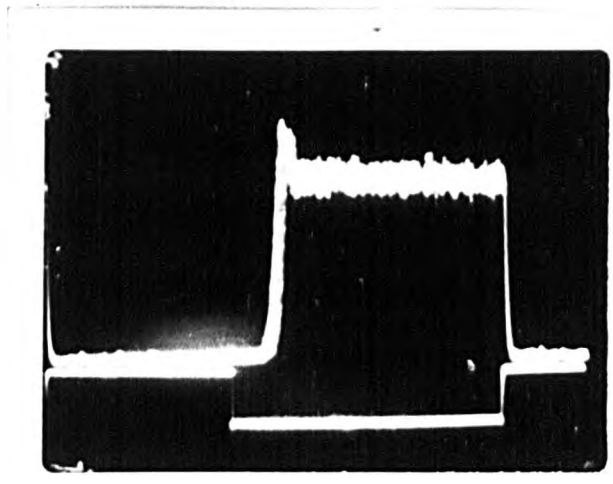

Figure 3.13. Split-cavity amplitude transients (obtained with 1 kHz square-wave Stark pulses).

state-mixing will undoubtedly occur whenever the quench-field - induced "decoupling" between the molecules and the cavity field at $\nu_o$ is incomplete.

However, since the two halves of the split cavity were electrically isolated, and the Stark pulser, when nominally "off", was in fact offset from earth by about one volt (the saturation voltage of the transistors used), it is possible that this extremely small Stark field could have modified both the amplitude transients and the time of silence. This point was investigated by observing the transients produced in the split cavity under two different conditions when the single central Stark probe was used for quenching, (a) driving the single probe from the second channel of the pulser, while maintaining the original channel of the pulser (connected across the two halves) in a permanently "off" state, (b) linking the two halves electrically to earth, and using the single probe, in conjunction with either channel of the pulser, as before.

There was no detectable difference between these transients and those obtained at the same beam flux (but with lower separator voltages) in an unsplit cavity with a single probe. It therefore seems reasonable to think of this type of split cavity as equivalent to an infinite number of probes, each producing an inhomogeneous Stark field, in contrast to the parallel-plate type of maser resonator, (when operated with a Stark field across the plates).

It is interesting to note in passing that the enhanced time of silence associated with the use of several Stark probes for quenching purposes at high excitation, and ascribed here to state-mixing, was not observed in related experiments which used a multiple-probe arrangement (Shakhov 1969). It should be mentioned at this stage that the present work on Stark quenching was stimulated not by Shakhov's paper (which only appeared in the West in

1973) but by a preliminary study, in the maser used by the author, of the effects of partial oscillation quenching with a single Stark probe (Bardo and Lainé 1971). The results obtained by Shakhov are reproduced for convenience in figure 3.14. It will be seen that the superradiant overshoot effect which follows the removal of the quenching perturbation was marginal; clearly, the value of the self-excitation parameter $\beta$ in the maser of Shakhov was far below that obtained in the present work.

Less difference might have been expected, however, since Shakhov sent molecular beams into the resonator from both ends, thereby increasing the flux, and hence the excitation. This discrepancy may have been due in part to an inappropriate choice by Shakhov of the number of probes used (six, needing six holes in the side of the resonator, each hole presumably comparable in size with the microwave coupling hole) and of the insertion depth for these probes (since it was apparently necessary to apply 1000 volts to all six of these probes simultaneously to quench these weak oscillations). However, it is more likely that a single chamber apparatus was used, in contrast with the differential-pumping arrangement described previously in this thesis (Bardo and Lainé 1971); the use of a single chamber would set a much lower limit to the attainable beam flux, even allowing for the fact that some of the results of Shakhov were obtained with opposed beams.

One important feature of the ammonia maser is that the maser characteristics depend on the particular combination of focuser and molecular beam source used, since the beam passes completely through the system. In an hydrogen maser, however, the resonator contains a storage bulb, where the atoms remain, on average, for a "dwell-time" $T_b$ of perhaps half a second before diffusing out. Many collisions will occur inside the bulb in this time, with the result

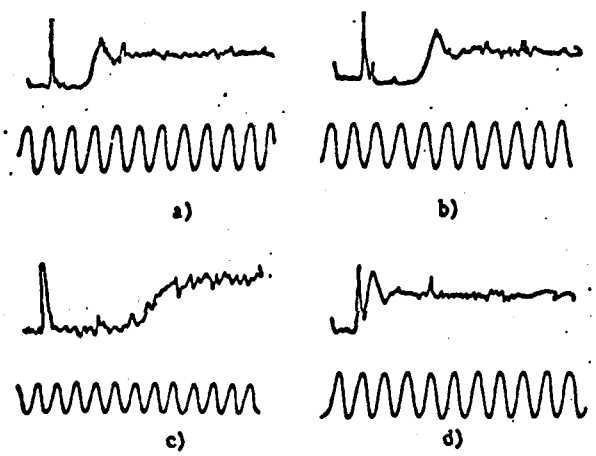


Experimental characteristics of the amplitude build-up in a maser: a) $A = A_{max}$, $u_{cc} = 26$ kV; b) $A = 0.5\ A_{max}$, $u_{cc} = 26$ kV; c) $A = 0.1\ A_{max}$, $u_{cc} = 18$ kV; d) the case of two opposed beams.

FIGURE 3.14. Multiple-probe transients (After Shakhov 1969).

that the characteristics of the beam source would not be expected to affect the probability of the presence of upper-state atoms; this probability is characteristically of the form $\exp(-t-t_o)T_b$ (Audoin 1966), where t is the moment of observation and $t_o$ is the moment of arrival in the bulb.

Furthermore, while the resonance line in the hydrogen maser is much narrower than the resonance line in the ammonia maser, the excitation parameter $\beta$ for hydrogen usually takes a much lower value, since the spin-exchange loss mechanism in hydrogen is density dependent, (and hence increasing the atomic beam flux to give a population density comparable with that in the ammonia maser only results in a decrease in the output).

It is found as a result that the value of $\beta$ is insufficient to observe amplitude transients unless the hydrogen maser is operated with the natural frequency of the cavity set close to the frequency of the atomic transition. Any change in frequency (and hence relative phase) which can occur during the build-up process will thus be very small (indeed, much smaller than in the ammonia maser). The non-linear maser equations can therefore be separated with confidence into almost completely uncoupled equations, as explained in chapter two, with one set here describing amplitude fluctuations and another describing phase fluctuations.

Since the probability function in the hydrogen maser is exponential in form, these considerations lead to a simple expression for the build-up process in an hydrogen maser (Audoin 1966):

$$\mathcal{E} = A\left[\exp(-t / 2T_1)\right]\left[\cos(\omega_1 t + \Phi)\right] \qquad 3.10.$$

with

$$\omega_1^2 + \left(\frac{1}{2T_1}\right)^2 = 2b_s^2 \qquad 3.11.$$

where $\mathcal{E}$ is the amplitude of the electromagnetic field in the cavity, $\omega_1$ is the frequency of the damped oscillation, $\Phi$ is the phase of

the oscillator at any time, and $b_s$ characterises the steady-state value of $\varepsilon$, $\varepsilon_s$, i.e. is a simple function of $\beta$, being in fact equivalent to the nutation frequency, $(\mu\varepsilon_s/\hbar)$.

Both these equations have been verified in the hydrogen maser, using an inhomogeneous Zeeman field (provided by opposed Helmholtz coils around the bulb) to achieve atomic Q-switching in hydrogen (Audoin et al 1968). Typical results for the amplitude transient are shown in figure 3.15.

The establishment process did have an associated time of silence, although the degree of overshoot, even with artificial Q-enhancement, (to increase $\beta$), was only perhaps one-third of that observed by the author in the ammonia maser. However, no information is available regarding any time-of-silence enhancement in hydrogen. With partial quenching, the fractional change in oscillation level was small (less than 5%), but there was rather more oscillatory build-up behaviour than in ammonia.

This difference in behaviour must be due to two factors: the effect of source characteristics on the velocity distribution in the ammonia maser, and the greater degree of non-linearity (and hence increased coupling between the amplitude and phase transients) which occurs in Q-switched ammonia masers. Although considerable effort was expended by the author on the construction of phase-measurement instrumentation when this difference was found, it did not prove possible at that stage to investigate any modification to the phase transient in the ammonia maser which could have resulted from the higher value of $\beta$ used. Nevertheless, it would be expected that such transients would be considerably different from those observed in the hydrogen maser. This follows since second-order calculations (Audoin 1968) show that when the overshoot is more than about 10% of the steady-state oscillation level,

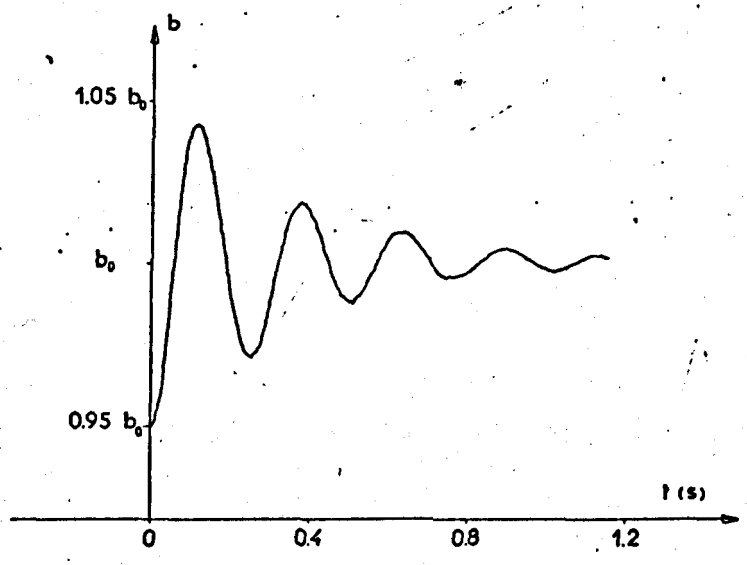


Example of recorded amplitude transient.

FIGURE 3.15. Q-switching in an hydrogen maser (after Audoin et al 1968).

the associated non-linearity manifests itself as a modification of the amplitude transient. Thus, while the maser performs damped oscillations at $\omega_1$, (as before), according to this theory it should also undergo damped oscillations at twice this frequency; the interference between these two motions will therefore be expected to cause the system to stabilize much faster than at low levels of excitation, such as obtained in the hydrogen maser. This effect is a feature of the amplitude transients of figures 3.5 et seq, but the very non-linearity of these results means that a quantitative comparison with the predictions of Audoin may be difficult.

Two other aspects of the Q-switching process in masers do not appear to have been investigated previously - the changes which may occur in the values of the polarization and the population excess during Q-switching. In ammonia, any such changes may be detected by using a second cavity in cascade with the first, but, as explained in chapter two, it is difficult to monitor even low frequency fluctuations in the population excess, while it is a comparatively easy matter to investigate changes in the polarization signal. Thus, it was found by the author that the polarization (and hence the magnitude of the "pulse" received by the beam in the first cavity) varied with time during Q-switching, as shown in figures 3.16 and 3.17.

This behaviour may be explained by representing the evolution of the total Bloch vector of the system geometrically (Feynman et al 1957), as explained in chapter one. In this representation, provided the first cavity is tuned to the molecular resonance frequency $\omega_o$, switching the Stark field off will cause the vector to trace out a path in the II - III plane which eventually joins that locus obtained as a parametric function of focuser voltage (Bardo and Lainé 1971). It will be recalled from

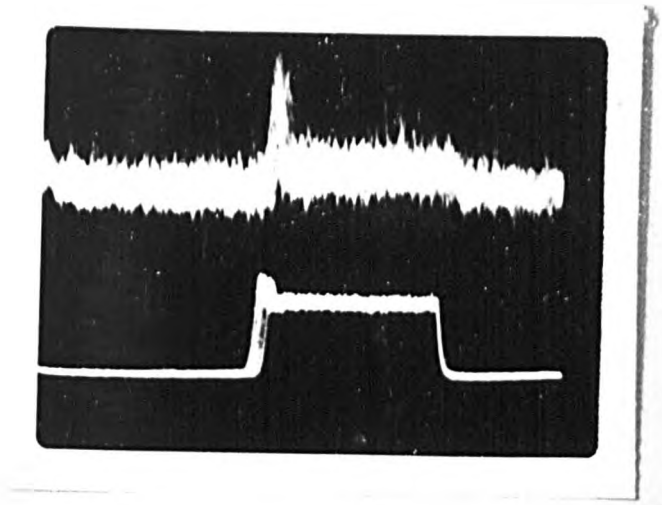

(a)

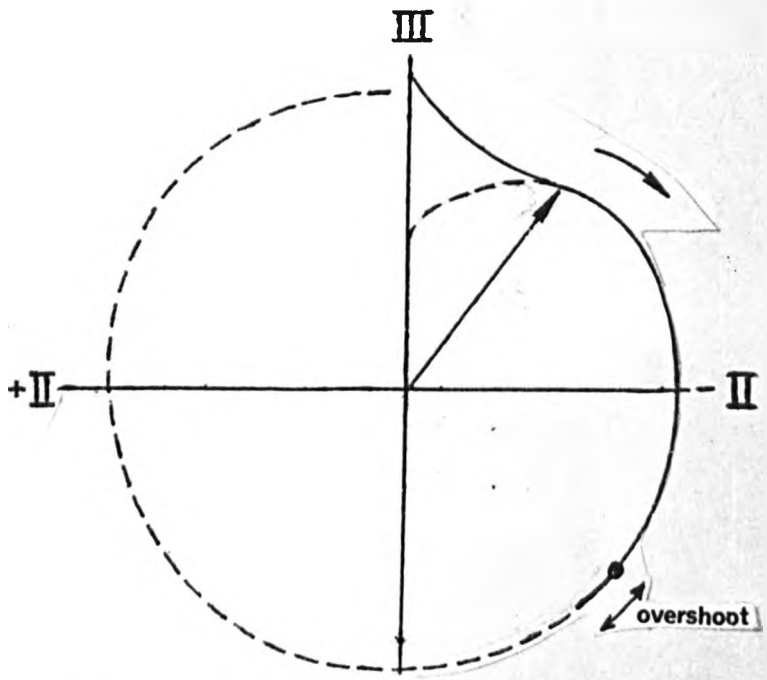


(b)

Figure 3.16 (a) Simultaneous fluctuations in amplitude ($C_1$ signal, lower trace) and polarization ($C_2$ signal); (b) the corresponding geometrical representation.

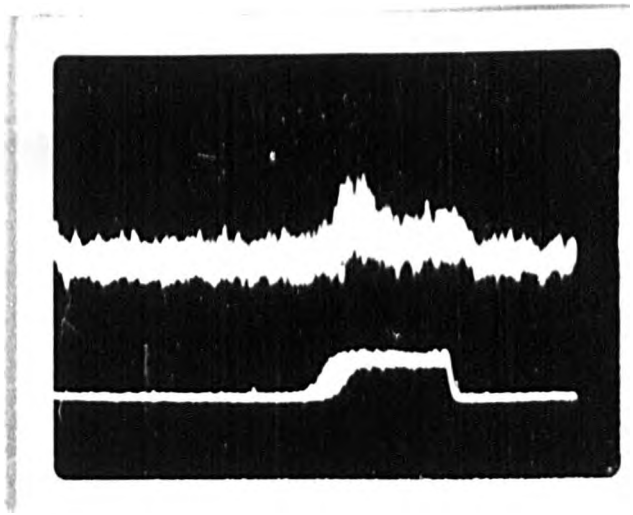

(a) 17 kV ; gain x 10

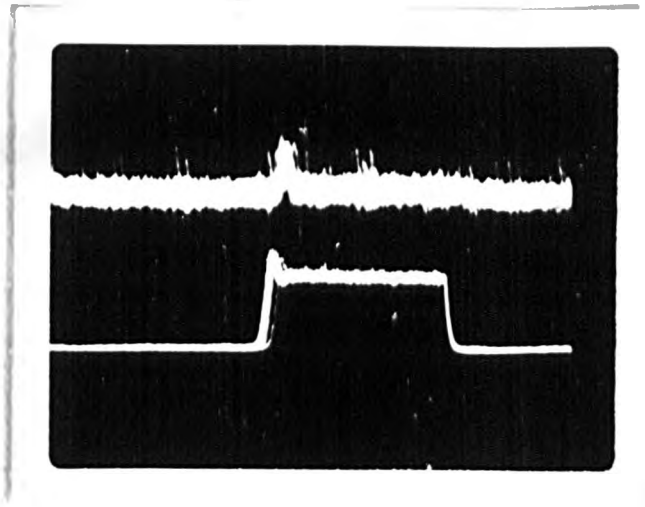

(b) 19 kV ; gain x 1

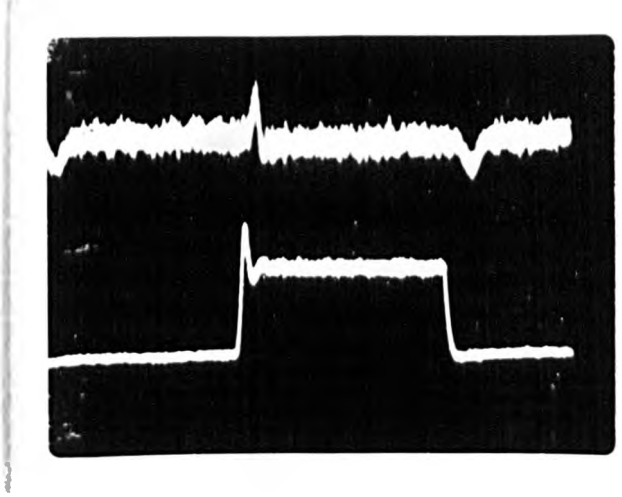

(c) 25 kV ; gain x 1

Figure 3.17. Polarization fluctuations after Q-switching; lower trace shows corresponding amplitude changes.

chapter one that the projection of the vector on axis III is proportional to energy (or to the difference in level populations for an ensemble of molecules), while the projection on the II - I plane is proportional to the polarization, (or to the experimental value of the induced dipole moment). In the case shown in figure 3.16, 20kV was applied to the focuser. Close inspection of the associated transient revealed that as the oscillation signal in the first cavity increased, the polarization signal in the second cavity went through a maximum (corresponding to a $\pi/2$ pulse in the first cavity), then, as the vector moved past this point on the locus, decreased (showing that the excitation was between $\pi$ and $\pi/2$), before settling down quickly to a slightly higher level (nearer $\pi/2$ excitation). A similar argument shows that when 17 kV was applied to the focuser (figure 3.17), the polarization must have gone through the $\pi/2$ point stabilizing at a point between $\pi/2$ and $\pi$, while at 25 kV the final polarization corresponded to excitation past the $\pi$ condition. These results are particularly interesting because they appear to provide the first confirmation of the predictions of a semiclassical approach to Q-spoiling in superradiant systems (Buley and Cummings 1963), viz. that overshoot can occur even though the system may be past the $\pi$ condition, (i.e. be inverted), as shown in figure 3.18.

The two other methods of transient production in masers which remain to be discussed involve inducing a sudden change in either the losses of the system ("Q-spoiling") or the rate at which molecules enter particular energy levels (Grasyuk and Oraevskii 1964).

The quality factor of a resonator can be changed very rapidly in lasers by using the optical modulation provided by a Kerr cell or a saturable absorber (although, as stated previously, excitation levels in Q-switched lasers are insufficient for cooperative build-up to be important). However, in the microwave region of the

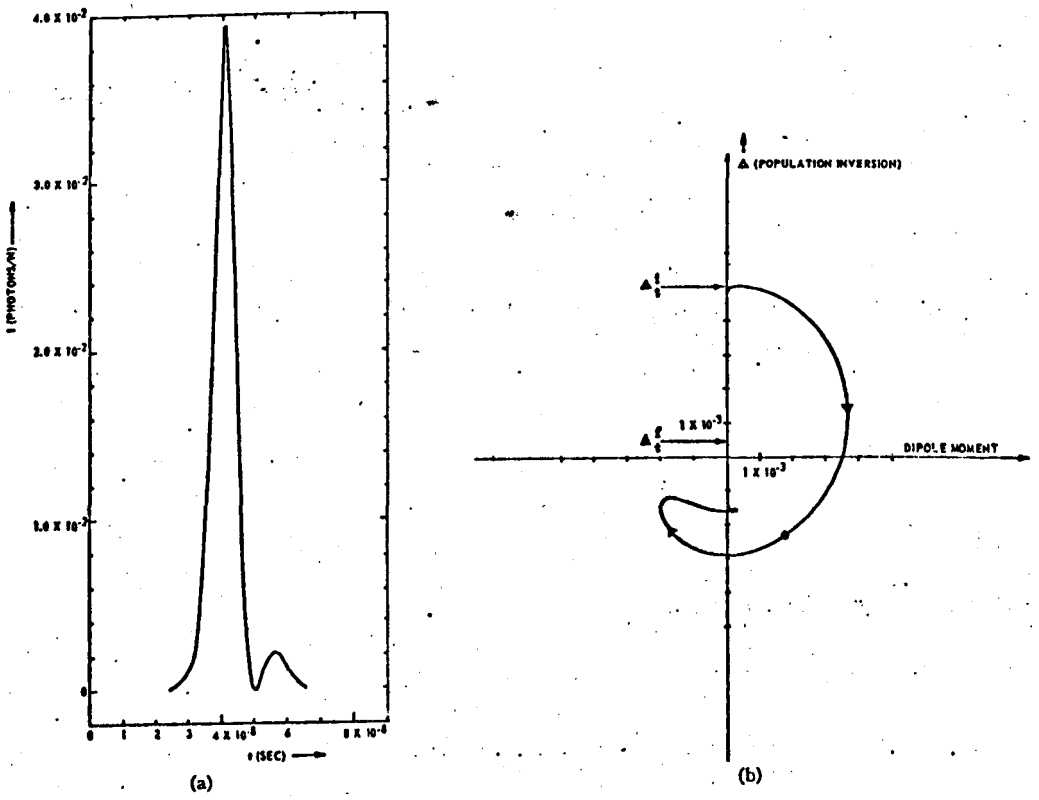


FIGURE 3.18. Q-switching in a superradiant system; (a) observed signal, (b) corresponding evolution (After Buley and Cummings 1963).

spectrum the decrease in level of excitation which is associated with the use of analogous devices generally precludes intracavity switching, and external Q-modulation techniques must therefore be used.

Thus, superradiant transients similar to those shown in figure 3.15 have been induced in both an hydrogen maser (Audoin et al 1968) and a nuclear spin maser (Combrisson 1960) by switching into circuit a (cavity) Q-multiplier, operating at the maser frequency, thereby reducing the effect of losses in the system. The author has found that a Q-multiplier based on what may be termed "frequency-conversion" feedback (with gain provided by the intermediate frequency amplifier, a fraction of whose output was fed back to the maser cavity after upconversion to the maser frequency) reduced the oscillation threshold in a like manner in an ammonia maser. In this case, while it increased the size of the amplitude transients, it prevented a "free" build-up of the oscillation signal, since it introduced an undesirable amount of noise into the system; a similar criticism could doubtless be leveled against any oscillator based on an external Q-multiplier. It is noted in passing that the effects of noise on build-up are much reduced if the impedance presented to the cavity is modulated, either with the diode switch described in connection with the Zeeman maser, or with the equivalent mechanical arrangement, a toothed wheel providing a variation in matching as it moves relative to the coupling hole (Smith and Lainé 1968).

The final method of Q-switching, that of altering the "pumping rate" between one (or more) pairs of energy levels, has one major drawback - the effective speed of switching may be too slow to allow the observation of transitory behaviour. Thus, even if a change is induced in a time $T \ll T_1, T_2, \tau_R$ in the flux of atoms or molecules leaving the source-cum-focuser combination in a particular energy

state, (e.g. by driving the focuser with a square-wave), the build-up process will be slower than that which would occur using one of the methods previously described. This follows from equation 3.9: $\tau_f$ then depends on the time of flight outside the cavity, which can be 100 $\mu$seconds or more in typical systems. The switching speed therefore effectively decreases, and the time of silence increases, although this change in speed is negligible when other characteristic times are long, as in hydrogen. Superradiant transients can not, therefore, be induced in ammonia masers by altering the source pressure, or by varying the focuser voltage (as found by Grasyuk and Oraevskii 1964), but have been induced in an hydrogen maser by pulsing the discharge tube (Nikitin and Strakhovskii 1966).

However, transients can be induced in ammonia if the effective switching speed is increased by changing the rate at which the molecules actually in the cavity can contribute to the transition of interest (in this case, the 3,3 line of ammonia). For example, since the quadrupole lines in ammonia share energy levels in common with the maser line, intra-cavity saturation of one of the quadrupole lines will change the transition probability at the maser frequency. The resulting population depletion may be sufficient to completely quench maser oscillations, even though, in contrast to the situation outlined in chapter two, excitation and detection of quenching occur at two different frequencies (Shimoda and Wang 1955). In the $^{14}NH_3$ maser, the relevant selection rules are $\Delta F = 0$ for the main line, and $\Delta F = 1$ for the nearby (upper) quadrupole transitions (or $\Delta F = -1$ for the lower frequency pair of quadrupoles). That this procedure can lead to quenching in the steady-state will be seen if it is assumed that the quenching signal used to irradiate the system at either of the upper quadrupole frequencies causes perhaps 20% of the molecules in the $F_1 = 3$ upper

state to make a quadrupole transition. The $F_1 = 3$, $\Delta F = 0$ transition rate will therefore be reduced by this factor, as will the $F_1 = 2$, $\Delta F = 0$ rate (assuming that the $F_1$ sublevels are equally populated initially). The intensity of the main maser line will therefore be reduced by about 16% while the intensity of the $F_1 = 2$, $\Delta F = 1$ transition is enhanced and the strength of the $F_1 = 3$, $\Delta F = 1$ transition is reduced. The author has found that this method of quenching can be modified to cause rapid population depletion, by sweeping across the quadrupole resonance (in a time less than other characteristic times of the system, if transients are to be observed). Although this modification is <u>without</u> the complications associated with quenching directly at the oscillation frequency, (Lainé 1967), such as the presence of an injected signal near $\nu_o$ throughout the build-up, it has not, so far, resulted in complete saturation, with the result that the transients produced are not yet as marked as those obtained with the most effective method of quenching, that of Stark broadening.

Section 3.4. Stark transients in an ammonia maser.

As explained in the previous section, one advantage of the probe technique of Q-switching via Stark broadening of the spectral line is that the quality factor of the maser cavity is not appreciably degraded by the presence of the probes if they are made of fine wire. However, since the region of inhomogeneous field produced by such probes is very localized, it is possible that if only a single probe is used, and the maser oscillation level with the probe earthed is well above that required for observation of an oscillatory build-up transient, then even large probe voltages will leave the maser above oscillation threshold.

If a square-wave is applied to the probe in such a case, two distinct stabilization regimes result, one being associated with the build-up of oscillations (a "switching-on" transient), and the other with switching the maser from a high level of oscillation to a lower level by Stark broadening (a "switching-off", or "Stark" transient). The first type (obtained following the removal of the perturbation) appears identical to the superradiant transients of the previous section (which are the result of complete quenching), but the second type of transient (which follows partial quenching) has completely different characteristics, as will be seen from figure 3.19.

For example, the decay constant and the frequency of the oscillatory switching-off transient are typically much slower than for the switching-on transient, although the frequency of both types of transient increases as the oscillation level increases. The final oscillation level reached after the switching-off transient is also usually lower than that required for observation of an oscillatory switching-on transient. Thus, whereas the switching-on transient appears because of the radiation damping

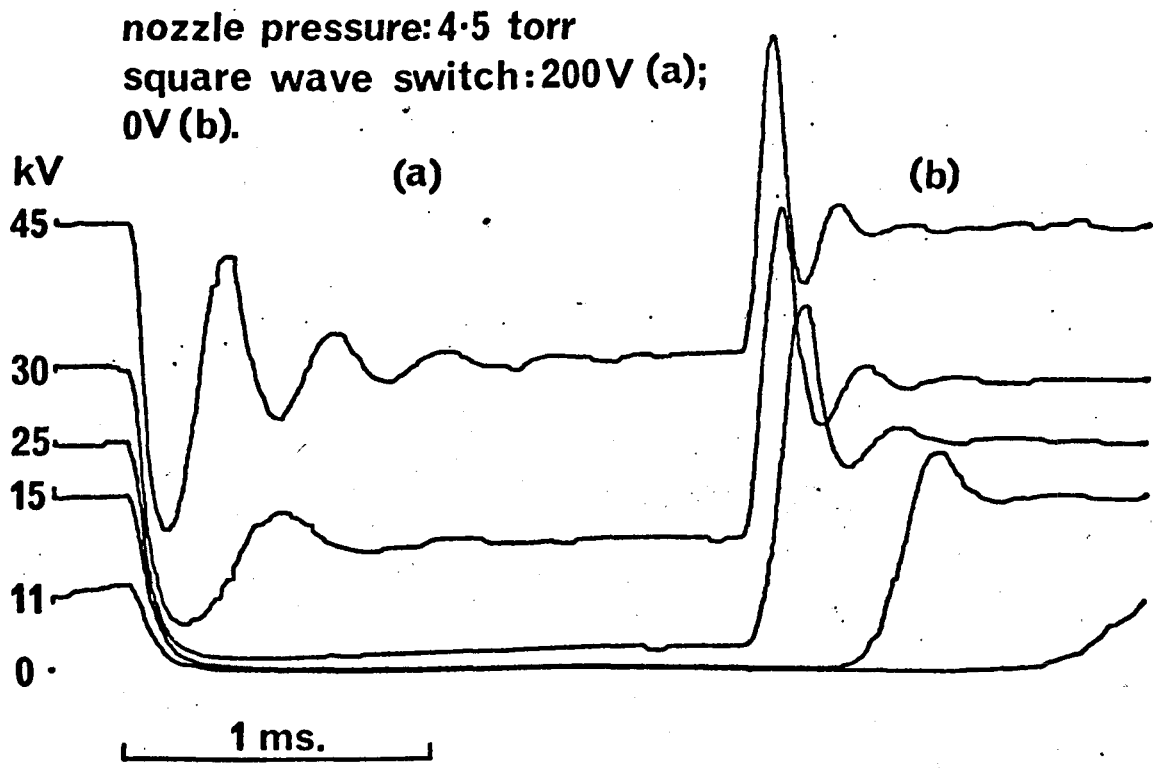


FIGURE 3.19. Amplitude transients, accompanying the build-up and decay of oscillations, induced by the central Stark probe.

effects associated with a sudden over fulfilment of the condition for oscillation in a quantum mechanical oscillator, it may be assumed that this phenomenon is not the prime cause of the oscillatory Stark transients.

When attempts were made to provide an alternative explanation, in terms of models based upon other effects known to occur in either passive systems or masers, however, two major difficulties preventing an immediate interpretation of the present phenomenon were discerned:

(a) the sudden application of a Stark perturbation to a passive system which is pumped by a coherent source will generally induce the simultaneous appearance of several transient effects, these having broadly similar characteristics (Brewer and Shoemaker 1972).

(b) if any of these effects occur in a Stark-perturbed maser oscillator, they will be modified by regeneration, because of the active nature of such a system.

These difficulties were overcome by comparing particular aspects of each model, such as magnitude of relaxation times, and dependence of relaxation times on Stark field. This procedure provided a cogent explanation of the Stark-probe transients, (as will be seen in subsequent pages), based upon the nutation effect observed when a Stark field is used to switch a passive system in or out of resonance with a coherent source (Brewer and Shoemaker 1972). This section therefore shows, by analogy with passive systems, that the maser Stark transients are due to what is termed "regenerative nutation" by the author.

The first possibility explored was that the maser transients could be explained with the aid of a free induction decay (FID) model.

If FID is to be observed in a passive system where the Stark field is homogeneous, molecules must be excited by a coherent source and then be suddenly shifted far off resonance. The signal emanating from these molecules at the Stark-shifted frequency will decay exponentially with a homogeneous field relaxation time constant $T_2$, being detected as a heterodyne beat with the source (Brewer and Shoemaker 1972). Similar FID effects should arise in any beam maser which is based upon an open resonator of the Fabry-Perot type, if the two plates can be maintained at different potentials, since this parallel plate arrangement will provide a highly homogeneous Stark field.

If ammonia is proposed as a working substance to test this hypothesis, however, the fact that molecules in different $M_F$ states of the 3,3 transition Stark-tune at different rates (Shimoda, Wang and Townes 1956) should be considered.

When an $E_{010}$ mode cavity is used, however, as in the present experiments, the Stark field must be produced either by a probe or by slicing the cavity into electrically isolated sections. In either case the field will be considerably less homogeneous. The FID signals from molecules in different regions of the cavity will therefore interfere. A substantial decrease in the time for which FID signals can be observed from the complete system should then result. It was because of this that a model based on the FID phenomenon seemed incapable of accounting for the signals actually observed in an $E_{010}$ mode cavity.

In passing, it will be appreciated that some molecules will only be slightly perturbed by the (inhomogeneous) probe field, even when it is large, and if such molecules remain within the amplifying bandwidth of the maser the decay rate of their polarization signals will be reduced by regeneration. Later discussion will

show that while such an "active" decay appears superficially similar to FID, it is in fact better described in terms of the nutation effect.

With the shortcomings of the FID model in mind, an explanation was sought which was based upon the existence of inhomogeneous fields near the probe. Accordingly, the observation that the upper state molecules needed for maser operation are normally selected by means of inhomogeneous electric fields in the state separator prompted contemplation of the possible effects of intra-cavity space quantization.

Equation 2.1 shows that the oscillation frequency of a beam maser is a function of the amplitude of the cavity radiation field. This amplitude depends upon spatial re-orientation (see, for example, equation 2.26), because the probability of emission from molecules in the resonator is greatest when the interaction between the molecules and the radiation field is strongest. This occurs when molecules are in a state of maximum M (relative to the micro-wave electric field in the resonator).

Thus, since the stray electric fields between the ends of the focuser and the resonator have a longitudinal character (regardless of whether the state separator used has a transverse or a longitudinal electric field), the excitation of the maser resonator will be strongest when the resonator radiation field is longitudinal with respect to the axis of the molecular beam (Krupnov and Skvortsov 1966). Furthermore, if weak magnetic or electric fields of the order of $10^{-4}$T, $10^{4}$ $Vm^{-1}$ respectively, acting on the molecular beam outside the resonator, are present, altering the magnitude of these fields will cause the amplitude of oscillations in the resonator to change substantially (Basov, Oraevskii et al 1964).

As discussed in connection with the Zeeman maser in chapter two, these observations can be explained if it is assumed that the weak fields cause the molecules to "rotate". The question therefore arose as to whether the Stark transients were in fact amplitude fluctuations associated with an analogous reorientation process, albeit in a localized intra-cavity field. For the purpose of discussion of this question it will be assumed that three groups of molecules exist at any time: (a) those which have just entered the cavity, (b) those which are close to the probe, and (c) those which are about to leave the cavity. It will be assumed in addition that the amplitude of oscillations in the absence of the Stark field is high, so that molecules near the exit absorb energy from the cavity radiation field, while molecules in the first part of the resonator make downward transitions, hence augmenting the field. It can then be stated that any reorientation effects which accompany Stark quenching will only be important for those molecules which are far from the probe, since the inhomogeneities in the electric field (and hence the quenching effects of this field) are greatest close to the probe.

Any emission or absorbtion in the immediate region of the probe would therefore be quenched, as explained previously, as soon as the Stark field was applied, but molecules in a particular M state in groups (a) and (c) might be "rotated" (e.g. from M = + 3 to M = 0, or perhaps to M = - 3). At the instant of switch-on, therefore, this would cause a decrease in any emission from molecules in group (a) and in any absorbtion from group (c), causing a change in oscillation amplitude additional to that expected from quenching considerations. This additional "reorientation-induced" change could be oscillatory, as molecules in group (a) eventually moved into group (c), but any such oscillations would damp out in

a time less than the time of flight $T_1$ through the cavity, even if all molecules had the same velocity. Furthermore, their frequency would not be expected to vary with oscillation level. It would therefore appear that since the switching-off transients do depend on oscillation level, and also decay several times more slowly than $T_1$, any contribution from intracavity reorientation effects must be small.

This was confirmed by using combinations of the three probes available, probes 1, 2 and 3, but applying the Stark pulses sequentially to each probe, with a variable delay between the pulse on one probe and the pulse on the next probe. An appropriate delay would cause the Stark field to "follow" any such group of molecules, hence augmenting any reorientiation transients which might be present. However, although time delays ranging from zero to as much as 100 $\mu$seconds were used, sequential pulsing only had the effect of increasing (relative to the zero-delay case) the damping of the Stark transients. This definitely indicates that some mechanism other than pure spatial reorientation was responsible for their appearance.

Reconsideration of this model indicated a third possible explanation: that probe Stark fields could perhaps effectively modify the molecular energy-level diagram, in a manner similar to the (magnetic) level-mixing/crossing described in chapter 2. Any associated transient phenomenon would be a manifestation of interference between a coherent superposition of states which do not normally interact. Such "level-perturbations" could be the result of either Majorana-type transitions (eq.2.27) or "sideband-generation" - type effects (Brewer 1971).

Perturbations of the first type could arise in two ways: (i) by the generation of Stark pulses with Fourier components which

cause an increase in the appropriate (magnetic- or quadrupole-associated) transition rates. This mechanism seems unimportant, since neither a hundred-fold increase in the rise time of the Stark pulses nor a similar variation in p.r.f. had any visible effect on the transients.

(ii) molecules moving past a probe would perceive a field which varied with time. Although the amplitude of maser oscillations might vary if the frequency of this variation corresponded to the separation between suitable energy levels, any resulting transients would be damped out, (and hence be shorter-lived than those actually observed), because a beam maser is not a univelocity system.

The second type of perturbation (which involves the generation of coherent "sidebands" by modulation of the molecular level spacings) is well-known in passive systems (Autler and Townes 1955, Luntz 1971), and has been observed to cause parametric resonance modulation in an hydrogen maser amplifier (Audoin et al 1969). However, since even in a passive system such a process is critically dependent on p.r.f. and perturbing-field homogeneity, it seems that this cannot be the cause of the present transients.

The fourth possibility explored was that these transients were the result of a "two-photon" Raman process, analogous to that observed in passive systems (Shoemaker and Brewer 1972). These workers induced this effect in certain degenerate molecules by using a resonant laser pump to establish a high degree of coherence among the magnetic sublevels. In these molecules the Stark effect was linear, so that all M states Stark-tuned in the same way. Accordingly, once the degeneracy had been resolved by a uniform Stark field, the molecules began to emit, generating both short-lived FID signals and, by non-linear mixing, long-lived

(lifetime $\sim T_2$) Raman signals, the latter being produced at a frequency corresponding to forbidden transitions with $\Delta M = \pm 2$.

Three factors make this seem particularly relevant to the present work:

(i) sublevel-coherence is automatically present in a self-oscillating maser,

(ii) those molecules making transitions from one sublevel to another and back again can therefore maintain a certain degree of coherence in this "pumping cycle",

(iii) The amplitude stabilization process in a self-oscillating system is inherently nonlinear.

Since the probability of occurrence of such a "two-photon" process would be expected to depend on the homogeneity of the Stark field, this point was checked by using an $E_{010}$ mode cavity which had been split longitudinally, as described in section 3.3.

One half of this cavity was always earthed, so that pulsing the other half subjected all the molecules within the cavity to approximately the same degree of Stark broadening. This half had also been drilled out to take a single, centrally placed Stark probe. Although this machining process degraded the cavity quality factor substantially, making the oscillation threshold condition perhaps twice as difficult to satisfy, the flux of active molecules was sufficient for the observation of strong superradiant build-up transients. However, while oscillatory Stark transients were observed when the two halves of the cavity were earthed and the central probe was used for Stark pulsing, no oscillatory decay of any kind was detected when this probe was earthed and a Stark field was applied across the two halves of the cavity.

One would expect that if a two-photon process can take place in an $E_{010}$ mode cavity, the accompanying transients would be more

pronounced with a more homogeneous (split-cavity) field. This therefore indicates that the Raman model is not in fact an appropriate one to use for these experiments. Indeed, even the "mixing" aspect of this model, when considered in isolation, appears to be unrelated to the present experiments, as will be seen if the effect (on a simple mixing model) of a small, localized Stark perturbation, such as is produced by a Stark probe, is considered. Use of the probe will:

(a) shift the maser oscillation frequency, from $\omega_o$, the unperturbed frequency of oscillation, to $\omega_{stark}$, the frequency with the Stark field on,

(b) allow the superradiant emission (at $\omega_o$) from unperturbed molecules to mix with the signals at $\omega_{stark}$, producing a signal modulated at the difference frequency.

However, this modulation must be extremely small, because although increasing the Stark field increases $\omega_{stark}$, the Stark transient modulation frequency $\Omega$ actually decreases.

This is not really surprising, because our mixing model did not include either the relative strengths of these two signals or the effect that regeneration would have. For examples, experiments on electric dipole systems which are suddenly irradiated by a coherent source have shown that when the source and sample are separate, the sample nutates about an effective driving field, the nutation frequency $\Omega_n$ being given by the formula (Tang and Silverman 1966):

$$\Omega_n = \left[ (\omega_s - \omega_o)^2 - (\mu E / h)^2 \right]^{\frac{1}{2}} \qquad 3.12.$$

where $\omega_s$ is the frequency of the source, $\omega_o$ is the resonance frequency of the transition in question, E is the strength of the driving field, and $\mu$ is the dipole matrix element.

Nutation is a particular kind of forced motion, and it is known that a qualitative similarity exists between the "free" nutation behaviour of equation 3.12 and the time evolution of coherently-prèpared passive ensembles undergoing forced motion (Nurmiko and Schwarz 1972, Lefrèreand Lainé 1972).

The final model we consider here, therefore, takes as its basis

(i) the field strength - cum - detuning aspects of a "free" nutation experiment, together with

(ii) the effects of regeneration on a nutating system consisting of a coherently-prepared sample, which has an oscillating polarization at one frequency, suddenly coupled to a source of another frequency by a common radiation field.

The output of such a system will be amplitude modulated, and the frequency of this modulation will depend on both the detuning parameter ($|\omega_s - \omega_o|$, using the notation of equation 3.12) and the strength of the source "oscillator" involved. Furthermore, regeneration will reduce the decay rate of the sample polarization signal, and will therefore make these settling transients relatively long-lived.

It was stated previously that when a single Stark probe is used, switching the probe field on and off generates two signals, one being at the new, Stark-shifted frequency, $\omega_{stark}$, and the other (a decaying polarization signal, associated with those molecules far from the probe) being at the frequency of the unperturbed maser, $\omega_o$. If the signal at $\omega_{stark}$ is equated with the "source" signal, and the unperturbed moles are taken to represent the "sample", this appears to provide a particularly apposite model of the maser Stark transients described in this thesis.

For example, if other parameters are kept constant, an increase in the effective saturation parameter, $\mu E/\hbar$ (and hence of the regeneration), achieved by increasing either beam flux or separator EHT, should result in an increase in both $\Omega$ and the decay time of these transients. Indeed, this decay time may well be longer than the time of flight through the cavity, provided $\omega_o$ is within the amplifying bandwidth of the Stark-perturbed maser.

Similarly, increasing the Stark field should reduce the stabilization time (since $\mu E/\hbar$ will decrease) and increase the detuning parameter. However, since any change in saturation parameter is always greater than the corresponding change in $\omega_{stark}$ when the probe technique is used (Shakhov 1967), the modulation frequency $\Omega$ should decrease. Both these sets of predictions are in agreement with experiment. Furthermore, the increase in damping observed when 2 or 3 probes are used can be explained quite simply by assuming that the decaying polarizations (which, in our present model, are associated with different regions of the cavity) are initially out of phase; the separate modulation signals will then interfere.

It can therefore be seen that all aspects of the Stark transients generated by the author in an $E_{010}$ mode cavity can be explained using this qualitative "forced regenerative nutation" model.

Section 3.5. Polarization transients in a beam maser.

The Stark transients just described were produced with the aid of an intracavity electric field. In this section another Stark-induced effect, obtained with an intercavity field, is reported and interpreted.

Early experiments on two-cavity beam masers in which the cavities were coupled unilaterally by the beam showed that when the first cavity $C_1$ was tuned to the centre of the molecular resonance, at a frequency $\omega_o$, an oscillation signal in $C_1$ was accompanied by oscillations at the same frequency in the second cavity $C_2$. The strength of these oscillations varied with the tuning of $C_2$, being greatest when $C_2$ was also tuned to $\omega_o$ (Higa 1957, Reder and Bickart 1960).

Later investigations into the case where both cavities were tuned to $\omega_o$ showed that the emission power in $C_2$ could be varied by applying a weak inhomogeneous electric field, of the order of $10^3$ $Vm^{-1}$, between the cavities. Indeed, the level of these induced second-cavity signals went through a pronounced maximum as the field was increased, decreasing to zero when a value of about $10^4$ $Vm^{-1}$ was reached, since such fields were sufficient to destroy the oscillating polarization carried by the beam (Basov, Oraevskii et al 1964).

These results may be contrasted with the present work, where an intercavity Stark field is suddenly switched on and off. The concomitant changes observed in the level $A(C_2)$ of the signal from the second cavity are of a transitory nature, as shown in figure 3.20. The particular system used was the differentially-pumped ammonia beam maser previously described, using $E_{010}$ mode single-port resonators tuned to the $J = K = 3$ transition as before, with the addition of a short (30 mm) intercavity ring focuser (Bardo and

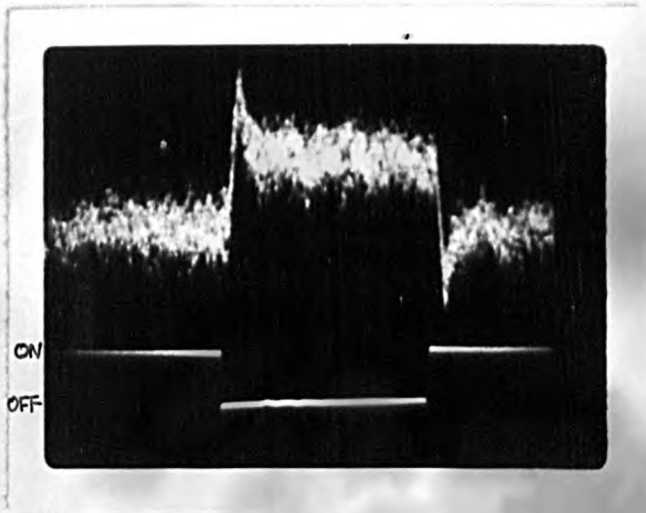


Figure 3.20. The effect of an intra-cavity Stark field on the polarization signal detected in the second cavity.

for self-oscillations in $C_2$ (Strakhovskii and Tatarenkov 1962). Since such a final state corresponds to a situation in which the oscillating polarization carried by the beam synchronizes the weaker self-oscillation of $C_2$, it can be surmised that the intermediate stage (corresponding to a sudden increase in $C_2$ signal) is related to the forced (and damped) precession observed in coherently prepared systems driven by a pulsed coherent source (Nurmiko and Schwarz 1972). Simultaneous momentary changes in $A(C_2)$ resulting from the spatial reorientation phenomenon previously mentioned should also take place, but these will generally be masked by the much larger amplitude fluctuations associated with the locking process.

In conclusion, it is noted that the characteristics of the synchronization transients should be strongly dependent on the relative detuning of either $C_1$ or $C_2$ from $\omega_o$, a result which could perhaps be applied to the problem of tuning a mutually synchronized two-cavity maser employing two opposed beams (Belenov and Oraevskii 1963).

Section 3.6. Summary and proposals for further work.

As explained in chapter one, the initial stages of this work were primarily concerned with one specific aspect of coupled molecule - radiation field interactions in an ammonia maser: discovering whether self-induced radiation-damping type instabilities ("spiking") would occur at high levels of excitation. Although this question has still to be fully answered, the excitation levels actually reached were sufficient for the observation of a number of related phenomena.

Chapters two and three show that many of the results thereby obtained were of a preliminary nature. Accordingly, the author's suggestions for further experiments fall into two groups: the first group involves more detailed investigations, preferably quantitative, on the effects described here for which only qualitative results exist; secondly, further qualitative experiments should be undertaken to check the validity of certain of the conclusions reached in this thesis. Since this second group contains "new" experiments, this area will be discussed first.

(a) A delayed-peak effect of the type described in chapter three should arise in an ammonia beam maser if the criteria of equations 3.7 and 3.8 can be satisfied. The difficulty here lies not in tipping the system with a microwave pulse, since the size of the tipping angle is not particularly critical, but in mechanically chopping the beam in a time $t_s < 100$ μsec. However, light choppers are now made which satisfy this stringent requirement. A suitable type based on a resonating torsion bar can be obtained from Bulova Time Products (Catalogue No. L46).

(b) Continuous self-pulsing may be achieved artificially in two ways. If the monitoring amplifier used in the Stark-pulse experiments of section 3.3 is connected through a suitable interface unit

to the Stark pulser itself, a feedback loop whose time constant is the radiation damping time of the maser should result. The interface unit could contain two integrated circuits, a limiting amplifier (e.g. Plessey type SL 630) and a Schmitt trigger (e.g. SN7413). The first of these would activate the second as soon as a predetermined oscillation level was reached. This would in turn cause the Stark pulser to switch on, and this would remain on until maser oscillations had ceased. The cycle would then be repeated. This technique would be suitable for optimization of beam maser systems, since the frequency of the resulting pulsations will increase if the excitation parameter is increased.

Alternatively, a Q-multiplier could be used to reduce cavity losses to a point where the maser becomes unstable. With a low-noise system such as a K-band parametric amplifier, the conditions under which self-induced spiking occurs could then be evaluated.

(c) Spoiling the quality factor of the cavity, rather than perturbing the molecules directly, would enable cavity-dumping type experiments analogous to those once performed on lasers (Vuylsteke 1963) to be tried in a superradiant system. This would also be interesting because information on the time evolution of ordered systems enables the predictions of quantum electrodynamics to be compared with those of semiclassical radiation theory. Q-spoiling of the requisite speed might be achieved by biassing a microwave varactor or a PIN diode which has been placed in an appropriate place in the cavity.

(d) A maser analogue of the saturable-absorber laser system could be evaluated. The particular scheme envisaged would use an isolator to couple the microwave signals externally and unilaterally from the second cavity of a two-cavity beam maser oscillator back to the first, with both cavities tuned to the peak of the molecular

resonance line. Some degree of pulse sharpening, akin to that observed in lasers containing saturable absorbers (De Maria et al 1969), should then result. The loop-delay between these circulating signal pulses should correspond to the time of flight of molecules between cavities. However, it may be found necessary to initiate this process by including an attenuator, such as the diode switch previously described in the feedback loop, this being set for maximum attenuation until such time as strong oscillations have been obtained in the first cavity.

(e) The time evolution of both the phase of oscillations in the first cavity during either Stark or radiation-damping induced pulsations and the accompanying population changes offer fertile ground for study. The problem here is solely one of devising an arrangement whereby microwave signals with a frequency stability no worse than the unperturbed maser may be obtained.

One possible approach would be to try the "flywheel synchronization" technique used in television receivers. This is employed in situations where contact with a stable reference oscillator is occasionally lost for short periods. An internal oscillator which is normally locked in phase to this external source will "drift" during these times, but this "drift" will be so low with a well-designed circuit that for all intents and purposes the receiver always maintains synchronization with the stable external source. There is no reason why the short-term (1 msec) frequency stability of a temperature-controlled klystron or Gunn oscillator with a well-smoothed power supply should be any worse than that of an ammonia maser. Furthermore the stabilisation process takes less than1 msec, and the time between perturbations can be chosen to be much greater than this.

Accordingly, the author proposes offsetting the local

oscillator klystron by a convenient frequency, (e.g. 30 MHz), equal to that obtainable from a quartz crystal-based oscillator. The local oscillator may then be locked in phase to the unperturbed maser by using a commercially available feedback loop (such as one of the Micronow range). Such loops usually have a "capture time" of 5 msec, or more, so will not follow the rapid changes in frequency associated with a Stark pulse.

The phase of the local oscillator at the beginning of any such transient should therefore be completely reproducible, provided the ratio of Stark pulse on-to-off times is suitable. Use of the sideband - generation technique of chapter two should also allow production of a signal,at the molecular resonance frequency,suitable for second-cavity studies of the populations of the molecular beam.

(f) Experiments on microwave <u>echoes</u> may well be feasible, either with the scheme outlined above, this being used in conjunction with a second maser (the "sample") and a microwave switching diode, or with a two cavity arrangement.

The pulse sequences required for echo effects, such as $\pi/2$, $\tau$, $\pi$, must be over in a time less than the transit time through the pulsed cavity, and must be at frequencies within the maser linewidth. Both these requirements can be met in a two cavity system by swtiching the Stark probe voltage in the first cavity on and off in a suitable fashion. The resulting rapid changes in oscillation level in the first cavity will result in the production of equally large changes in the polarization carried by the beam into the second ("sample") cavity, where echoes may arise.

This really completes the list of untried experiments which follow naturally from this thesis, and it only remains to point to two areas where <u>detailed</u> experimentation would prove fruitful. These are firstly, studying <u>population changes</u> in a Zeeman maser

during the transition from a locked to an unlocked state, and secondly, investigating locking and quenching in an ammonia maser on a quantitative basis, to see if the van der Pol results can be applied to this system.

References

Alsop L.E. et al, (1957), Phys.Rev.107, 1450 - 1

Anderson P.W., (1957), J.Appl.Phys.28, 1049 - 53

Audoin C., (1966),C.R.Acad.Sci.263, 542 - 5

Audoin C., (1968),Phys.Lett.A 28, 372

Audoin C. et al, (1968),Proc.22nd Symp. on Frequency Control, USAEC, Fort Monmouth, New Jersey, p.493

Audoin C. et al., (1969), IEEE J. Quantum Electron.5, 431 - 4

Autler S.H. and Townes C.H., (1955), Phys.Rev.100, 703

Bambini A. and Vallauri R., (1971),Optics Comm.3, 209 - 12

Bardo W.S. and Lainé D.C., (1971),J.Phys.E. (Sci.Instr.)4, 595 - 6

Bardo W.S. and Lainé D.C., (1971),J.Phys.D. (Appl.Phys.)4, L42 - 44

Basov N.G., Oraevskii A.N. et al, (1964),Sov.Phys.-JETP 18, 1211 - 7

Basov N.G., Oraevskii A.N. et al, (1966), IEEE J. Quantum Electron. 2, 542 - 8

Basov N.G., Morozov V.N. et al, (1969), IERE "lasers and Opto-electronics" conference report,London, pp.S7 - S15

Belenov E.M. and Oraevskii A.N., (1963),Radio Engng.Electron.Phys.8, 140 - 3

Bender P.L. and Driscoll R.L., (1958),IRE Trans.Instr.7, 177

Bennett Jr. W.R., (1962), Phys.Rev.126, 580 - 593

Bevensee R.M., (1963), Proc.IEEE 51, 215

Bloom A.L., (1962), Appl.Optics 1, 61 - 8

Bloom S., (1956), J.Appl.Phys.27, 785 - 8

Bloom S., (1957), J.Appl.Phys.28, 800 - 805

Brewer R.G. and Shoemaker R.L., (1972), Phys.Rev.A6, 2001-7

Brousseau R. and Vanier J., (1971), Physics in Canada 27, 56

Buley E.R. and Cummings F.W., (1964), Phys.Rev. 134, A1454

Collins R.J. et al, (1960), Phys.Rev.Lett.5, 303 - 5

Combrisson J., (1960), in "Quantum Electronics" (C.H.Townes, ed.),

Columbia Press, New York, pp.167 - 76

Davidenko D.F. et al, (1969), Optics and Spectros.26, 437-440

De Maria A.J. et al, (1969), Proc.IEEE 57, 2-25

Dicke R.H.,(1954), Phys.Rev.93, 99 - 110

Di Domenico Jr. M., (1964), J.Appl.Phys.35, 2870

Dzhibladze M.I. et al, (1969), Sov.Phys.Dokl.13, 1047

Feynman R.P. et al. (1957), J.Appl.Phys.28, 49-52

Grasyuk A.Z. and Oraevskii A.N., (1964), Radio Engng.Electron. Phys. 9, 424 - 8 and 443 - 6

Greifinger C. and Birnbaum G., 91959), IRE Trans,Electron.Devices 6, 288-93

Grigor'yants V.V. and Mazurov Yu.A., (1968), Radio Engng.Electron. Phys. 11, 126-8

Haken H., (1966), Z.Physik 190, 327-356

Higa W.H., (1957), Rev.Sci.Instrum.28, 726-7

Hocker G.B. and Tang C.L., (1969), Phys.Rev.Lett.21, 9

Khaldre Kh.Yu. and Khokhlov R.V. (1958), USSR News of Higher Educ. Inst., Radiophysics Ser.1, 60-5

Krupnov A.F. and Skvortsov V.A., (1966), Radiophys.Quantum Electron. 10, 74-5

Lainé D.C., (1967), Electron.Lett.3, 454-5

Lainé D.C. and Bardo W.S., (1969), Electron.Lett.5, 323-4

Lefrère P.R. and Lainé D.C., (1972), Phys.Lett.4 A, 93-4

Livshits B.L. et al, (1966), JETP Lett.3, 179

Luntz A.C., (1971), Chem.Phys.Lett.11, 186-7

Nikitin A.I. and Strakhovskii G.M., (1966), Radio Engng.Electron. Phys.11, 1650-3

Nurmiko A.V. and Schwarz S.E., (1972), Appl.Phys.Lett.20, 346-8

Oraevskii A.N., (1964), "Molecular Generators", Nauka (publ.), Moscow.

Oraevskii A.N., (1967), Sov.Phys.-Usp.10, 45-51

Reder F.H. and Bickart C.J., (1960), Rev.Sci.Instrum.31, 1164-5

Risken H. and Nummedal K., (1968), J.Appl.Phys.39, 4662

Shakhov V.O., (1967), Quantum Radiophys.10, 257-9

Shakov V.O., (1969), Quantum Radiophys.12, 1152-5

Shapiro S.L. et al, (1968), Appl.Phys.Lett,12, 36-7

Shimoda K. and Wang T.C., (1955), Rev.Sci.Instrum.26, 1148-9

Shimoda K. et al, (1956), Phys.Rev.102, 1308-21

Shoemaker R.L. and Brewer R.G. (1972), Phys.Rev.Lett.28, 1430-3

Singer J.R. and Wang S., (1961), Phys.Rev.Lett.6, 351-4

Sinnet D.M., (1962), J.Appl.Phys.33, 1578-81

Smith A.L.S. and Lainé D.C., (1968), J.Phys.D.(Appl.Phys.)1, 727-32

Smith P.W., (1967), IEEE J.Quantum Electron.3, 627-636

Statz H. and deMars G.A., (1960), in "Quantum Electronics" (C.H. Townes,ed.), Columbia Press, New York, pp.530-7

Strakhovskii G.M. and Tatarenkov V.M., (1962), Sov.Phys.-JETP 15, 625-6

Stratton J.A., (1941), "Electromagnetic Theory", McGraw Hill (publ.), New York, pp.448-454

Stroud C.R. et al, (1972), Phys.Rev.5A, 1094-1104

Tang C.L., (1963), J.Appl.Phys.34, 2935-40

Tang C.L. and Silvermann B.D., (1966), in "Physics of Quantum Electronics", (P.L. Kelley, B.Lax, P.E.Tannenwald, eds.), McGraw Hill, New York, pp.280-93

Uspenskii A.V., (1963), Radio Engng.Electron.Phys.8, 1145-8

Vanier J., (1968), Phys.Rev.168, 129-50

Vuylsteke A.A., (1963), J.Appl.Phys.34, 1615 - 22